Validation of the COSMO Land-Surface Parameterization TERRA-ML with discharge measurements

Dissertation
zur
Erlangung des Doktorgrades (Dr. rer. nat.)
der
Mathematisch-Naturwissenschaftlichen Fakultät
der
Rheinischen Friedrich-Wilhelms-Universität Bonn

vorgelegt von
René Graßelt
aus
Stralsund

Bonn, 2009

Angefertigt mit Genehmigung der Mathematisch-Naturwissenschaftlichen Fakultät
der Rheinischen Friedrich-Wilhelms-Universität Bonn

1. Referent: Prof. Dr. Clemens Simmer

2. Referent: Prof. Dr. Susanne Crewell

Tag der Promotion: 29.01.2010

Diese Dissertation ist auf dem Hochschulschriftenserver der ULB Bonn
http://hss.ulb.uni-bonn.de/diss_online elektronisch publiziert.

Erscheinungsjahr: 2010

Abstract

The objective of this study is to eliminate known deficits in the operational land-surface parameterization (LSP) TERRA-ML of the numerical weather prediction (NWP) model COSMO (Consortium for Small-Scale Modeling). A large deficit represents the drying out of TERRA-ML which leads to an unrealistic runoff simulation during long-time simulations. Earlier studies show that the vertical soil water formulation influences the generation of runoff. The operational TERRA-ML uses a formulation which is not often used in NWP models. This study investigates the impact of the vertical soil water formulation on the runoff generation. This investigation is needed due to the objective of this study to use the LSP scheme as potential flood prediction tool for river catchments

This study uses a TERRA-ML version coupled to a river routing scheme. The extended system is able to transform the grid based calculated runoff into discharge and allows therefore the prediction of discharge. In addition to the successful implementation of the routing scheme, an alternative vertical soil water transport parameterization is implemented into TERRA-ML in order to estimate the uncertainties on runoff generation. The newly implemented vertical soil water parameterization overestimates total discharge less (6%) than the operational parameterization (20%) when compared to a gauging station located at the lower reaches of the river Sieg during a time period 2005. Due to the drying out of TERRA-ML, the lower boundary condition of the LSP is replaced by SIMTOP (Simple TOPMODEL based runoff scheme), a variable ground water table parameterization. The simulations with SIMTOP show a clearly improved base flow simulation especially during drier periods. A sensitivity analysis based on a factorial design is performed to gain deeper insight into the influence of the crucial parameters on model performance. The result is that the ground water table parameters and the initial soil water conditions influences the model performance strongly.

A complete system is build which allows the prediction of discharge. The drying out deficit in TERRA-ML is removed. The alternative vertical soil water movement parameterization improves the simulation of runoff.

Zusammenfassung

Das Ziel dieser Studie ist die Eliminierung bekannter Defizite im operationellen Landoberflächenmodell TERRA-ML des numerischen Wettervorhersagemodells COSMO (Consortium for Small-Scale Modelling). Ein grosses Defizit sind die Austrocknungseffekte während Langzeitsimulationen, die zu unrealistischen Abflusswerten führen. Frühere Studien zeigen das die vertikale Wassertransportparametrisierung die Abflussgenerierung beeinflusst. Die in TERRA-ML operationell verwendete vertikale Wassertransportparametrisierung entspricht einer in der numerischen Wettervorhersage nicht häufig verwendeten Formulierung. Diese Studie untersucht den Einfluss der vertikale Wassertransportparametrisierung auf die Abflussgenerierung. Diese Untersuchung is notwendig um das Ziel dieser Studie umzusetzen, das Landoberflächenmodell TERRA-ML als potenzielles Gerinne-Abflussmodell in Flusseinzugsgebieten zu verwenden.

Diese Studie benutzt eine TERRA-ML Version, die an ein Routing Schema gekoppelt ist. Das somit erweiterte Modell ist in der Lage, den für jede Gitterzelle berechneten Abfluss in Gerinne-Abfluss zu transformieren und somit Abflussvorhersagen zu ermöglichen. Neben dem Routing Schema wurde in TERRA-ML eine alternative vertikale Wassertransportparametrisierung implementiert, um dessen Einfluss auf die Abflussgenerierung abzuschätzen. Die alternativ implementierte vertikale Wassertransportparametrisierung überschätzt den totalen Gerinneabfluss für einen gewählten Beispielzeitraum in 2005 um nur 6% während die operationelle Parametrisierung um 20% überschätzt. Durch Defizite in den Parametrisierungen in TERRA-ML zeigt auch das erweiterte Modellsystem Austrocknugseffekte in Langzeitsimulationen, die zu einer unrealistischen Basisabflussentwicklung führen. Daher wurde als Konsequenz die untere Randbedingung des Landoberflächenmodells durch SIMTOP (Simple TOPMODEL based runoff scheme), einer variablen Grundwasserspiegelparametrisierung, ersetzt. Nach der Implementierung des SIMTOP Ansatzes, zeigt das erweiterte TERRA-ML eine deutliche Verbesserung der Modellgüte. Des Weiteren wurde eine Sensitivitätsstudie basierend auf einem factorial design durchgeführt um zu untersuchen welche Parameter die Modellgüte am meisten beeinflussen. Das Ergebniss zeigt das die Grundwasserspiegelparameter und Bodenfeuchteinitialisierung die Modellgüte wesentlich beeinflussen.

Insgesamt konnte ein komplettes Modellsystem geschaffen werden, was die Vorhersage von Gerinne-Abfluss erlaubt. Des Weiteren konnten die Austrocknungseffekte behoben werden und durch eine alternative vertikale Wassertransportparametrisierung zusätzlich eine Verbesserung in der Abflussgenerierung erreicht werden.

Contents

Chapter 1

Introduction

The atmospheric branch of the hydrologic cycle is a crucial component of the weather and climate system, and is significant for many aspects of society and health of life on earth (USGCRP 2001). Much of the motivation for weather and climate prediction stems from the importance of precipitation (Dirmeyer et al. 2008). An accurate prediction of precipitation is of major interest for the society. Flood forecasts, agricultural and water resources management could be improved and severe weather warnings could be issued more precisely. Nevertheless, quantitative precipitation forecast (QPF) is still a major challenge in numerical weather prediction (e.g. Warrach-Sagi et al. 2008; Hohenegger et al. 2008a; Wulfmeyer et al. 2008). The problem of the numerical weather prediction (NWP) is to a large extent an initial and boundary value problem (e.g. Kalnay 2002). The water vapor field of the continental lower troposphere and therefore cloud formation and precipitation is influenced by the interaction of the atmosphere with the land-surface through the energy and water fluxes. A very wet soil on a sunny day gives rise to more evaporation, while a dry soil allows more solar radiation to warm the surface resulting in higher maximum temperatures. Earlier studies show the soil moisture influence on quantity and spatial distribution of precipitation at the local (e.g. Seuffert et al. 2003) and regional scale (e.g. Schär et al. 1999). Due to the still insufficient quality of the NWP precipitation for hydrological purposes, however, observed precipitation is used instead of model-generated precipitation. Precipitation can be observed by rain gauges and/or radar. Rain gauges provide high quality point observations. The magnitude of errors depends on wind speed, siting characteristics, type of precipitation (rain or snow), and temperature. Additionally, rain gauge measurement is difficult in a variety of settings, including mountain ridges, forests, and water bodies (Smith 1993). More serious, however, is the representativeness error when the necessary area-covering products are derived from these point observations. Weather radars are less accurate for point observations due to numerous error sources, such

as uncertain so-called Z-R-relations (reflectivity-rainfall rate relationship), evaporation of falling rain and the distortion of the precipitation field due to below-cloud winds. They provide, however, quite realistic area distributions of rainfall.

The treatment of the land-surface processes has always been a difficult problem in atmospheric models because of the complicated interactions between atmosphere, vegetation and soil (Beljaars et al. 1995). Recognizing the importance of the land-surface processes, detailed parameterizations have been introduced in atmospheric models. Beljaars et al. (1995) indicate that current land-surface schemes are mainly physically based and use Monin-Obukov similarity for the atmosphere-surface interactions. The complexity of these models ranges from simple bucket models to sophisticated land-surface parameterization (LSP) with multiple vegetation, soil and snow layers (e.g. Koster et al. 2000; Slater et al. 2001). Avissar (1998) divided the LSPs in three types: (i) the "bucket" type, introduced by Manabe (1969); (ii) the "Soil-Vegetation-Atmosphere Transfer (SVAT) schemes" type, introduced by Deardorff (1978); and (iii) the "mosaic-of-tiles" type, introduced by Avissar and Pielke (1989). Especially in the NWP the interface between the atmosphere, soil and vegetation is usually described by LSPs based on SVAT schemes, which mainly focus on a correct representation of the energy and mass fluxes between atmosphere, soil and vegetation (e.g. Chen et al. 1996; Warrach et al. 2002).

The LSP schemes employ a one-dimensional (vertical) treatment of sub-surface moisture transport and surface moisture and energy fluxes that assume homogeneous soil moisture conditions across horizontal areas spanning up to hundreds of kilometers (Warrach-Sagi et al. 2008). The LSPs partition the precipitation into evapotranspiration, runoff, and soil moisture change, and the net incoming radiation into a latent and sensible heat flux, ground heat flux and snow melt energy. The water and energy fluxes between the land-surface and the atmosphere are linked via the evapotranspiration. Many models consider potential evaporation from snow and/or an interception reservoir, and they may also approximate of hydrologic processes (e.g. Dickinson et al. 1993; Sellers et al. 1986; Viterbo and Beljaars 1995). The consideration of these processes becomes apparent in the calculation of runoff which is strongly related to evapotranspiration. Hence, a poor runoff calculation results in an unrealistic latent heat flux, regardless of which scheme is used (Koster et al. 2000). Basic equations of the LSPs for vertical water flow, vertical heat conduction, surface energy and water balance are nearly the same, but the numerical solutions, assumptions and the applied parameters differ (e.g. Richards 1931; Pitman et al. 2004). Beljaars et al. (1995) suggest that although most schemes have been validated and calibrated with the help of field data, the differences between individual models can still be large, which has been demonstrated the project for intercomparison of land-surface parameterization schemes (PILPS; Henderson-Sellers et al. 1993; 1995). PILPS, a seven year project, focuses on evaluating and improving land-surface schemes for climate and NWP models. General conclusions of PILPS

are that different land-surface schemes deal with incoming precipitation differently partioning it into runoff plus drainage, soil storage and evaporation differently at different times and depending (differently) upon the antecedent conditions. Moreover, LSP schemes can be tuned to observations but no single scheme predicts all the variables describing the land-surface climatology and hydrology well (Henderson-Sellers 1996).

The land-surface atmosphere interactions were investigated during the global Energy and Water Cycle Experiment/Climate Variability and Predictability (GEWEX/CLIVAR) Global Land-Atmosphere Coupling Experiment (GLACE). This project has provided an estimate of the global distribution of land-surface coupling strength during boreal summer based on the results from a dozen weather and climate models (Dirmeyer et al. 2006). There are numerous variations among models, due to differences of the model outcome by the simulation of both the terrestrial and the atmospheric branches of the hydrologic cycle. They found evidence that systematic biases in near-surface temperature and humidity between the models may contribute to incorrect surface flux-sensitivities. However, the multi model mean generally performed better than most or all of the individual models. Up to now, a single LSP scheme has deficiencies in the quality of the simulation of the water and energy cycle.

In contrast to hydrological models LSP schemes do not taken into account the lateral flow of water. The LSP grid based generated runoff represents the amount of water which can be transformed into discharge. Discharge is one of the major components of the global water cycle and accounts for about 40% of the precipitation on land. Therefore, it plays an important role in the global climate system by affecting evapotranspiration and fresh water inputs to the oceans, which in turn affect the ocean thermohaline circulation (Niu et al. 2005). There is a growing interest, however, to use LSP schemes also for flood prediction, because the atmospheric model component automatically provides physically consistent driving parameters to the LSP scheme. The existing well-developed data assimilation techniques of the NWP community are able to adjust the physical state optimally to observations. In the last few decades hydrologists have made considerable progress in the development and application of watershed models for the analysis of hydrologic systems and to provide accurate flood forecasting techniques. The predictions with these models are often deterministic, focusing on the most probable forecast, without an explicit estimate of the associated uncertainty. However, uncertainty arises from incomplete process representation, initial conditions, input, and parameter errors. Quantifying these uncertainties is necessary to assess model quality and predictive capability (Vrugt and Robinson 2007). Using LSPs for discharge prediction necessitates also to consider lateral flow of water as stressed by Lohmann et al. (1996) and others. There is also interest by the NWP community in predicting discharge with their models, because this extension opens up the possibility to evaluate the LSP mod-

ules by discharge measurements and eventually to use observed discharge for data assimilation.

In principle, hydrological models instead of LSPs can also be directly coupled to NWP models for discharge prediction. Hydrological models are often physically-based simulation models of the hydrologic budget of a watershed. Hydrologic models represent only a small part of the overall physical processes occurring in nature. The hydrologic models are aimed at flood forecasting and long term hydrologic simulation using observations and precipitation data from radar. The modeled processes include interception, infiltration, evaporation, snow accumulation and ablation, interflow, recharge, base flow, and overland and channel routing. The missing of energy conservation in the most hydrological models, however, results either in inconsistencies within the coupled model or forces us to implement the missing component in the hydrological module — usually a very cumbersome and error-prone business. Even when hydrological models are already equipped with LSPs, the correct coupling to an atmospheric model causes considerable problems due to different treatments of the near-surface processes. An example of such a system has been provided e.g. by Seuffert et al. (2002), who coupled an older COSMO (Consortium for Small-Scale Modelling) model version to the hydrological model TOPLATS. In addition to physical consistency also the computational architecture does frequently cause problems: modern operational NWP systems are adjusted to high-performance computing environments (vector or cluster architectures) while many hydrological models are not, or are differently organized. These circumstances usually slow down processing by an order of magnitude.

Another problem for fully coupled atmosphere-hydrology model systems is the scale gap between the atmosphere and the surface. The NWP models lower boundary calculate the coupled water and energy balance at each grid cell of the atmospheric model. On these typical grid scales ($\geq 1km^2$), soil texture, topography and vegetation and, therefore, water and energy fluxes, soil moisture, runoff and soil temperature are highly heterogeneous (e.g. Kabat et al. 1997). This heterogeneity can not be modeled explicitly at acceptable computational cost. The LSPs differ in their way to account for the heterogeneity of soil and vegetation parameters due to the use of mosaic approaches (e.g. Ament and Simmer 2006), effective and aggregated parameters (e.g. Claussen 1999; Kabat et al. 1997) and probability density functions of the most important land characteristics (e.g. Avissar 1992).

Recent developments of LSPs try to eliminate hydrological deficiencies in the NWP. The Community Land Model 3.5 includes sophisticated hydrological parameterizations to take horizontal soil water fluxes and ground water table fluctuations into account (Oleson et al. 2008). Lohmann et al. (1996) consider horizontal water transport processes by coupling the VIC (Variable Infiltration Capacity) LSP (Liang et al. 1996) to a horizontal routing scheme. The major task was to utilize this runoff

information to check the reliability of the LSP scheme, giving the opportunity to include discharge data as an integrated quantity for validation. The routing scheme developed by Lohmann et al. (1996) channels the runoff generated in the different vertical soil layers within each model column including surface runoff to the river taking account of the time delay in water flow. A disadvantage of this routing model is that, when runoff water has left the grid cell, no re-infiltration into the soil is allowed. In general, three different approaches are implemented in the various LSPs for the runoff generation: 1) saturation excess runoff and free drainage (e.g. Abramopoulos et al. 1988; Doms et al. 2005) 2) the "VIC"-model and "ARNO"-model concept (e.g. Dümenil and Todini 1992; Liang et al. 1996; Wood et al. 1992) and 3) the "TOPMODEL"approach (e.g. Beven and Kirkby 1979). Warrach et al. (2002) summarized and analyzed these approaches in the LSP SEWAB (e.g. Mengelkamp et al. 1999; Warrach et al. 2001). For the TOPMODEL approach a simplified formulation based on the physical architecture of TOPLATS is investigated by different scientist (e.g. Gulden et al. 2007; Niu et al. 2005; Stieglitz et al. 1997). They often used the simplified TOPMODEL approach to minimize the computational costs and to make it usable for meteorological models.

1.1 Motivation and organization of the thesis

The introduction of the LSP schemes leads to the conclusion that these models do not provide optimal boundary values for the NWP. Further research is needed such as the implementation of additional hydrological processes or the forcing of LSP schemes with high quality input information. A major key for the NWP is to consider the computational efficiency in the implementation of new approaches.

A central motivation of this study is to use the LSP scheme TERRA-ML for the prediction of discharge. TERRA-ML is part of the NWP model designed by the Consortium for Small-Scale-Modelling (COSMO; Doms and Schättler 2002). The grid based architecture of the LSP and a drying out during long-time simulations represent disadvantages for the use of TERRA-ML as a flood prediction tool. Hence, this study extends TERRA-ML with the objective to build a model system which is able to simulate discharge processes correctly.

Simulated runoff depends on the correctly designed processes at the land-surface and in the soil. There are several hydrologic processes which are insufficiently parameterized in the operational version of the LSP. The result is a bad model performance for the simulated discharge. Hence, new parameterization approaches are implemented into TERRA-ML. For example, the treatment of the vertical soil water flow is an important compartment for the runoff generation. A formulation following Campbell (1974) is implemented into TERRA-ML to estimate its impact on

the model efficiency and to compare the evolution of runoff with the operational approach of Rijtema (1969). For the objective of this study to validate the LSP of the COSMO model with discharge measurements, an accurate surface and base flow component are needed. TERRA-ML does not have a variable ground water table parameterization which provides an accurate base flow simulation. Hence, an additional goal of this study is the implementation of a variable ground water table in TERRA-ML. The introduced simplified approach based on the physical architecture of TOPLATS (e.g. Gulden et al. 2007; Niu et al. 2005; Stieglitz et al. 1997) is implemented as a novel formulation in TERRA-ML.

The grid based architecture of NWP models only allows the calculation of runoff for individual grid cells and is therefore unable to consider horizontal flow which is needed to describe river catchment properties correctly. This study uses a one-way mode (decoupled from the NWP model) extended LSP scheme of COSMO. The LSP scheme TERRA-ML is coupled to a river routing scheme following Warrach-Sagi et al. (2008). The coupled model system is used to describe discharge processes realistically. With the used one-way mode it is aimed to evaluate a model system which can be integrated in the COSMO model in later studies as a useful application. For example, the generated discharge can be assimilated in the NWP model and can help to improve the soil moisture prediction. Therefore, the LSP represents a preliminary stage version to a full coupled model system.

An evaluation with observed discharge requires the knowledge of realistic rainfall information. This study uses the so-called RADOLAN RW data set (Radar Online Calibration, a product of DWD with a one km spatial resolution, and hourly temporal resolution), which is especially derived for hydrological applications. The newly build model system is forced with RADOLAN RW and applied to the catchment of the river Sieg located in Western Germany.

The hydrological cycle is a major component of the earth's climate system and the subject of this work. The hydrologic processes which are implemented in TERRA-ML are explained in an overview in Chapter 2. To understand the architecture of the LSP TERRA-ML, the configuration including all recently applied parameterizations (e.g. vertical water flow, ground water table parameterization) are presented in Chapter 3. A detailed description of the research area is given in Chapter 4. A description of the data sets which are used for forcing and evaluation are presented in Chapter 4. In Chapter 5, the results of the impact of the alternative vertical soil water formulation on the simulation of discharge are shown. In the next step the evaluation of the simulated discharge by applying the novel implemented variable ground water table parameterization is shown. A statistical evaluation is presented in Chapter 5. Conclusions are drawn and future work is discussed in Chapter 6.

Chapter 2

Hydrologic cycle

The global hydrologic cycle is a major component of the earth's climate system (Famiglietti and Wood 1994). The hydrologic cycle interacts with other system components like the solid Earth, the oceans, and the atmosphere over a wide range of spatial and temporal scales. These interactions affect a number physical, chemical, and biological processes including weather, climate, biogeochemical cycles and ecosystem dynamics. The hydrologic cycle is driven by incoming solar radiation, supplying the energy for evapotranspiration from land-surfaces and the ocean and for the atmospheric transport of water. This water eventually precipitates over land areas and the oceans.

This Chapter introduces the hydrological processes at the global scale and additionally provides a detailed description of the hydrologic cycle over land on regional scale and the connection to the surface energy balance.

2.1 The global hydrologic cycle

The global hydrologic cycle characterizes the distribution as well as the spatial and temporal variations of moisture in the terrestrial, oceanic, and atmospheric compartments of the global water system. The global hydrologic cycle is commonly portrayed by a diagram that shows the major transfer of water between continents and oceans (Fig. 2.1).

Water evaporates from the oceans and the land-surface, is carried by the atmospheric circulation as water vapor, precipitates as rain or snow, is intercepted

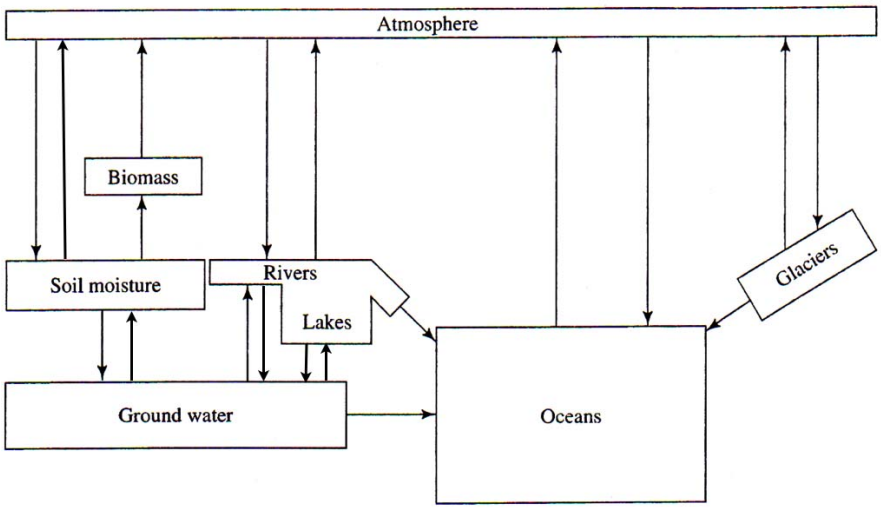

Figure 2.1: *Principal storages (boxes) and pathways of water in the global hydrologic cycle after Dingman (2002).*

by trees and vegetation, provides runoff on the land-surface, infiltrates into soils, recharges ground water, discharges into streams, and ultimately, flows out into the oceans from which it will eventually evaporate again. This immense water engine, fueled by solar energy, driven by gravity, proceeds endlessly in the presence or absence of human activity. The relative magnitudes of the individual components of the global hydrologic cycle, such as evapotranspiration, may differ significantly even at small scales, for example an agricultural field and a nearby woodland (Maidment 1993).

Maidment (1993) presented the volume of water flowing annually through the components of the hydrologic cycle. He used for the quantitative description of the global water balance units relative to the annual precipitation on the land-surface (119 000 $km^3/year$). The annual volume of evaporation from the ocean (424 units) is seven times larger than that from the land-surface (61 units), making oceans the primary source of precipitation over the earth's surface. The annual volume of discharge from the land-surface to the oceans (39 units) comes nearly all from surface water (38 units) and is counterbalanced by an equal net inflow of atmospheric water vapor from the oceans to the land areas.

2.2 The regulation of hydrologic processes over land

The U. S. Committee on Opportunities in the Hydrologic Sciences (Eagleson et al. 1991) defined the land part of the hydrologic cycle as the movement of water on and under the earth's land-surface, the physical and chemical interactions with earth materials accompanying that movement, and the biological processes that conduct or affect that movement.

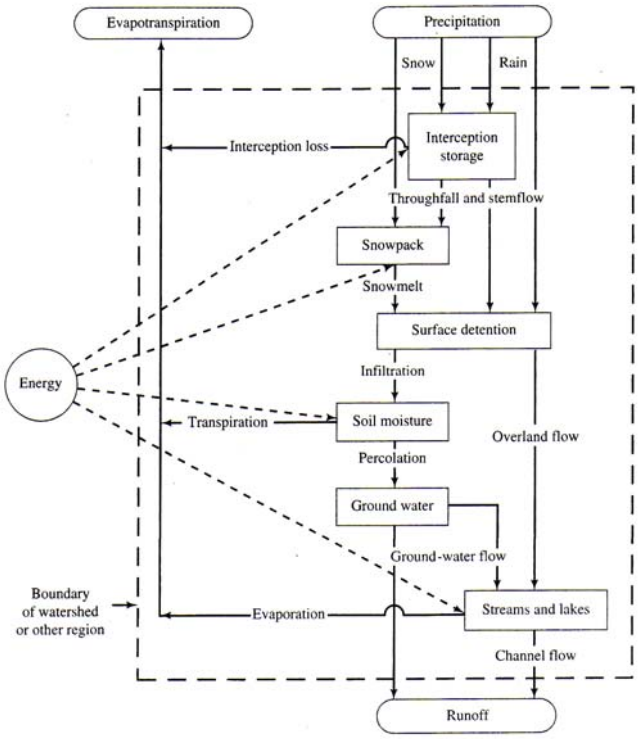

Figure 2.2: *Principal storages (boxes) and pathways of water in the land part of the hydrologic cycle (Dingman 2002).*

The terrestrial hydrologic cycle undergoes changes of state between liquid, solid and gas in four main processes. In contrast to the open water surface, the evapotranspiration over land is controlled by several mechanism. For example, plants reduce the transpiration by closing stomata and prevent that water can delivers from the root zone to the atmosphere. The open water surface is always able to evaporate with the potential rate. The potential evaporation process describes the amount of water that could be evaporated if there was sufficient water available.

This demand incorporates the energy available for evaporation and the ability of the lower atmosphere to transport evaporated moisture away from the surface.

At watershed level the hydrologic cycle can be described in a mathematical form by the water balance equation. The main source is Precipitation (P); the sinks are evapotranspiration (E), runoff (Q), infiltration (I) and storage ΔS.

$$P - E - Q - I = \Delta S \tag{2.2.1}$$

All terms can be divided again into different sub-processes (Fig. 2.2). The terms of equation 2.2.1 can be described as follows: Precipitation P is the source of virtually all-fresh water in the hydrologic cycle, falls nearly everywhere, but its distribution is highly variable in time and space. The dramatic consequence of precipitation variability, droughts and extremes floods, have determined broad features of human settlement and commerce since ancient times. Describing and predicting the variability of precipitation is a fundamental requirement for a wide variety of human activities (Smith 1993). For example, in high and midlatitudes, melt of the seasonal snow cover is the most significant hydrologic event of the year (Gray and Prowse 1993). Gray and Prowse (1993) also mentioned that in these regions, runoff from the shallow snow covers often provides 80 percent or more of the annual surface runoff, augments soil water reserves, and recharges ground water supplies. Even at lower latitudes, particularly in alpine regions, snowmelt is a primary source of water.

The soil water transport during precipitation events depends on the characteristics of the land-surface, especially the type and density of vegetation, buildings, pavement, or roads. Interception covers a variety of processes that results from the temporary storage of precipitation on vegetation or man-made covers. Intercepted precipitation can be either evaporated to the atmosphere or ultimately transmitted into the soil. The main processes are throughfall, stemflow, and interception loss. Throughfall occurs either when precipitation falls through spaces in the vegetation canopy or when precipitation drips from leaves and twigs. Stemflow designates water that flows along twigs and branches with its ultimate delivery to the land-surface at the main stem or trunk. Interception loss accounts for precipitation that is retained by plant surfaces and later evaporated or absorbed by the plant (Smith 1993).

Evaporation and transpiration (E) (Eq. 2.2.1) is the second component in the hydrologic cycle. During evaporation water is converted into water vapor. The rate is controlled by the variability of solar energy at the evaporating surface, and the ease with which water vapor can diffuse into the atmosphere. Different processes are responsible for the diffusion, but the physics of water vapor loss from open-water surfaces and from soils and crops is essential identical. Local evaporation is a function of both local climate and regional air movement (Shuttleworth 1993).

In hydrology, potential evaporation and reference crop evaporation are used for

evaporation estimates, e.g. published by Shuttleworth (1993). He also told that these concepts are based on idealized situations. In particular they ignore the fact that meteorological parameters near the surface are influenced by upwind surface energy exchange. The potential evaporation is defined as the quantity of water evaporated per unit area, and per unit time free from an idealized water surface under existing atmospheric conditions. In contrast, the reference crop evaporation is defined as the rate of evaporation from idealized grass crop with a fixed crop height of 0.12 m, an albedo of 0.23, and a surface resistance of 0.69 s/m.

The extent to which the energy available at the ground is used to evaporate water is determined by the processes controlling vapor diffusion through the air. Movement occurs by variations in vapor concentration, and because the molecules making up the air are in permanent, random motion, either individually or coherently as turbulent eddies. Diffusion is divided in molecular and turbulent diffusion. Turbulent diffusion occurs when wind blowing horizontally over natural surfaces is retarded by interaction with the ground and vegetation. This interaction creates random and chaotic air motion in which portions of air, of varying size, move in an imprecisely defined yet coherent way during their transient existence. The most important resistance associated with molecular diffusion is that which controls the movement of water vapor from inside plant leaves to the air outside through small apertures in the surface of the leaves which are called stomata. This transpiration process is described as follows: the air inside the stomata cavity beneath the leaf surface is nearly saturated, while that outside is usually less. Water vapor movement is controlled by the plant, which opens or closes the stomata aperture in response to atmospheric moisture demand and the amount of water in the soil. In this way, plants control their water loss to the atmosphere, and seek to ensure their survival when water is limited (Shuttleworth 1993).

During precipitation events over bare soil the water can be stored (interception store) at the surface, infiltrate into the soil I or drain off at the land-surface (surface runoff). Percolation is the movement of water in the soil. Infiltration is defined as the process of water entry into a soil from rainfall, snowmelt, or irrigation (Rawls et al. 1993). This infiltration process into the soil depends on the soil water movement (percolation) which is defined as the process of water flow from one point to another within the soil. The infiltration process depends on the soil properties on the land-surface e.g. the pore volume and the soil moisture distribution at the beginning of the precipitation event. Due to a gradient in the matric potential at the beginning of the precipitation event the infiltration shows a higher capacity. During the process the infiltration capacity is close to the conductivity of the saturated soil (Fig. 2.3). Exceeds the intensity of precipitation the conductivity the water will be stored or drain off at the land-surface (Dingman 2002). The vertical soil water transport in the soil is driven by gravitation and difference in matric potential.

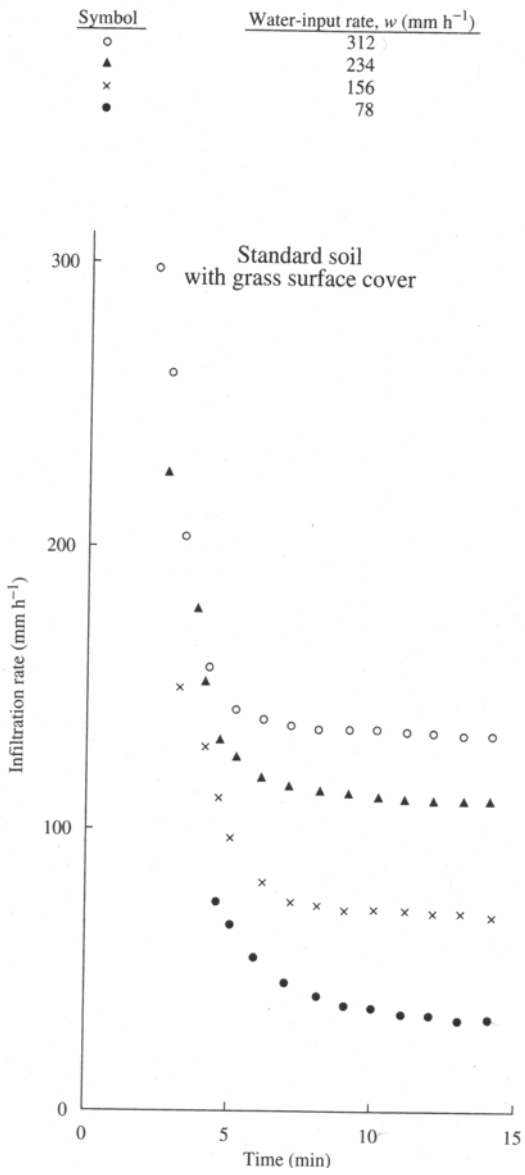

Figure 2.3: *Infiltration rate into grassed loam plots as measured in laboratory studies using artificial rainstorms of 15-min; infiltration rate as a function of time for various water input rates. (Dingman 2002)*

Discharge Q (Eq. 2.2.1) is defined by Mosley and McKerchar (1993) as the flow rate of water in cubic meters per second, along a defined channel. Mosley and McKerchar (1993) described discharge as the part of the hydrologic cycle which transfers water, originally falling as rain or snow, onto a watershed, from the land-surface to the oceans. Hence, discharge at a particular point in a channel network consists of surface runoff from the watershed, and return flow from the aquifer.

Discharge is generated by a combination of base flow (return flow from the ground water), interflow (rapid sub-surface flow through pipes, macro pores and seepage zones in the soil) and saturated overland flow from the surface. Interflow and saturated overland flow together comprise surface runoff, the rapid runoff during and after rainfall. This means that discharge Q is divided into surface runoff Q_s and in the base flow component Q_b. Surface runoff and base flow are conventionally separated on a discharge hydrograph (Fig. 2.4) by a line extended from the foot of the rising limb of the hydrograph to the falling limb (surface runoff), or recession (base flow).

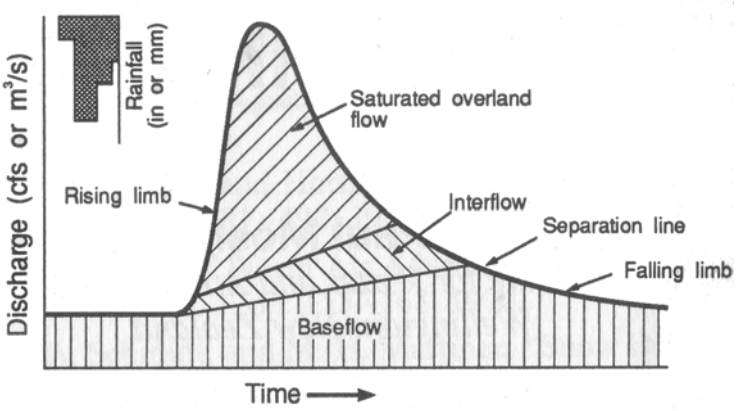

Figure 2.4: *Separation of sources of discharge on an idealized hydrograph (Mosley and McKerchar 1993)*

For a complete description of the hydrologic cycle the energy budget has also to be taken into account because the energy budget between surface and atmosphere is connected to the water balance (Fig. 2.2). Similar to the water budget, an energy budget can be established for an area based on the fundamental law of energy conservation. It is usually expressed as the surface energy balance (SEB) equation. (e.g. Schüttemeyer 2005; Meyers and Hollinger 2004; Stull 1988).

$$H + LE + G + S_p + S_g + S_c - R_n = 0 \tag{2.2.2}$$

Net radiation (R_n) is balanced by the sum of sensible heat flux (H), latent heat flux (LE), and the soil heat flux (G), in addition to the energy fluxes for photosynthesis (S_p), canopy heat storage in biomass and water content (S_c), and soil heat

storage (S_g). The surface energy balance equation describes the interaction of many processes occurring at the land atmosphere interface. The equations of water and energy balance are closely connected through actual evapotranspiration or latent heat flux (compare Eq. 2.2.1 and 2.2.2). This means that both balances have to be taken into account in a LSP scheme.

Chapter 3

Land-Surface Parameterizations

3.1 Overview

The Consortium for Small-Scale Modelling (COSMO) develops and advances an operational meso-γ to convective scale weather prediction system. The COSMO model (Doms and Schättler 2002), used by various European weather services (e.g. German Weather Service, Meteo Swiss, Institute of Meteorology and Water Management Poland) encompasses regional scale weather models with different versions and spatial resolutions. The COSMO model constitutes a limited area forecast model based on the non-hydrostatic unfiltered Euler equations. The model equations are formulated in rotated geographical coordinates and a generalized terrain following height coordinate. A variety of physical processes are taken into account by parameterization schemes.

Before 2007 the COSMO model was known as Lokal Modell (LM) and was available in three different versions, whereas only two were operational at the same time. The main differences are in size of model areas and grid resolutions. The first version of the LM has been developed at Deutscher Wetterdienst and became operational in 1999. The LM was the direct successor of the former DM (Deutschlandmodell) which was a hydrostatical model with a grid resolution of 14 km x 14 km. The LM was available with a spatial resolution of 7 km x 7 km and covered Germany plus its surroundings (Fig. 3.1). In 2005 LM-E (Lokal Modell Europe, now COSMO-EU) replaced the LM and covered completely Europe with a grid resolution of 7 km x 7 km. Since 2007 the so-called LM-K (now COSMO-DE) is also operational. It is nested in the COSMO-EU and covers Germany with a high spatial resolution (2.8 km x 2.8 km).

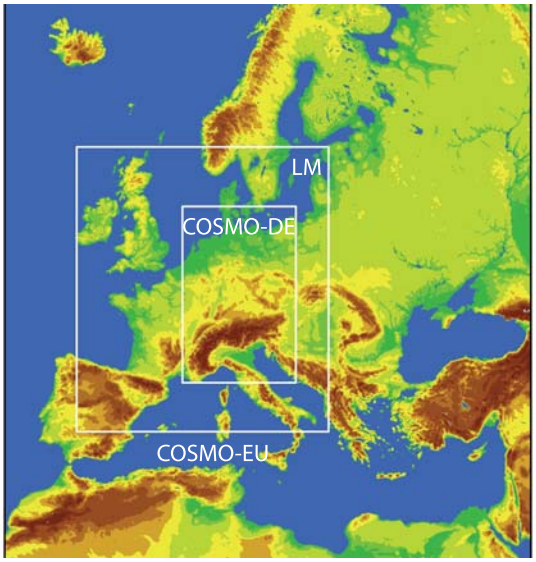

Figure 3.1: *Model domains of the LM and the successor COSMO-EU as well as of the COSMO-DE which is nested in the COSMO-EU model.*

In order to turn the COSMO model into NWP-mode, or for case studies, a number of components such as data assimilation, interpolation of boundary conditions from a driving host model, and post processing utilities are required. The boundary and initial values of the COSMO-EU are interpolated from the analysis and predictions of the Global Modell (GME) and from the continuous COSMO data assimilation scheme stream. The GME, in which the COSMO-EU is nested, describes a triangular mesh global grid point model and builds together with the corresponding data assimilation schemes the COSMO NWP system at the DWD.

The current operational COSMO-EU model has the objective to predict accurately the near-surface weather conditions, focusing on clouds, fog, frontal precipitation and thermally forced local wind systems. The COSMO-DE model with its finer resolution allows a direct simulation of severe weather events triggered by deep convection, such as super cell thunderstorms, intense mesoscale convective complexes, prefrontal squall-line storms and heavy snowfall from wintertime mesocyclones (Doms and Schättler 2002). The physical parameterizations of the model cover among other things a sub-grid scale turbulence scheme, sub-grid-scale clouds, moist convection, a radiation parameterization, and a multi-layer LSP. The improvement of latter is one objective of the study.

The land-surface processes in COSMO are contained in the land-surface parameterization (LSP) scheme TERRA. The turbulent exchange between the atmosphere and the underlying surface is modeled by a stability and roughness-length dependent surface flux formulation. These surface fluxes constitute the lower boundary

conditions for the atmospheric part of the model. Until September 2005 a 2-soil layer version TERRA-2L was operational. In 2001, Schrodin and Heise (2002) began developing a new multi-layer version, TERRA-ML. Aside from more layers, TERRA-ML considers freezing and melting processes in the soil. TERRA-ML became operational with the implementation of the LM-E in 2005. Additionally, the temperature prediction with the extended force-restore method (Jacobsen and Heise 1982) was replaced by a direct solution of the heat conduction equation.

The central tool of this study is the LSP TERRA-ML of the LM model version 3.16 in a decoupled mode. TERRA-ML describes the exchange processes between the land-surface, atmosphere and soil. There are numerous advantages by using an LSP-scheme in a decoupled mode. A decoupled model enables the LSP-scheme to be upgraded without additional computational cost. Hence, it is also simple to test new parameterization approaches. A disadvantage of this decoupled model is that TERRA-ML is driven by the atmospheric boundary values at the surface, meaning that changes in the state of the land-surface do not feed back into the development of the atmosphere. TERRA-ML determines the variables of the hydrological cycle using the multi-soil layer concept with soil moisture diffusion and soil heat conduction equations for different soil textures as well as frozen soil processes. The operational TERRA-ML uses six model layers for the calculation of the water balance. The model does not consider any sub-grid variability. This means that the LSP considers only the vegetation type and soil texture which dominates the area of a grid cell. However, both parameters are spatially distributed based on different data sets which create more variability in soil moisture distribution of the overall model domain. An important parameterization is the Biosphere-Atmosphere Transfer Scheme (Dickinson et al. 1993) which is implemented for the parameterization of evapotranspiration. The turbulent exchange is based on the Monin-Obukhov similarity for the constant-flux layer. A river routing scheme is not contained in the operational version. This work uses an extended TERRA-ML scheme which is already coupled to a river routing scheme. The river routing scheme based on the work of Lohmann et al. (1996) has the task to channel the runoff generated in the different vertical soil layers within each model column including surface runoff to the river, taking into account the time delay in water flow.

The implemented hydrologic parameterizations in TERRA-ML are used in numerous LSPs. There are also, however, some differences between the LSPs. One of these LSP models is Noah. Since 1993 the Noah community has been developing the LSP in collaboration with investigators from public and private institutions, e.g. the National Centers for Environmental Prediction (NCEP; Chen et al. 1996; Koren et al. 1999). Noah is a stand-alone, one-dimensional column model which can be executed in either coupled or uncoupled mode. The LSP is employed for studies related to the impact of land use on regional climate. The evapotranspiration is according to TERRA-ML the sum of bare soil E_{bare}, the interception reservoir E_I

and vegetation E_{veg}. The formulation of the evapotranspiration components are different in TERRA-ML and Noah. The latter model does not use the Dickinson scheme. The bare soil evaporation is determined via the potential evaporation based on the Penman approach that includes a stability-dependent aerodynamic conductance (Mahrt and Ek 1984). The turbulent exchange coefficient is calculated with a formulation of Paulsen (1970). For the canopy conductance the parameterization of Jarvis (1976) and Stewart (1988) is applied. For the soil moisture diffusion, soil heat conduction equations, and frozen soil processes Noah considers only four soil layers. Noah has been used operationally in NCEP models since 1996, and it continues to benefit from a steady progression of improvements (Betts et al. 1997; Ek et al. 2003).

A more detailed sub-grid LSP is used in the present NWP model of the European Centre for Medium-Range Weather Forecasts (ECMWF). The model is called TESSEL and based on the work of Viterbo and Beljaars (1995). TESSEL also follows a multi-layer concept based on four model layers. In comparison to TERRA-ML and Noah, TESSEL considers the sub-grid variability over land and uses the tile approach for calculating the surface fluxes. In detail, the evpotranspiration is calculated as in Noah with the difference that TESSEL distinguishes between high and low vegetation. Among other things, each grid cell of TESSEL has more than one variable of leaf area index (LAI), root distribution ($root$) and roughness length (z_0). For each tile of the grid cell, a surface temperature is calculated which influences the atmospheric processes of the NWP model. For the canopy conductance the parameterization of Jarvis (1976) and Stewart (1988) is applied. A disadvantage of TESSEL is that only one universal soil texture is used.

The Community Land Model (CLM) was created at the 1998 National Centre for Atmospheric Research (NCAR) Climate System Model (CSM) and subsequently developed by a collaboration of scientists. CLM includes superior components from each of three contributing models: the NCAR land-surface model (Bonan 1998), the Biosphere-Atmosphere Transfer Scheme (Dickinson et al. 1993), and the LSP of the Institute of Atmospheric Physics of the Chinese Academy of Sciences (Dai and Zeng 1997). The model is also the land model for NCAR's coupled Community Climate System Model (CCSM). The difference to the already introduced LSPs is that the CLM parameterizes the runoff based on TOPMODEL (Beven and Kirkby 1979; see section 3.3.2). The CLM land-surface model considers a river routing component in contrast to the operational versions of TERRA-ML, TESSEL and NOAH.

The Variable Infiltration Capacity (VIC) model (Liang et al. 1994; Liang et al. 1996) was originally developed in the early 90s and is maintained and upgraded at the University of Washington. The land-surface is modeled as a grid of large, flat, uniform cells. The VIC model also considers sub-grid heterogeneity (e.g. elevation, land cover) which is handled via statistical distributions. Moreover, the

VIC model is in comparison to the other introduced LSP models only available in a two-layer version. The evapotranspiration is calculated with the formulation of Penman-Monteith (Lohmann 1996). This macro-scale hydrology model is used extensively in research over the watersheds in the U.S. as well as globally (e.g. Liang et al. 1998; Hamlet and Lettenmaier 1999; Nijssen et al. 2001). The grid cells of the VIC model are simulated independently of each other and considers no lateral flow via river routing schemes as in CLM.

The introduced alternative LSPs show that each model has different methods to handle the hydrologic cycle. Therefore, it is difficult to decide which simulation of the hydrologic cycle leads to the best agreement with the reality. Nevertheless, there are advantages and disadvantage for the use of a model. For example, the VIC model with only two soil layers and the LSP TESSEL with an uniform soil texture present disadvantages. Thus, compared with multi-layer models a two layer LSP is not able to simulate the same detailed soil hydrology. An uniform soil texture leads to a smaller variability in the soil moisture distribution compared to LSPs with more classes of soil texture. The CLM with the consideration of a ground water table parameterization and the use of a routing scheme has clear advantages. Both approaches describe the runoff processes more realistically. The reason to use TERRA-ML in this study, is the objective to improve the already available operational LSP of the COSMO model. Furthermore, the experience in the operational mode are an additional advantage. The already existing TERRA-ML coupled to a routing scheme and the one-way mode of TERRA-ML which allows to extend the model easier are also reasons to use the LSP.

3.2 The operational land-surface parameterization TERRA-ML

The hydrologic processes, which are described in the following Section, are based on the publication of Doms et al. (2005) and Ament (2006). The layer thickness of TERRA-ML can be chosen arbitrarily. In the operational version, the energy balance is calculated in eight layers (Fig. 3.2), but the solution of the heat conduction equation takes into account only seven layers with a total thickness of 7.29 m. The 8th layer is the so-called climate layer, where the annual mean 2 m-temperature is prescribed as a boundary value. For the solution of the water balance the same layers as in the thermal section are used, but the number of active layers, in which the water balance is calculated, is restricted to six. The lower boundary condition at the bottom of the deep layer is free drainage. Soil water can drain from the lowest layer, but the flux due to diffusion is neglected. This means that ground water cannot moisten the soil by capillary rise from below.

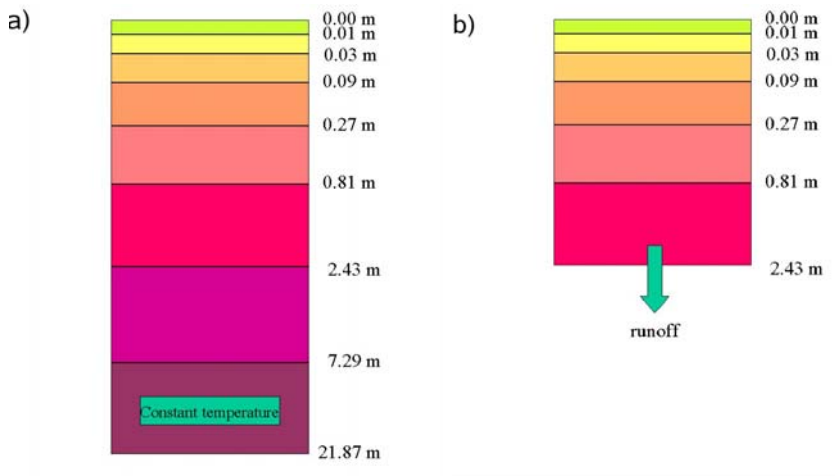

Figure 3.2: *The operational and in this study used layer structure of TERRA-ML* **a)** *for the energy balance and* **b)** *water balance.*

3.2.1 Evaporation and transpiration

The net evapotranspiration of a grid box is the sum of bare soil evaporation E_{bare}, plant transpiration E_{trans}, sublimation from snow E_s, and the evaporation from the interception store E_I weighted by their areal coverages:

$$E = (E_{bare} + E_{trans}) + f_I E_I + f_{snow} E_s \tag{3.2.1}$$

with f_I being the areal fraction covered by interception water, f_{snow} the areal fraction covered by snow. The starting point for all components is the potential evaporation rate E_p:

$$E_p(T_s) = -\rho K_h |\overrightarrow{v_h}| (q_{atm} - q^*(T_s)) \tag{3.2.2}$$

with the transfer coefficient for heat K_h which is calculated diagnostically and based on the Monin-Obukov similarity for the constant-flux layer, the air density ρ and wind speed $\overrightarrow{v_h}$ at the height h. The variable T_s describes the temperature of the respective surface (interception store, snow store, uppermost soil model layer) and q^* denotes the saturation specific humidity.

During soil ice conditions the bare soil evaporation E_{bare} is formulated by the potential evaporation (Eq. 3.2.2). In this case no changes of soil water content are considered. During ice free conditions the following formulation is used: If $E_p(T_s) < 0$, the evaporation rate of bare soil E_{bare} is parameterized using the assumption

$$E_{bare} = (1 - f_I) \cdot (1 - f_{snow}) \cdot (1 - f_{veg}) \cdot Min[-E_p(T_s); F_m] \tag{3.2.3}$$

where f_{veg} is the areal fraction covered by plants and F_m is the maximum moisture flux through the surface that the soil can sustain (Dickinson 1993). The determination of F_m results from tuning a two layer land-surface model with the results of a multi-layer land-surface model. The tuning is based on average values of soil water content normalized by the pore volume η_{PV} of the soil texture for an uppermost layer of 0.1 m thickness and for the soil water content for a total active layer of 1 m thickness (Doms et al. 2005).

The BATS scheme of Dickinson (1993) is applied for the plant transpiration E_{trans}. In the multi-layer version of TERRA-ML the moisture flux between the plant foliage and the air inside the canopy is assumed to be equal to the flux between the air inside and the air above the canopy. It is also assumed that the foliage temperature is equal to the surface temperature. Hence, total transpiration E_{trans} is computed by taking into account both the resistance for water vapour transport from the foliage to the canopy air (foliage resistance r_f) and the resistance for water vapour transport from the canopy air to the air above the canopy (atmospheric resistance r_a):

$$E_{trans} = f_{veg} \cdot (1 - f_I) \cdot (1 - f_{snow}) \cdot E_p(T_s) r_a (r_a + r_f)^{-1} \tag{3.2.4}$$

r_a^{-1} is given by $r_a^{-1} = K_h |\overrightarrow{v_h}|$ and r_f^{-1} is parameterized by $r_f^{-1} = r' f_{LAI} r_{la}^{-1}$. It is assumed that r_{la}^{-1} is proportional to the square root of the friction velocity $r_{la}^{-1} = K_m u_\star^{1/2}$ (with a transfer coefficient for momentum K_m) and a factor of proportionally of 0.05 $(m/s)^{1/2}$. The parameter f_{LAI} describes the leaf area index which depends on the plant type and $r' = r_{la}(r_{la} + r_s)^{-1}$ represents the resistance which describes the reduction of transpiration by the stomatal resistance r_s. The stomatal resistance r_s is minimal when environmental conditions are optimal for photosynthesis/transpiration, and maximum under unfavorable conditions. The actual value is determined by four stress factors, which are zero if the stress is highest. They consider stress due to shortage of insolation (F_{rad}), shortage in soil moisture (F_η), improper ambient temperature (F_{tem}) and humidity (F_{hum}):

$$r_s^{-1} = r_{max}^{-1} - (r_{min}^{-1} - r_{max}^{-1}) F_{rad} F_\eta F_{tem} F_{hum} \tag{3.2.5}$$

Radiation stress F_{rad} depends on incoming photosynthetically active radiation. Soil moisture stress F_η is evaluated from the average soil moisture content down to the root depth. F_{tem} and F_{hum} are based on the interpolated temperature at 2 m height and the humidity at the lowest atmospheric level (Ament 2006).

After the determination of the evapotranspiration according to Equation (3.2.1), the following bulk formula is inverted to derive a virtual specific humidity q_s at the surface:

$$E_0 = -\rho K_h |\overrightarrow{v_h}| (q_{atm} - q_s) \tag{3.2.6}$$

where q_{atm} is the specific humidity at the lowest grid level above the ground and q_s is the virtual specific humidity. The virtual specific humidity equals the humidity that

is required at a flat surface to sustain the diagnosed latent heat flux. Since most surfaces are not flat, e.g. due to leaves, q_s is in general not measurable and may be greater than the saturation humidity $q^*(T_s)$ (Ament 2006; Doms et al. 2005).

3.2.2 Interception store and infiltration rate

During rain, the interception store is used to collect the water partly which is formulated according to:

$$\rho_w \frac{\partial W_i}{\partial t} = \alpha \cdot P_r + E_i - I_{perc} - R \tag{3.2.7}$$

with the density of water ρ_w, the water content of the interception store W_i, the precipitation rate P_r, the evaporation E_i which is assumed to be at the potential rate. Runoff R from interception store as well as a distribution factor α of the interception store are also included. The parameter α depends on the ratio between actual interception store W_i and the maximum interception store content $W_{i,max}$ which is parameterized as:

$$W_{i,max} = W_{i,0}(1.0 + 5.0 \cdot f_{veg}). \tag{3.2.8}$$

The maximum capacity of this store is estimated depending on the fractional area of plants f_{veg} with $W_{i,max}$ the maximum water content of interception and snow store and $W_{i,0} = 5 \cdot 10^{-4} m$. If the water content of the interception store W_i is greater than 0, part of the water will percolate (I_{perc}) to the uppermost layer. A basic assumption of the LSP is that the interception store can only contain water if the snow store is empty and vice versa. That is, snow and interception water can not be present simultaneously and the corresponding water contents will be uniquely related to the surface temperature T_s due to $W_i = 0$ for $T_s < T_0$ and $W_{snow} = 0$ for $T_s > T_0$, where T_0 is the freezing point (Doms et al. 2005).

If the water enters the soil, the maximum infiltration rate I_{max} is given by a simplified Holtan-equation (Hillel 2004):

$$\begin{aligned} I_{max} &= 0 && : T_s \leq T_0 \\ I'_{max} &= (f_r S_{oro}[Max(0.5; f_{veg}) I_{K1}(\eta_{PV} - \eta_1)/\eta_{PV} + I_{K2}] && : T_s > T_0 \end{aligned} \tag{3.2.9}$$

The parameter f_r considers the reduction of I_{max} if soil ice exists in the uppermost layer:

$$f_r = 1 - \frac{\eta_{ice,1}}{\eta_{PV}}, \tag{3.2.10}$$

with the pore volume of the soil texture η_{PV} and the ice content of the first soil layer $\eta_{ice,1}$.

Additionally I'_{max} is limited by the available pore volume of the uppermost soil layer:

$$I_{max} = Min(I'_{max}; \frac{\eta_{PV} - \eta_1}{2\Delta t} \Delta z_1 \rho_w). \tag{3.2.11}$$

At present the influence of the sub-grid scale orographic variations is neglected ($S_{oro} = 1$). The parameter for the determination of the maximum infiltration (Eq. 3.2.9) I_{K1} and the infiltration parameter I_{K2} depend on soil texture. If percolation I_{perc} exceeds the maximum infiltration rate, a contribution to the runoff R results.

3.2.3 Soil water movement and runoff generation from soil layers

After infiltration the vertical soil water transport is driven by gravity and the capillary forces. Horizontal transport is neglected due to the coarse horizontal resolution and therefore the flux of soil water F can be written as a one-dimensional Darcy equation (e.g. Ament 2006, or Dingmann 2002)

$$F = K(\eta) + D(\eta)\frac{\partial \eta}{\partial z}. \tag{3.2.12}$$

Hydraulic conductivity K and hydraulic diffusivity D depend both on the soil moisture η, the pore volume η_{PV}, and the air dryness point η_{ADP}. The soil moisture is the ratio of water volume to soil volume which can vary in both time and space (Dingmann 2002). The pore volume η_{PV} is the proportion of pore spaces in a soil volume. The air dryness point η_{ADP} is the water content which can not be removed from the soil under natural conditions. Hydraulic conductivity K and hydraulic diffusivity D are parameterized in TERRA-ML by the exponential laws of Rijtema (1969):

$$K(\eta) = K_0 exp\left(K_1 \frac{\eta_{PV} - \eta}{\eta_{PV} - \eta_{ADP}}\right) \tag{3.2.13}$$

$$D(\eta) = D_0 exp\left(D_1 \frac{\eta_{PV} - \eta}{\eta_{PV} - \eta_{ADP}}\right) \tag{3.2.14}$$

The pore volume η_{PV} and air dryness point η_{ADP} as well as the hydraulic conductivity parameters K_1, K_0 and hydraulic diffusivity parameters D_0, D_1 depend on soil texture (for the reference table see Schrodin 1995 or Doms et al. 2005).

Runoff generated within the individual soil layers is used to generate the base flow component in TERRA-ML. Runoff from a soil layer k occurs when its total water content η_k exceeds field capacity η_{FC} and/or when the divergence of the fluxes in the layer is negative. The field capacity is the amount of soil moisture held in the soil after excess water has drained and the rate of downward movement has stopped. Thus TERRA-ML calculates runoff from one soil layer as follows:

$$R_k = -\frac{\eta_k - \eta_{FC}}{\eta_{PV} - \eta_{FC}} \left(\frac{\partial F}{\partial z}\right)_k \Delta z_k \tag{3.2.15}$$

3.3 Extensions of TERRA-ML

In one-way mode TERRA-ML allows an easier testing of parameterization approaches as well as the coupling with other models. The validation of TERRA-ML with discharge measurements which is a fundamental objective of this study requires the accurate calculation of the grid based runoff. In this study different parameterization approaches and its influences on runoff calculation are tested.

3.3.1 The replaced vertical soil water movement equations

The operational relationships for hydraulic conductivity and hydraulic diffusivity (Eq. 3.2.13; 3.2.14) as implemented in TERRA-ML are not used in most other LSP schemes. Usually relationships of e.g. Van Genuchten (1980) or Rawls et al. (1993) are preferred. The VIC (Variable Infiltration Capacity) model (Lohmann 1996) uses a formulation by Brooks and Corey (1964). TESSEL, the operational LSP of the ECMWF (European Centre for Medium-Range Weather Forecasts, documentation 2001) uses the parametric relations of Clapp and Hornberger (1978). The most meteorological models use the formulation of Campbell (1974) or Brooks and Corey (1964) due to the numerical efficiency (Braun 2002). In order to evaluate the possibly negative influence of the operational scheme on runoff generation the latter formulation by Campbell (1974) is implemented. The operational hydraulic conductivity and diffusivity are replaced as follows:

$$K(\eta) = K_0 \cdot \left(\frac{\eta}{\eta_{PV}}\right)^c, \qquad c = 2 \cdot b + 3, \tag{3.3.1}$$

$$D(\eta) = -b \cdot \eta_{ADP} \cdot K_0 \cdot^{-b-3} \cdot \eta^{b+2}. \tag{3.3.2}$$

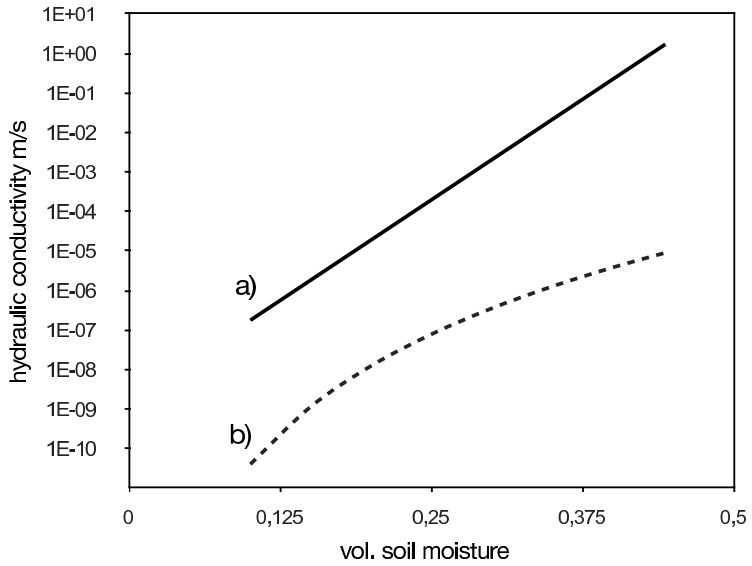

Figure 3.3: *Hydraulic conductivity of sandy loam calculated by the functions of a) Rijtema (1969) and b) Campbell (1974)*

The pore size distribution index b is now an additional parameter, which can be estimated empirically by measured soil properties (see e.g., Clapp and Hornberger 1978, or Pielke 1984).

A variation of the pore size distribution index b by Ek and Cuenca (1994) leads to a high sensitivity of the calculated heat flow. Due to this sensitivity the soil moisture distribution is modified. The changed soil moisture distribution is able to influence atmospheric conditions. Thus sensitivity indicates the importance of a correct parameterization of the vertical soil water movement. A fundamental different evolution of the calculated hydraulic conductivity during an increase of soil moisture (Fig. 3.3) provides the argument for an implementation of the formulation based on Campbell (1974). The calculation used the soil characteristics which are applied in the operational TERRA-ML (see Doms et al. 2005).

The hydraulic conductivity applied for sandy loam results in both a different pattern and different order of magnitudes. This means that the formulation of Rijtema (1969) leads to much higher values of the hydraulic conductivity as well as a curve following a strong increasing evolution. In contrast, Campbell (1974) shows an evolution of the hydraulic conductivity which increases slower with higher soil water contents. Furthermore, a comparison with the hydraulic conductivity

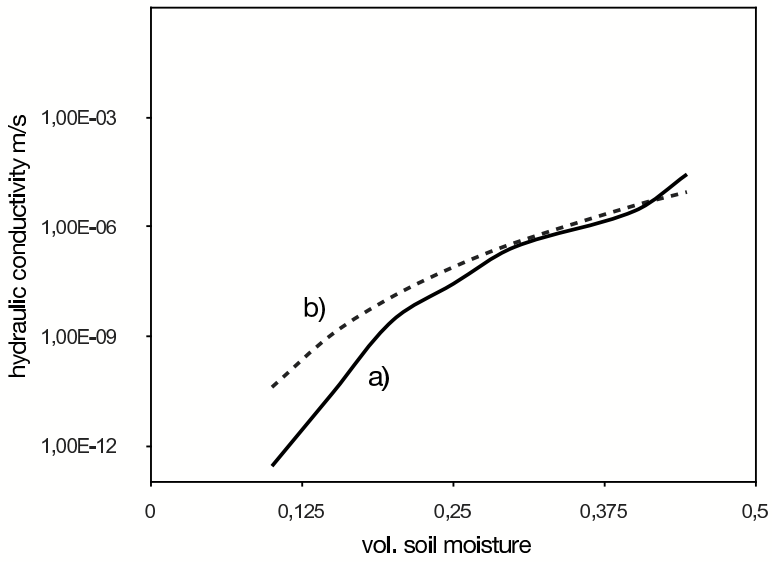

Figure 3.4: *Hydraulic conductivity of sandy loam calculated by the functions of a) van Genuchten (1980) and b) Campbell (1974)*

evolution of van Genuchten (1980), another frequently used formulation, compares well with Campbells (1974) formulation (Fig. 3.4). The introduced results motivate the objective of this study to investigate the relevance of the hydraulic conductivity on TERRA-MLs runoff generation.

3.3.2 Ground water table parameterization

With the growing recognition of ground water-atmosphere interaction as a potentially significant influence on the surface energy balance (Kollet et al. 2009), and thus on spatial and temporal weather variability, increasing attention focused on improving the process representations of sub-surface hydrology within LSP schemes. The complexity of such parameterizations ranges from multi-layer models with relatively shallow soil columns in which ground water storage is implicitly represented because of the model conserves mass to multi-layer soil columns models coupled to lumped, unconfined aquifer models (Gulden et al. 2007).

In the operational version of TERRA-ML the ground water table is practically kept constant. The lower boundary condition at the bottom of the deepest layer contains a free drainage boundary condition; i.e. soil water can drain from the lowest layer, but any upward diffusion flux from below is neglected. Thus ground

water cannot wet the soil by capillary rise. Probably due to this lower boundary condition TERRA-ML tends towards drying out in summer periods and during long-time simulations. In this study a variable ground water table is implemented into TERRA-ML to remove the drying out effects. Different approaches have been developed by various authors (e.g. Chen and Kumar 2001; Famiglietti and Wood 1994).

An often used scheme is based on the TOPMODEL approach (Beven and Kirkby 1979). TOPMODEL formulations allow for the dynamically consistent calculations of both the saturated fraction of the watershed and the base flow that supports that saturation from knowledge of the mean watershed water table depth (Stieglitz et al. 1996). TOPMODEL incorporates topographic variations using the concept of the "topographic index" $\lambda = ln(a/tan\beta)$, where a is the upstream area of a pixel that drains through the pixel and $tan\beta$ is the local surface topographic slope. Following Stieglitz et al. (1996), the sub-surface runoff in the TOPMODEL approach is expressed as:

$$R_{sb} = \frac{K_{sat}(0)}{f} e^{-\lambda_m} e^{-f\bar{z}\nabla} \tag{3.3.3}$$

where λ_m is the grid cell mean value of the topographic index. K_{sat} defines the saturated hydraulic conductivity while f represents a decay factor of K_{sat}.

Famiglietti and Wood (1994) proposed a discretized framework in which the distribution of the topographic index is disaggregated into a number of intervals, each representing a fraction of the watershed with similar water table depth and soil moisture, to parameterize the sub-grid variability in soil moisture and runoff. However, this idea leads to structural conflicts with NWP models which causes extensive computational costs. To reduce the computational costs, Stieglitz et al. (1997) coupled the analytical part of the TOPMODEL approach with a standard one-dimensional LSP.

The TOPMODEL concept was originally developed for small catchments with areas up to $10^2 km^2$ and grid cells in the range of meters (Schmitz 2005). Nevertheless the TOPMODEL approach was also used for large catchments and coarser resolutions, but leads to problems in the calculation of the topographic index and the ground water table depth. The effects are flat slopes and high values of the topographic index, which lead to a large number of grid cells with negative ground water tables. Other consequences are permanent saturation also during drier periods.

LSP schemes and the TOPMODEL approach use different definitions of the soil saturated hydraulic conductivity, K_{sat} (Niu et al. 2005). LSPs usually define K_{sat} as a function of soil texture, while TOPMODEL assumes that K_{sat} decreases with soil depth to create a water table. In TOPMODEL the soil surface value of K_{sat} is an arbitrary parameter because it is solely used to produce runoff. However, LSP use

the soil hydraulic properties to determine soil moisture, which affects evaporation and transpiration. The original derivations of the TOPMODEL sub-surface runoff (Sivapalan et al. 1987) require larger values for the soil surface K_{sat} than LSP schemes do; researchers justified the very large K_{sat} with arguments about the role of macro pores (e.g. Beven 1982).

This study uses a simplified TOPMODEL-based runoff parameterization SIMTOP that mitigates several of the problems with TOPMODEL-based runoff schemes for meteorological models. This Section describes the sub-surface runoff scheme of the SIMTOP approach which is based on the publications of Niu et al. (2005) and Gulden et al. (2007). In this study the sub-surface formulation of SIMTOP is implemented into TERRA-ML in order to improve the base flow simulation and to eliminate drying out. For completeness the determination of a variable ground water table height is needed. This parameterization is provided by a formulation of Stieglitz et al. (1997).

SIMTOP uses a maximum sub-surface runoff coefficient in place of a complex product of coefficients as used by the TOPMODEL formulation. This simplification makes the parameterized sub-surface runoff independent of the soil surface K_{sat} defined by the soil texture profile. An additional simplification is that SIMTOP represents the discrete distribution of the topographic index with an exponential function instead of a three-parameter gamma distribution function.

In SIMTOP (Niu et al. 2005), the sub-surface runoff R_{sb} is parameterized as:

$$R_{sb} = R_{sb,max} e^{-f \bar{z}\bigtriangledown} \tag{3.3.4}$$

where $R_{sb,max}$ is the maximum sub-surface runoff when the grid cell mean water table depth $\bar{z}\bigtriangledown$ is zero. The decay factor, f, can be determined through a sensitivity analysis or calibration against the hydrograph recession curve.

The simplification compared to Equation (3.3.3) avoids the difficulties in determining the surface saturated hydraulic conductivity in horizontal direction $K_{sat}(0)$ and the uncertainties that result from computing the mean topographic index λ_m with coarse digital elevation models (e. g. at a resolution of 1 km x 1 km).

To calculate the base flow according to Equation (3.3.4) the determination of the ground water table depth $\bar{z}\bigtriangledown$ is needed. The ground water table depth is the interface between the saturated and unsaturated soil. This study uses the formulation of Stieglitz et al. (1997) and selected a soil moisture levels greater than or equal to 70% of the field capacity as the defining threshold, that is:

$$\bar{z}\triangledown = zb_i \qquad \eta_i \leq 0.7\eta_{FC}$$

$$\bar{z}\triangledown = zb_i = \left(\frac{\eta_i - 0.7\eta_{FC}}{\phi - 0.7\eta_{FC}}\right)\Delta z_i \qquad \eta_i > 0.7\eta_{FC} \tag{3.3.5}$$

where zb_i is the depth of the lower boundary for the layer i, ϕ is the porosity, η_{FC} is the field capacity and η_i is the soil moisture of layer i. This means that if the first layer i starting at the bottom of the soil column corresponds to the condition $\eta_i \leq 0.7\eta_{FC}$ then it is assumed that the ground water table is located at the bottom of layer i (Fig. 3.5). Otherwise the condition $\eta_i > 0.7\eta_{FC}$ leads to the ground water table depth which is calculated with the second algorithm in equation 3.3.5.

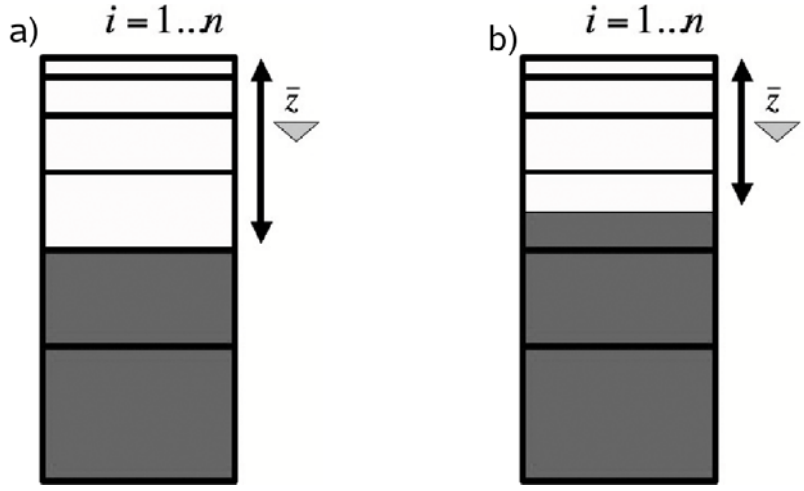

Figure 3.5: *Ground water table height (defined in text)* **a)** *for the first layer i starting at the bottom of the soil column which corresponds to the condition* $\eta_i \leq 0.7\eta_{FC}$ *is assumed that the ground water table is located at the bottom of layer i or otherwise* **b)** *the ground water table depth is calculated with the second algorithm in equation 3.3.5.*

Two major assumptions are made to derive the water table depth. The first is that by using the operational layer structure of TERRA-ML the depth of the soil column is limited to only a few meters. This assumption restricts the applicability of the approach to regions where the water table is shallower. This condition is valid for our research area (Chapter 4). The publishers of the SIMTOP approach

applied the model also on the global scale in which the condition is not achieved in all regions. In case that the water table is deeper than the model bottom, Niu et al. (2005) propose that the water table is decoupled from soil moisture but may still contribute to base flow. For such a case, a simple lumped aquifer model is suggested for the use in NWP or general circulation models (GCMs). The second assumption is that the water head throughout the soil column is at equilibrium which means that no variability of the water table height within the grid cell exits.

The operational base flow parameterization in TERRA-ML (Eq. 3.2.15) is changed by the total base flow equation (Eq. 3.3.4). This base flow is also extracted from each soil layer in which the base flow is weighted by the saturated conductivity K_{sat} of the layer times the amount of water in the layer. This means that the contribution to the total base flow, R_{sb}, by the six model layers in TERRA-ML is parameterized according to:

$$R_b, j = \left[\frac{K_{sat,j}(zb_j - \bar{z}\triangledown)}{K_{sat,j}(zb_j - \bar{z}\triangledown) + \sum_{i}^{6} K_{sat,i}\Delta z_i} \right] R_{sb} \tag{3.3.6}$$

j is the model layer that contains the ground water table and

$$R_b, i = \left[\frac{K_{sat,i}\Delta z_i}{K_{sat,j}(zb_j - \bar{z}\triangledown) + \sum_{i}^{6} K_{sat,i}\Delta z_i} \right] R_{sb} \qquad i = j+1, 6, \tag{3.3.7}$$

where the head of the ground water table is located, K_{sat} is the saturated hydraulic conductivity which is constant with the depth and Δz is the layer depth.

3.3.3 The routing scheme

Without a coupling to additional parameterizations a validation of the NWP calculated runoff with discharge measurements is difficult due to the grid based architecture of these models. Discharge measurements obtained from gauging stations on the course of a river represent the runoff integrated across the catchment. Very often in meteorological models the runoff calculated by the embedded LSP schemes disappears from the water balance immediately after being generated. Therefore, a validation is only possible by storage of the grid based calculated runoff and a

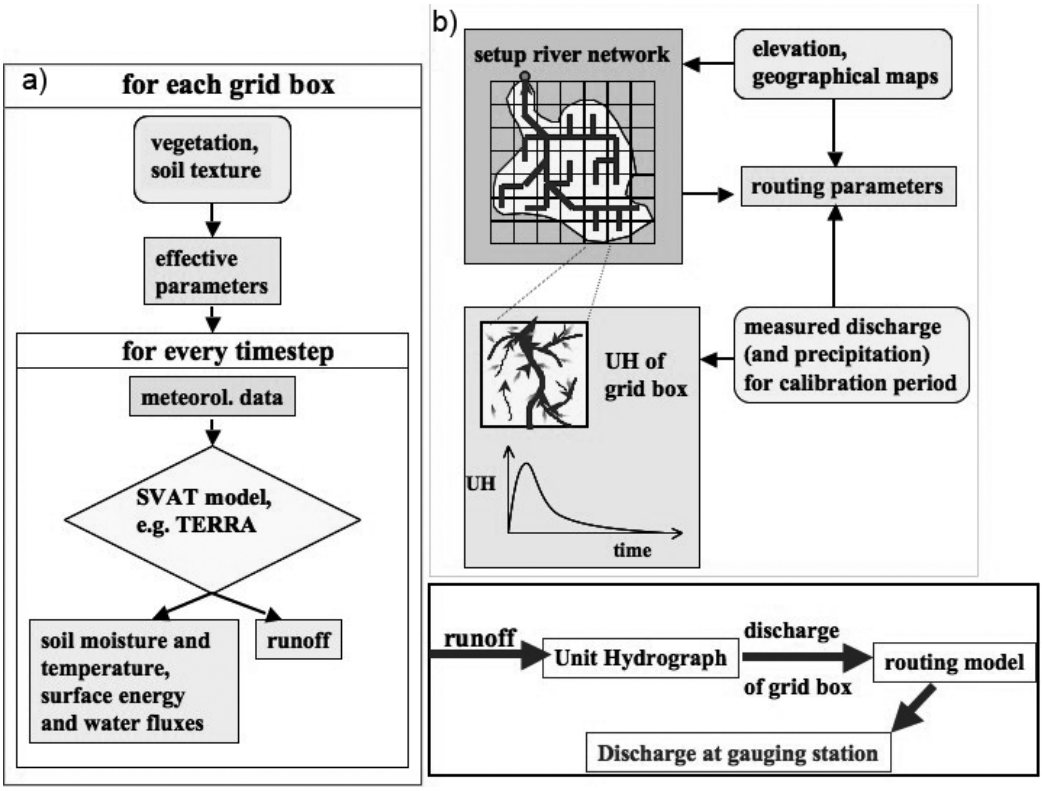

Figure 3.6: **a)** *The multi-layer LSP TERRA-ML describes exchange processes between soil, land-surface and the atmosphere. TERRA ML calculates for each grid cell the surface energy and water fluxes, soil moisture, surface and base flow by considering topography, soil texture and land use.* **b)** *The coupled routing model simulates the time runoff takes to reach the outlet of a grid cell and the water transport in the river network. For this realization the model uses impulse-response functions (Unit Hydrographs) and it is assumed that the routing process is linear, time-invariant and causal.*

transformation of runoff into discharge. This study describes a simple linear routing model for the transformation of runoff from an LSP scheme into discharge. The basic idea is based on the paper of Lohmann et al. (1996). He developed the routing model which was coupled to TERRA-ML by Warrach-Sagi et al. (2008; Fig. 3.6).

Flow routing is a mathematical procedure for predicting the changing magnitude, speed, and shape of a flood wave as a function of time i.e. the flow hydrograph at one or more points along a watercourse. The flow hydrograph can result i.e. from rainfall or snowmelt runoff, reservoir releases (spillway, gate, and turbine releases and or dam failures), landslides into reservoirs, or tides (astronomical and/or wind-generated storm surges; Fread 1993).

Table 3.1: *Approximate velocity, space and time scales for the different processes involved on horizontal water movement; the following values are only rough estimations, these process occur all simultaneously during a precipitation event (Lohmann et al. 1996)*

Processes	Velocity Scale	Space Scale	Time Scale
rivers	0.5-5 m/s	0-300 km	0-150 h
infiltration excess runoff	10-500 m/h	0-1 km	0-100 h
saturation excess runoff	0.3-100 m/h	0-2 km	0-600 h
ground water	1-10000 m/yr	0-? km	0-years

In the combined model all nonlinear processes (e.g. calculation of runoff) are included in TERRA-ML, while the horizontal transfer process from runoff into discharge is described by the routing scheme, which is based on a stable causal linear time invariant system. The theory of linear transfer functions (Lohmann et al. 1996; Box et al. 1994) assumes that the connection of two data sets of a linear system which consist of an input time series $X(t)$ and an output $Y(t)$ is linear and characterized by an impulse response function (IRF), called in hydrology unit hydrograph (UH). Therefore, the LSP scheme TERRA-ML is run for each grid cell, the runoff is then routed to the outlet of that grid cell with an internal unit hydrograph, and then added to the river routing scheme which couples all grid cells together. Once the water has left the grid cell, no re-infiltration into the soil is allowed. The river routing scheme distinguishes roughly between the in-grid-box-dynamics and the influence of the river network itself (Figure 3.6). Hydrological processes occur at a wide range of time, space, and velocity scales (see Tab. 3.1). In this approach all the travel paths are lumped together in the impulse response function.

3.3.3.1 Method details

Lohmann et al. (1996) assumes in this scheme that all horizontal routing processes within a river system behave like a causal stable, linear, time invariant system:

$$Q(t) = \int_0^\infty UH(\tau) p^{eff}(t-\tau) d\tau. \tag{3.3.8}$$

$Q(t)$ is the discharge at a gauging station and p^{eff} is the part of the precipitation which contributes to discharge. It is always assumed that the precipitation has fallen uniformly, which of course does not hold for convective precipitation. $UH(t)$ is the impulse response function with the condition $\int_0^\infty UH(t)dt = 1$.

Table 3.1 shows that the response to a precipitation event can cover a large range of time scales. A separation of the time scales into a slow and a fast component with a linear model approach is necessary and e.g. proposed by Rodriguez (1989). His approach can be written as a first-order differential equation:

$$\frac{dQ^S(t)}{dt} = -k \cdot Q^S(t) + b \cdot Q^F(t) \tag{3.3.9}$$

where the total discharge

$$Q(t) = Q^S(t) + Q^F(t) \tag{3.3.10}$$

is the sum of slow flow $Q^S(t)$ and fast flow $Q^F(t)$. The parameters k and b are constant over the period of calculation. Equation 3.3.9 is sort of a lowpass frequency filter (Press et al. 1992) transforming measured discharge $Q(t)$ into a fast flow and a slow flow component. Averaging both sides of equation 3.3.9 in time shows that the fraction of water flow in slow component to the water flow in fast component is given by

$$\frac{b}{k} = \frac{water\ \ in\ \ slow\ \ flow}{water\ \ in\ \ fast\ \ flow} \tag{3.3.11}$$

The parameter k can be estimated using regression analysis of the measured discharge $Q(t)$ in periods without and with small fast flow. It determines how fast the linear slow flow storage decreases if there is no or only small input from the fast component. The higher the values of k the smaller is the half time decay $ln(2)/k$ of the slow flow storage. The parameter b can be fitted using the condition $Q(t) - Q^S(t) \geq 0 \forall t$, as the slow flow component is never allowed to exceed the total flow. The higher it is the more water is in the slow flow component.

Assuming that there is an impulse response function $UH^F(t)$ for the fast component, $UH(t)$ can be written as the sum of the impulse response functions for the fast and the slow components

$$UH(t) = UH^F(t) + UH^S(t) \tag{3.3.12}$$

Having estimated the two parameters of the slow flow model from measured data (Eq. 3.3.9), it is possible to compute the fast impulse response function $UH^F(t)$ and the precipitation p^{eff} which contributes to the discharge. This is provided by solving the following iterative scheme (Eq. 3.3.13 - 3.3.16) with a least squares solution, starting with p^{eff} being the precipitation at time i:

If there are n data points of precipitation and if $(m-i)*$ time step is the assumed length t_{max} of the fast flow impulse response function, the equation

$$Q(t) = \int_0^\infty UH(\tau) p^{eff}(t-\tau) d\tau \tag{3.3.13}$$

can be written for the discrete case as

$$\begin{pmatrix} Q_m^F \\ \vdots \\ Q_n^F \end{pmatrix} = \begin{pmatrix} p_m^{eff} & \cdots & p_1^{eff} \\ \vdots & \ddots & \vdots \\ p_n^{eff} & \cdots & p_{n-m+1}^{eff} \end{pmatrix} \times \begin{pmatrix} UH_0^F \\ \vdots \\ UH_{m-1}^F \end{pmatrix} \tag{3.3.14}$$

for the calculation of UH_i^F. In the discrete case UH^F already includes the time step Δt. After each calculation the following constraint is applied:

$$\sum_{i=0}^{m-1} UH_i^F = \frac{1}{1+b/k} \qquad with \qquad UH_i^F \geq 0 \quad \forall i, \tag{3.3.15}$$

which follows from the fixed fraction of the water in the fast and slow component, the fact that $\int_0^\infty UH(t)dt = 1$ and the non-negativeness of $UH(t)$. UH^F is then put into the following matrix which is solved for p^{eff}:

$$\begin{pmatrix} Q_m^F \\ \vdots \\ \vdots \\ Q_n^F \end{pmatrix} = \begin{pmatrix} UH_{m-1}^F & \cdots & UH_0^F & 0 & \cdots & 0 \\ 0 & \ddots & \ddots & \ddots & \ddots & \vdots \\ \vdots & \ddots & \ddots & \ddots & \ddots & 0 \\ 0 & \cdots & 0 & UH_{m-1}^F & \cdots & UH_0^F \end{pmatrix} \times \begin{pmatrix} p_1^{eff} \\ \vdots \\ \vdots \\ p_n^{eff} \end{pmatrix} \tag{3.3.16}$$

Again, after each iteration, the constraint

$$0 \leq p_i^{eff} \leq precipitation \quad \forall i \tag{3.3.17}$$

is applied to p_i^{eff}, which afterwards is put into equation 3.3.14 for the next iteration.

According to Lohmann (1996), the difference to other schemes (e.g. Duband et al. 1993) is that this method does not use several single precipitation events, but long data series of precipitation and discharge. This is necessary due to the strong varying base flow component and the overlapping of precipitation events.

The routing model has some limitations. An important one is that the whole transport process is formulated as a linear system with homogeneous precipitation because it is difficult to find a transfer function without that assumption. Another limitation is the fixed relation of the fast flow to the slow flow. The coefficients k and b, as the UH^F itself, must be seen as lumped parameters, as the surface is heterogeneous. UH^F reflects a three dimensional water transport process, while the formulation is only one dimensional.

3.3.3.2 The river routing in TERRA-ML

The river network in the study area is constructed with the same spatial resolution as the atmospheric model. The routing scheme requires a flow direction for each grid cell as input within the Sieg catchment. This information is computed from the digital elevation model with the help of SAGA a geographic information system (GIS; source: www.saga-gis.uni-goettingen.de). The direction of the maximum hill slope of each grid box determines the flow direction for drainage. The lines in Fig. 3.7 reflect the main flow directions of the natural streams.

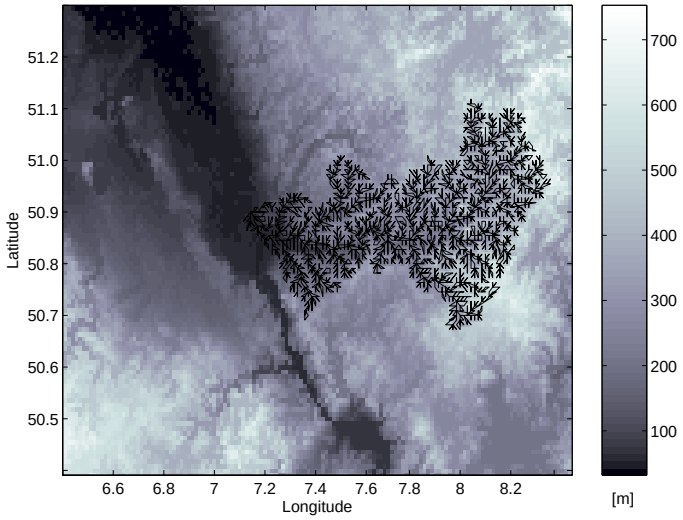

Figure 3.7: *Model domain topography in 1 kilometer spatial resolution. The grid cells in the Sieg catchment are shown with the directions of horizontal transport processes.*

While the sub-grid dynamics of the horizontal routing process are described with a transfer function model, the water transported out of the grid box through other grid boxes is modeled with a simple linear river routing model. This implicitly assumes that water is not transported out of a grid box with processes other than the river flow. River routing within the model is done with a linearized Saint-Venant equation (Mesa and Mifflin 1986; Fread 1993).

$$\frac{\partial Q}{\partial t} = D\frac{\partial^2 Q}{\partial x^2} - C\frac{\partial Q}{\partial x} \tag{3.3.18}$$

The parameters C and D can be found from measurements or by estimation from geographical data of the river bed. Wave velocity C and diffusivity D are only

effective parameters, because there is often more than one river in a grid cell and human made changes also influence these values. When these influences get too strong, equation 3.3.18 cannot describe the processes in the river system.

Chapter 4

Study area, forcing and validation data

This Chapter introduces the study area and discharge observations which are necessary for the evaluation of the extended TERRA-ML model. In addition, all driving parameters are introduced including the observed precipitation. The one-way mode of TERRA-ML allows to use a higher spatial resolution compared to the operational fully coupled NWP-system in which the computational costs have to be taken into account. The extended TERRA-ML is run with a spatial resolution of 1 km x 1 km for a total area of 142 km x 101 km. The resolution of the operational COSMO NWP system is either 7 km x 7 km (COSMO-EU) or 2.8 km x 2.8 km (COSMO-DE; since April 2007). Therefore, a set of adjusted input parameters consistent of invariant soil field and meteorological forcing are needed.

4.1 Study area

The model system is applied to the river Sieg, a tributary of the Rhine (Fig. 4.1). Its catchment has a north-south dimension of approx. 60 km and an east-west dimension of approx. 85 km and covers an area of 2.832 km^2 (Fig. 4.2). The largest part of the Sieg catchment is located in the federal state of North Rhine-Westphalia; a small part of 642 km^2 is located in Rhineland-Palatinate and Hesse. The region is characterized by a low mountain range in the middle and eastern parts and lowlands in the western parts near the Rhine. Elevations vary from about 50 m above sea level close to the river corridor to 606 m at the Rothaargebirge in the east (see Fig. 4.2). The river Sieg has an overall length of 155.2 km and is feed by several tributaries. The average discharge for the time 1965 - 1998 amounts to 52.1

Figure 4.1: *The left picture shows the gauging house of station Menden and the right picture the river Sieg on the underflow located near to the river Rhine (source of pictures: www.lds.nrw.de).*

m^3/s at the gauging station Menden, which is located on the lower reaches of the river Sieg. Discharge varied between 6.18 m^3/s and 570 m^3/s during low and high water conditions. The river Agger is the largest tributary for the river Sieg with a catchment size of 805 km^2.

The average annual precipitation in the catchment ranges from 600 to 1100 mm (Ministry of the environment, conservation, agriculture and consumer protection NRW 2004) with increasing values from the lower reaches of the river in the west to the headwaters in the east. Current land use is dominated by forestry (47.5%), and pasture (29.9%). Agriculture amounts in total to 7.4% and is concentrated in the eastern part of the catchment (Busche and Diekkrüger 2005; Ministry of the Environment and Conservation, Agriculture and Consumer Protection 2004; see Fig. 4.3). Urban areas cover 8.6% while the fraction of industrial real estate amounts to 1.7%. The soil texture is dominated by silt and silty loam (73%; Schmitz 2005).

4.2 Model parameters and initial values

The applied grid spacing of 1 km x 1 km covers an area of 142 km x 101 km. Earlier studies with the LSP TOPLATS showed that a higher spatial resolution in combination with more detailed soil information (e.g. soil texture) improves the soil moisture calculation and the runoff simulation (e.g. Schmitz 2005).

The high spatial resolution requires an adjustment of the invariant soil parameters provided by the operational TERRA-ML (Tab. 4.1). These parameters are used as constant information during the calculations.

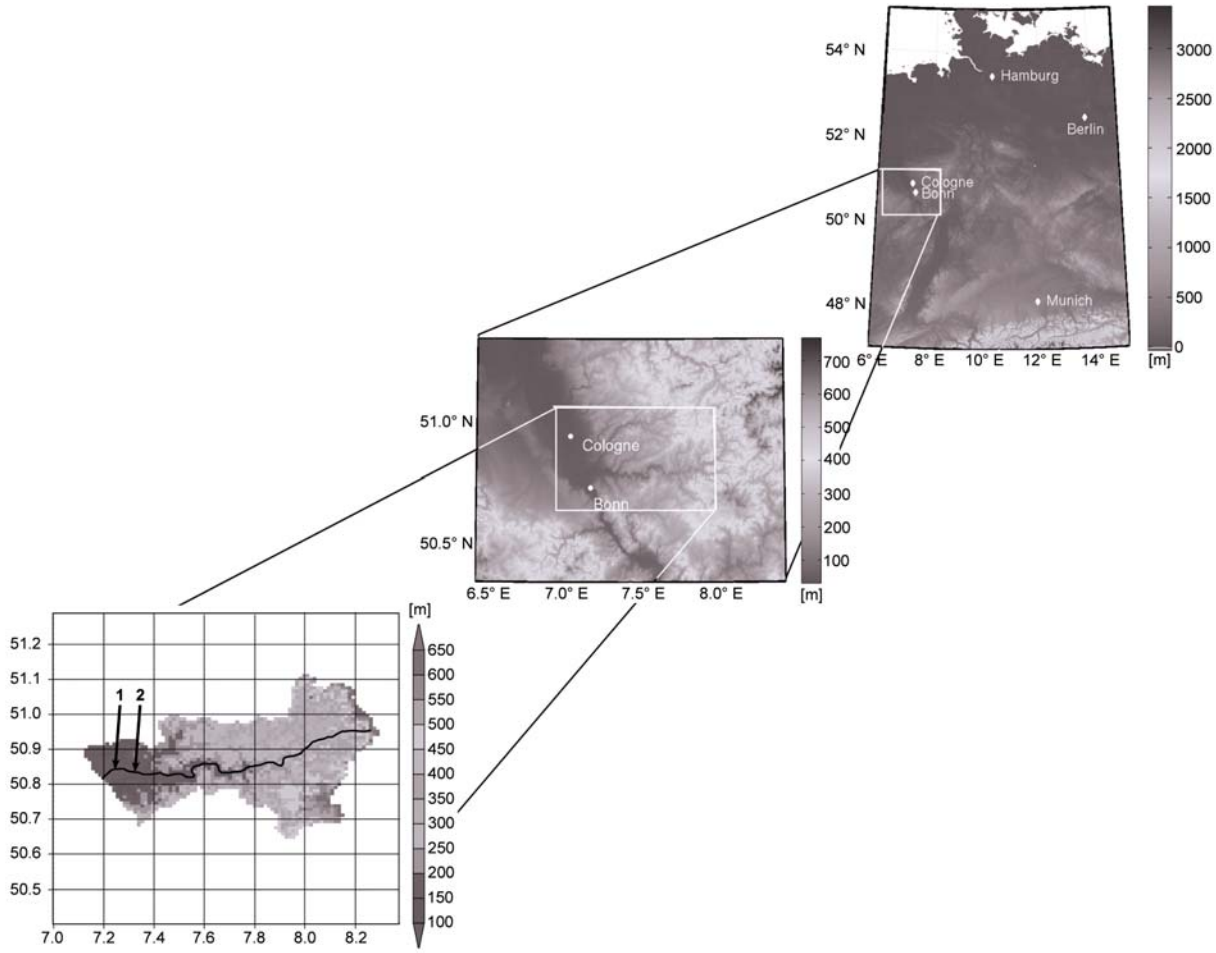

Figure 4.2: **a)** *Location and elevation (m) of* **b)** *the model domain and* **c)** *the Sieg river catchment in Western Germany (geographical coordinates in degree), arrow one denotes the location of gauging station Menden and arrow two gauging station Siegburg-Kaldauen.*

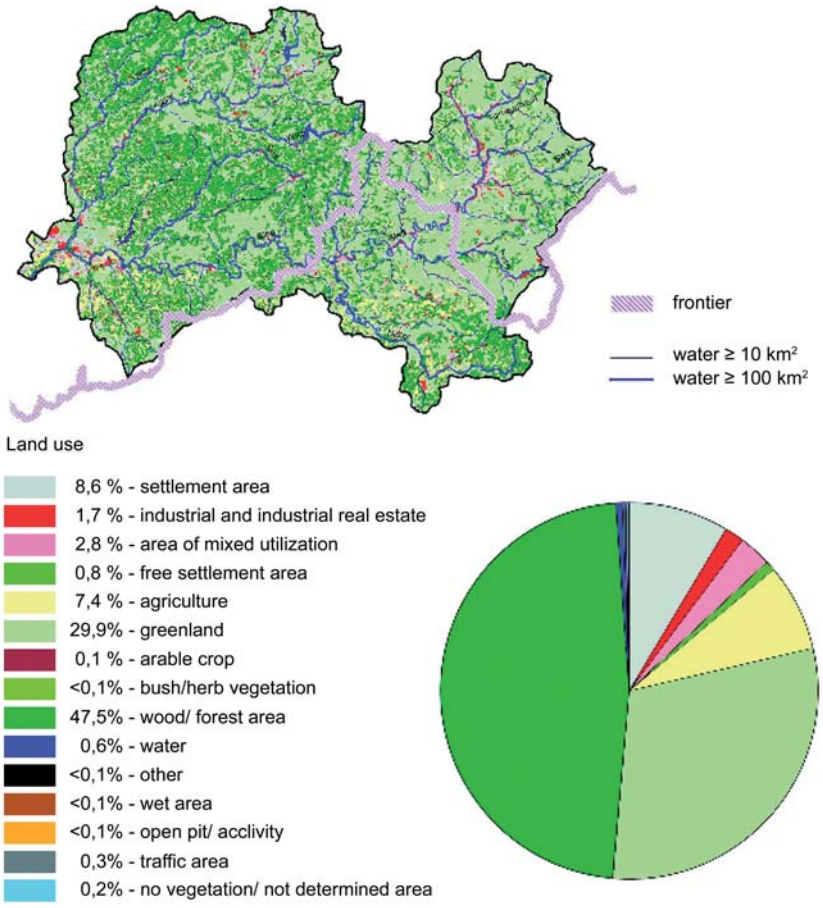

Figure 4.3: Land use for the Sieg river catchment (with Agger catchment) Source: Ergebnisbericht Sieg - Ministry of Environment, Conservation, Agriculture and Consumer Protection NRW

The surface elevation is adopted from the NASA-SRTM (Shuttle Radar Topography Mission, Farr et al. 2007) data set. The vegetation parameters are based on the CORINE Land Cover (CLC) data set (EEA, 2000) using a reference table for roughness length, plant cover, leaf area index, and root depth (Tab. 4.2). The CLC data set is derived from satellite observations and provided in a spatial resolution of approximately 100 m. For TERRA-ML a CLC data set is created with a spatial resolution of 1000 m. This is obtained using a GIS by selecting the most frequent vegetation parameter within the 1 km x 1 km TERRA-ML grid cell. Except for roughness length and rooting depth, all vegetation related parameters such as plant cover and leaf area index vary seasonally.

For the calculation of the soil processes TERRA-ML needs additional information of the pore volume, field capacity and hydraulic conductivity. These soil character-

Table 4.1: *Invariant soil fields for TERRA-ML*

Variable	Data set	Annotation
Topography	NASA-SRTM	elevation in meter
Soil texture	BK 50	ten classes
Plant cover min/max Leaf area index min/max	CORINE	minimum of plant cover in winter, maximum plant cover during the vegetation period
Root depth	CORINE	in meter
Roughness length	CORINE	in meter

istics depend strongly on soil texture. The operational soil texture in TERRA-ML is based on the global DSMW data set (Digital Soil MAP of the World) provided by the FAO (Food and Agricultural Organisation of UNO). The spatial resolution is quite coarse (5 arc minutes, appr. 10 km), and only 5 classes of soil texture are distinguished. This study uses the BK 50 data set provided by the geological state office of North Rhine-Westphalia and Rhineland-Palatinate for the Sieg catchment and its surrounding area, which allows us to use 10 classes of soil texture. Figure 4.4 represents the DSMW 10 km data set and in comparison the implemented 1 km BK 50 data set.

Table 4.2: *Look-up table of land-use dependent vegetation parameters adopted from the operational table of DWD*

Variable	town	grass	crop	shrub	Decid. forest	Confi. forest	Mixed forest
Roughness length (m) z_0	1.0	0.03	0.1	0.1	1.0	1.0	1.0
Plant cover f_{veg} min/max	0.05/0.1	1/1	0.5/1	0.1/0.5	1/1	0.5/1	0.5/1
LAI f_{LAI} min/max	0.1/4	0.5/4	0.2/4	0.1/3	0/6	8/8	2.25/7
Root depth (m) z_{root}	0.3	0.15	0.3	0.4	0.8	0.8	0.8

The routing scheme requires a flow direction in 1 km resolution for each grid cell within the Sieg catchment as input. This information is also derived by a GIS and based on the NASA-SRTM elevation model.

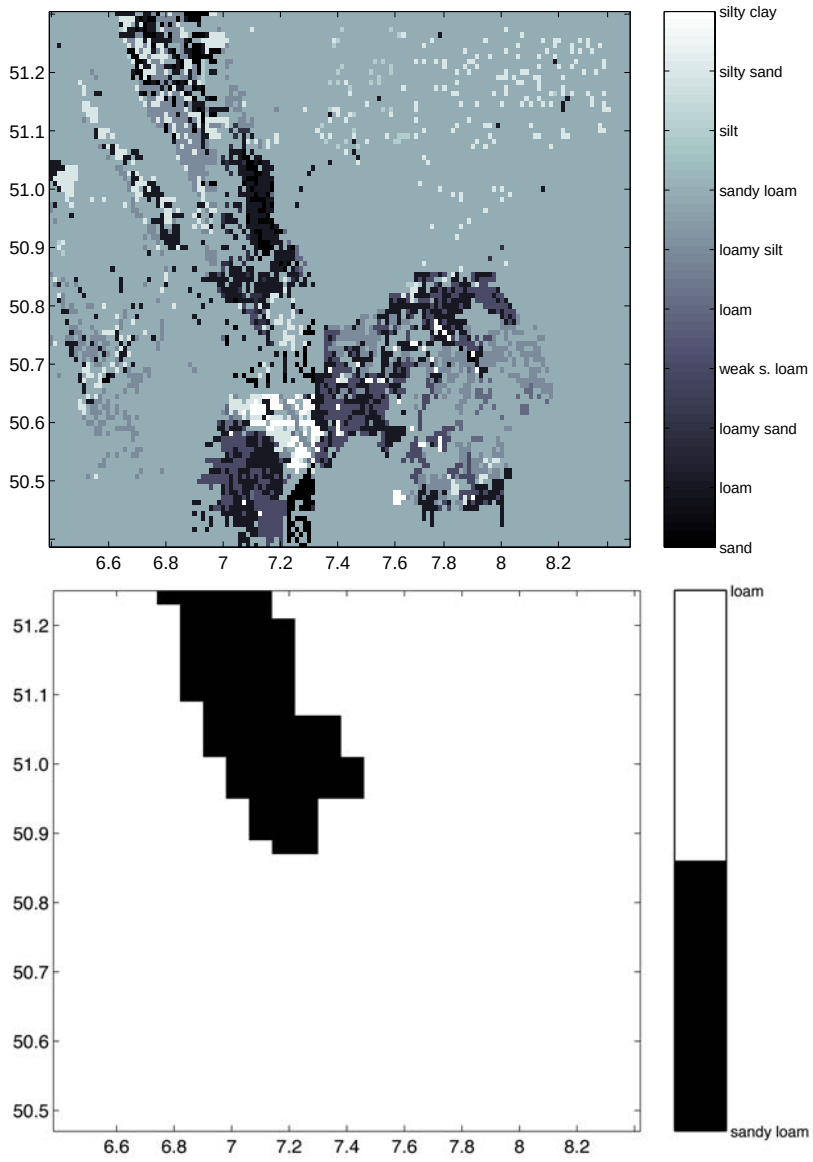

Figure 4.4: *New soil characteristics (BK 50, top) for the model domain in comparison with the information of the FAO (Food and Agricultural Organisation of UNO) data set (bottom)*

4.3 COSMO analysis data

Due to the restricted availability of measurements in high temporal and spatial resolutions in the study area the extended TERRA-ML is forced with the COSMO analysis data. The development of high resolution rainfall products at the DWD enables, however, the use of high resolution data (see next Section). The COSMO-analysis data are derived from nudging-assimilation runs of the COSMO system at DWD. This assures, that model values are continuously drawn towards the observed values during the forward integration of the model (Schraff and Hess 2003). The forcing data comprise incoming short- and long wave radiation and screen-level (2 m) temperature, specific humidity, wind and pressure. Observed 2 m-temperature and 10 m-wind speed compare reasonably to the interpolated COSMO analysis for the SYNOP-station Cologne/Bonn (Fig. 4.5). There are, however, noticeable underestimations of the maximum and minimum temperature by the COSMO analysis as well as some deviations of the 10 m-wind speed during high wind speed situations. The reason is the spatial resolution in which the model determines the 2 m-temperature and the 10 m-wind speed. Since the COSMO-analysis data produces grid based values in resolutions of 7 km x 7 km. In addition, the 2 m-temperature and 10 m-wind speed represent diagnostic values which are derived from prognostic values of the COSMO model. For example, the determination of the 2-m temperature depends on the interaction of the humidity at the surface and the first atmospheric model level (Section 3.2.1 and Eq. 3.2.5). Earlier studies show uncertainties of the 2-m temperature determination (e.g. Ament 2006). Nevertheless, the often marginal deviations between assimilation data and measurements legitimate the forcing of TERRA-ML with these data.

4.4 Precipitation forcing

The successful prediction of discharge with TERRA-ML depends on the quality of the precipitation input. This study uses the RADOLAN RW (Radar Online Calibration) product due to the still insufficient quality of NWP generated precipitation for hydrological purposes. The radar based rainfall product RADOLAN RW, an operational product by DWD designed for the use in high quality precipitation nowcasting. The product is available since March 2005. The hourly data set is based on a quality controlled radar composite created from 16 German radar sites (Fig. 4.6) and adjusted to online available rain gauge observations. Different adjustments and weighting procedures are combined to give optimal results when compared to the rain gauge observations. RADOLAN RW takes only about 500 at least hourly recording rain gauges suitable for online calibration into account. In case of strong precipitation events up to 800 additional rain gauges can be included

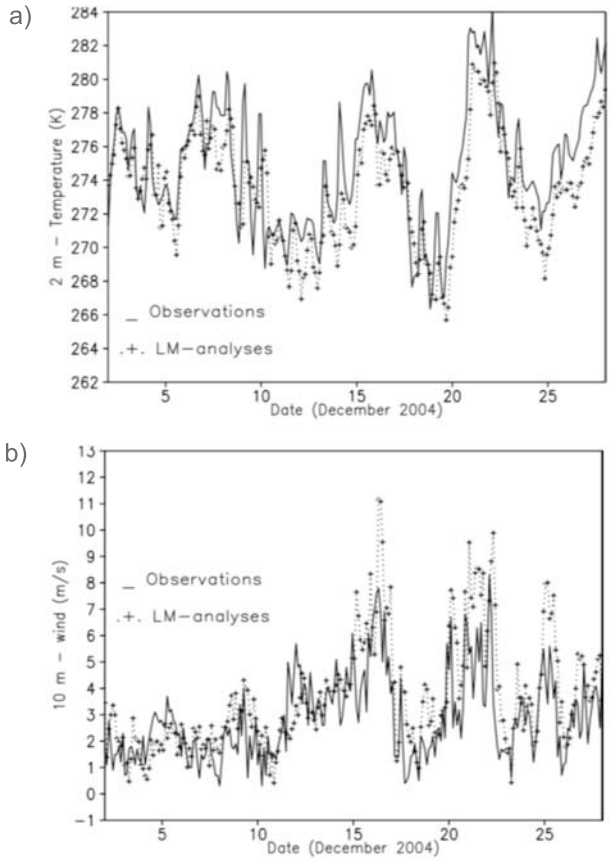

Figure 4.5: **a)** *2 m-temperature observed (solid curve) in comparison with the COSMO-analysis data (dotted/crosses curve) for SYNOP-station airport Cologne-Bonn of December 2004 with a temporal resolution of 3 hours.* **b)** *The same for 10m-wind speed.*

in the analysis. For the Sieg catchment there are up to 8 online-recording rain gauge available for adjustment.

A disadvantage of RADOLAN RW is the calibration with a low number of rain gauge measurements in the Sieg catchment which can influences the quality of the product. In an earlier study the REGNIE data set was used, a gridded 1 km x 1 km daily precipitation product of the DWD based on rain gauge observations covering Germany, for the simulation of discharge. The objective was to upscale the radar based rainfall product RADOLAN RW with rain gauge measurements. The study showed, however, only a marginal improvement of the discharge prediction thus we come to the conclusion that the radar based rainfall product calibrated with a larger density of high temporal resolution observations is able to improve the discharge prediction. In addition, the study showed that the parameterization

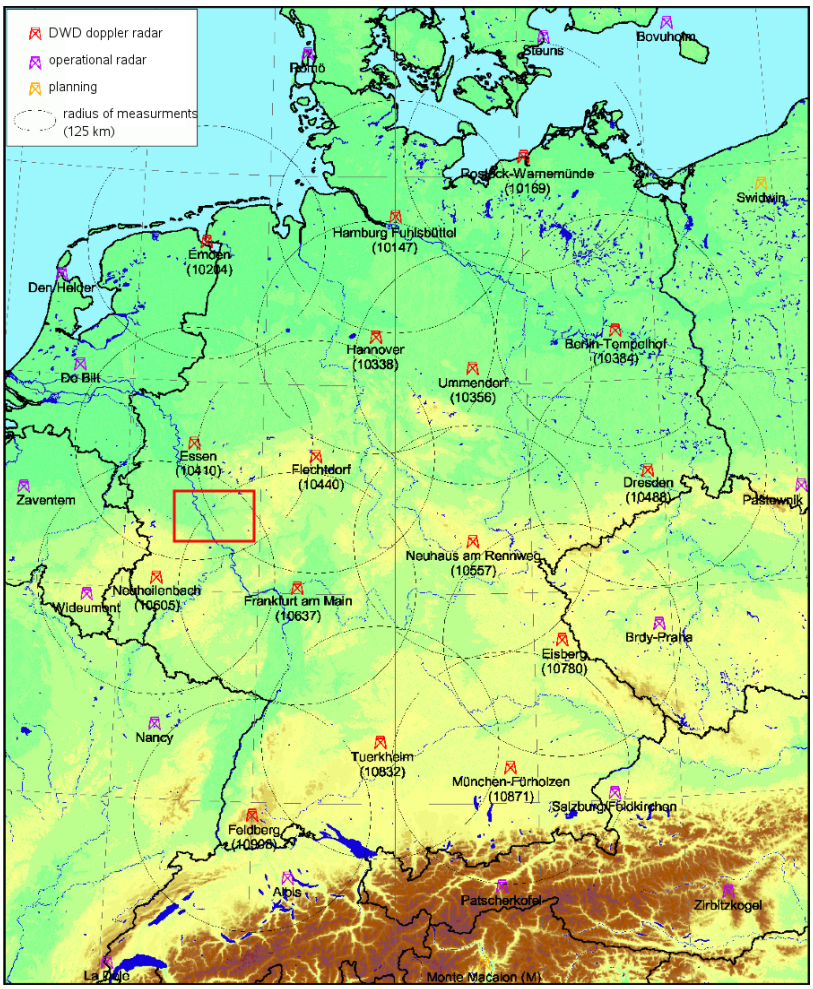

Figure 4.6: *The DWD radar network, the red marked area represents the study area.*

deficits in the LSP have a stronger influence on the simulated discharge and the model performance than the difference in precipitation data (Graßelt et al. 2008).

4.5 Discharge observations

In this study the simulated discharge is compared with the observations in order to evaluate the predictive quality of the the extended model system. The simulated discharge is compared with measurements of the gauging stations Menden and Siegburg-Kaldauen along the lower reaches of the river (Fig. 4.2). Data are available every 15 minutes; the study uses 30 minutes averages for comparison. Discharge

at both stations is measured with both current-meter (Baumgartner and Liebscher 1990) and Acoustic Doppler Current Profiler (Shields and Rigby 2005). The latter principle is more reliable for water levels above 70 cm while the prior method is applied for lower water levels. A current meter contains a rotating element whose speed of rotation is proportional to the water velocity. The expected errors are 5% for the current-meter method and 3% for the Acoustic Doppler Current Profiler (source: personal communication Johann Peters, Ministry for the Nature, Environment and Consumer Protection North Rhine-Westphalia).

An evaluation of the calculated discharge requires accurate measurements. To this purpose the measured discharge is evaluated by direct comparison with RADOLAN RW for two time periods in 2005 (Fig. 4.7) and 2006/2007 (Fig. 4.8).

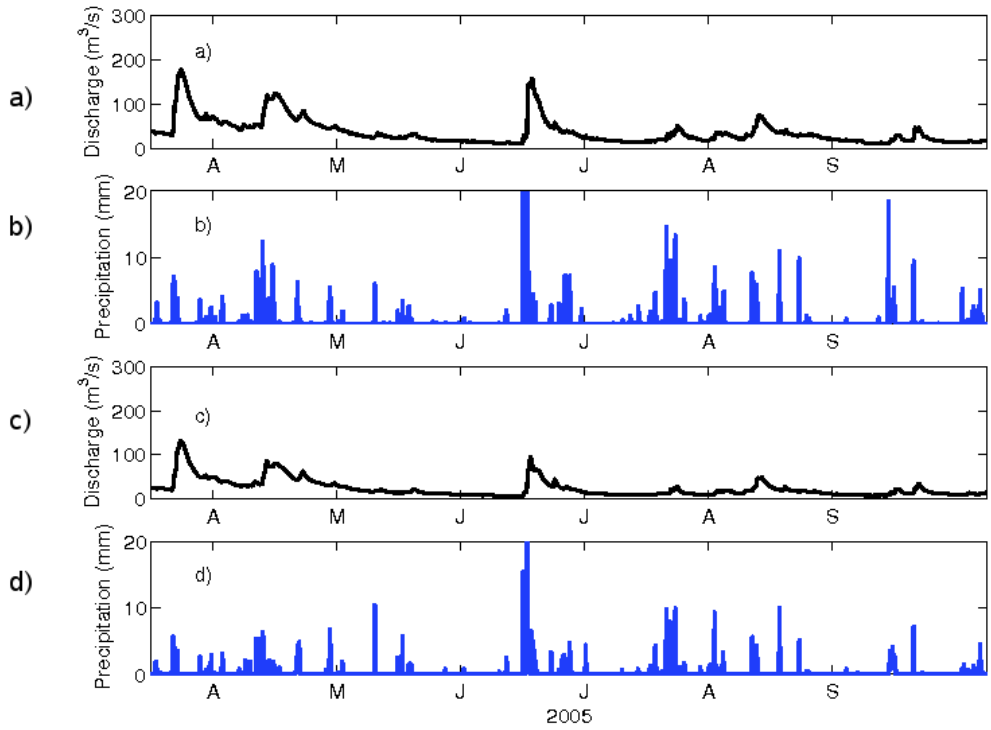

Figure 4.7: **a)** *Discharge* (m^3/s) *measured at gauging station Menden -3h averages for the time April - September 2005,* **b)** *precipitation data (mm) based on RADOLAN RW at gauging station Menden -3h averages,* **c and d)** *the same for gauging station Siegburg-Kaldauen.*

The measured discharge shows hydrographs with a short temporal delay during a strong precipitation event e.g. in the time period 2005 between June and July. During drier periods without higher precipitation events the measured discharge

shows in nearly all cases no significant hydrographs. For example, the time period in 2006/2007 between October and December indicates only small precipitation events and therefore only marginal peaks in the evolution of discharge. A similar result shows the measured discharge in the time period 2005 between May and June. In the winter months (December, January, Febuary; Fig. 4.8a,b) an overall higher discharge is represented. The reason is the typically saturated soil condition and

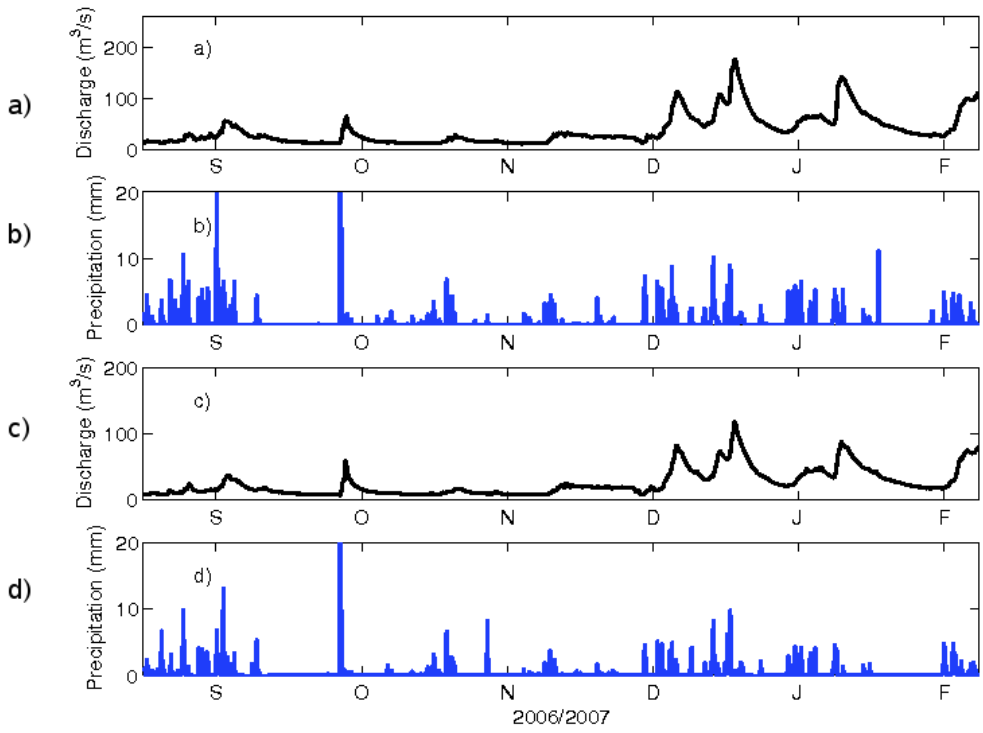

Figure 4.8: **a)** *Dischage* (m^3/s) *measured at gauging station Menden -3h averages for the time September 2006 - Febuary 2007,* **b)** *precipitation (mm) based on RADOLAN RW at gauging station Menden -3h averages,* **c and d)** *the same for gauging station Siegburg-Kaldauen.*

therefore higher surface runoff. In addition, stratiform rainfall leads to an increase of the measured discharge during this time period.

Both gauging stations indicate similar discharge measurements. Most differences occur during the summer period in 2005. The reason is the location of gauging station Menden at the confluence with the river Rhine which shows higher measured discharge compared to gauging station Siegburg-Kaldauen.

Chapter 5

Model Validation

This Chapter describes the validation of TERRA-ML and its extensions with discharge measurements. In the first Section the influence of the operational and the newly implemented vertical soil water formulation on runoff generation is evaluated. This investigation uses the version of TERRA-ML coupled to the routing scheme, called TERRA-R in this Chapter. In the second Section the results of the simulated discharge of TERRA-R-SIMTOP are shown. TERRA-R-SIMTOP is coupled to the routing scheme and uses the newly implemented variable ground water table parameterization SIMTOP. The last Section shows a statistical evaluation of the model system TERRA-R-SIMTOP.

5.1 Evaluation of the vertical soil water movement

The quality of the model runs are evaluated by employing the "Model Efficiency" diagnostic ME. This approach was proposed by Janssen and Heuberger (1995) and has the objective to compare model predictions with observations quantitatively. ME is a measure of the models ability to simulate the observed runoff amplitudes. The ME is determined via

$$ME = \frac{\left[\sum_{i=1}^{N}(O_i - \bar{O})^2 - \sum_{i=1}^{N}(S_i - O_i)^2\right]}{\left[\sum_{i=1}^{N}(O_i - \bar{O})^2\right]} \tag{5.1.1}$$

N denotes the total length of the data set. O_i and S_i denote the observed and simulated value at time i, respectively, and $\bar{O}$ is the observed mean value.

The ME quantifies the relative improvement of the employed model over the 'nominal' or 'bench-mark' situation, namely to the mean of observations $\bar{O}$. Different from the correlation coefficient, the ME indicates high model quality only if the long-term average discharge is captured well. The feature for which the improvement is studied is the variation in the model residuals $O_i - S_i$ or $O_i - \bar{O}$. Any positive value of ME can be interpreted as improvement over the 'nominal' situation $\bar{O}$; the closer to +1 the better. (Janssen and Heuberger 1995). Therefore, the ME ranges from one to infinite negative values.

ME is computed to estimate the influence of the new vertical soil water movement formulation on runoff generation. Hence, the model performance of TERRA-R with the vertical soil water parameterization based on Campbell (1974) is investigated. The results of the runs with TERRA-R are compared with observations at the two gauging stations situated at the lower reaches of the river Sieg. For the summer period 2005 the model runs are initialized with saturated soil conditions.

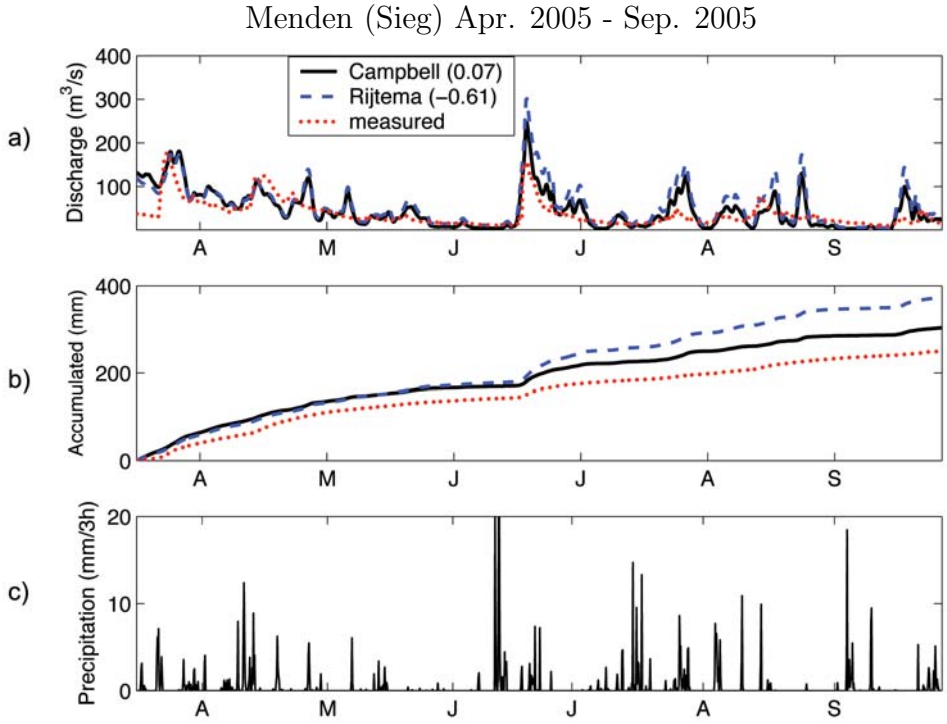

Figure 5.1: *Discharge for gauging station Menden (01.04.05 - 30.09.05) in m^3/s - 3h averages.* **a)** *The solid curve represents the parameterization by Campbell (1974), the dashed curve the parameterization by Rijtema (1969), and the dotted curve represents measured discharge;* **b)** *Accumulated discharge - 3h averages converted in mm.* **c)** *Areal precipitation by RADOLAN RW.*

The simulation for gauging station Menden (Fig. 5.1) with the hourly RADOLAN RW data set resulted in a better model performance for the Campbell (ME= 0.07) formulas compared to Rijtema (ME= -0.61). The evolution of discharge (Fig. 5.1a) represents an overall realistic simulation for both vertical soil water parameterizations between April and June. The modeled accumulated discharge (Fig. 5.1b) shows a good accordance of both formulations compared to measurements with only small overestimations until the first large discharge peak in July. Afterwards, the hydrograph (Fig. 5.1a) indicates discharge peaks which are often strongly overestimated particularly for Rijtema (1969). These higher values are also indicated in the accumulated discharge (Fig. 5.1b) in July, August, and September. Rijtema (1969) simulates 123 mm more discharge compared with measurements and 60 mm more compared to the formulation of Campbell (1974). The strong decrease in base flow is obtained with both applied vertical soil water formulations. Therefore, the newly implemented approach of Campbell (1974) is not able to remedy the drying out and to eliminate this parameterization deficit.

The results of gauging station Siegburg-Kaldauen (Fig. 5.2a) are similar to those obtained for Menden. The ME are low for both parameterizations (ME= -1.27 for Campbell (1974) and ME= -2.97 for Rijtema (1969)). The simulated discharge is overestimated during the total model run in which the operational formulation following Rijtema (1969) shows higher hydrographs during strong precipitation events. Therefore, the accumulated discharge (Fig. 5.2b) of both vertical soil water formulations is also overestimated during the total model run. The deviation between accumulated discharge and measurements amounts up to 106 mm for the Campbell (1974) parameterization and 173 mm for Rijtema (1969). Drying out is also observed and suggests that the decrease in base flow is caused by a parameterization deficit in TERRA-R.

Soil moisture and the latent heat flux (LHFL) are important parameters both influencing the determination of various values in the atmospheric part of the NWP model e.g. 2 m-temperature (Section 3.2.1). The evolution of both parameters are important in terms of a two-way coupling of the model system in later studies. A modified flux transfer from surface to atmosphere is able to influence the atmospheric conditions. Moreover, the development of the LHFL and the soil moisture can help to understand the overestimation of discharge as well as the drying out during the simulation.

TERRA-R determines the LHFL by using the evapotranspiration in the hydrological section of the LSP (Eq. 3.2.6). The influence of the vertical soil water movement on the LHFL as calculated by TERRA-R is shown by a scatter plot (Fig. 5.3). The diagram compares both formulations for the grid point of gauging station Menden.

The parameterizations of Rijtema (1969) and Campbell (1974) have obviously

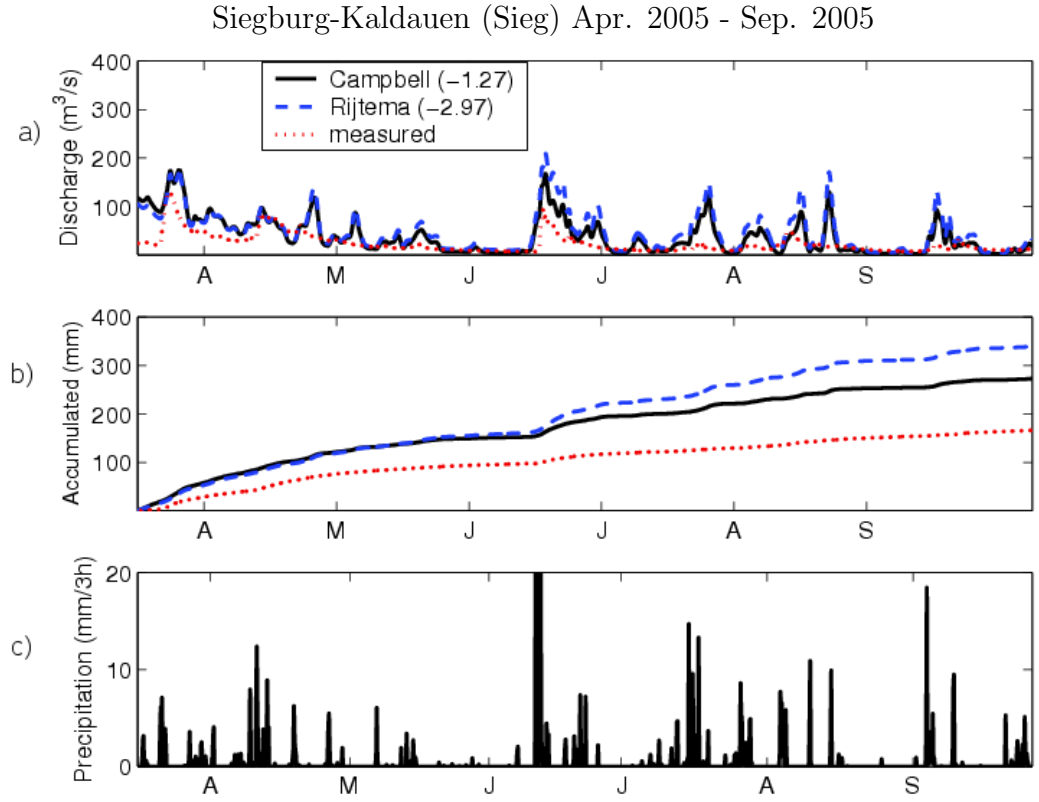

Figure 5.2: *Discharge for gauging station Siegburg-Kaldauen (01.04.05 - 30.09.05) in m^3/s - 3h averages.***a)** *The solid curve represents the parameterization by Campbell (1974), the dashed curve the parameterization by Rijtema (1969), and the dotted curve represents measured discharge;* **b)** *Accumulated discharge - 3h averages converted in mm.* **c)** *Areal precipitation by RADOLAN RW.*

very similar effects on LHFL. The marginal better model performance on the simulated discharge for the Campbell (1974) approach does not lead to a significant modification of LHFL. This means that in case of a two-way coupling the modified vertical soil water movement has marginal influence on the determination of the flux transfer.

In contrast to LHFL, the soil moisture distribution is differently affected by both vertical soil water formulations (Fig. 5.4). The simulations are again given for the grid point of Menden. The figure shows the total soil moisture content for the upper layers 1 - 4 (thickness 0.27 m) and lower layers 5 - 6 (2.16 m). A fast saturation of water in the first layers implies a higher surface runoff and therefore a higher hydrograph and less water for filling the soil water storage. The vertical soil water parameterization interacts with the soil moisture content (Eq. 3.2.12), thus the distribution of soil moisture will change using the alternative approaches. Over-

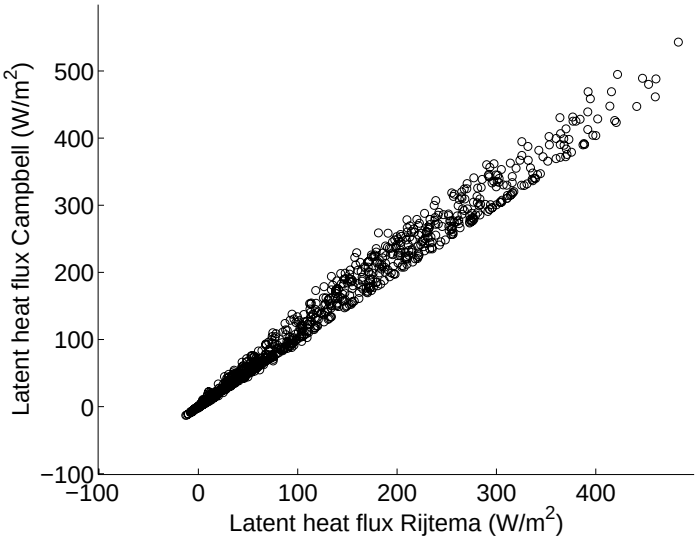

Figure 5.3: *Latent heat flux calculated by TERRA-ML including parameterization by Campbell (1974) and Rijtema (1969)*

all, smaller soil water values are simulated lower when the formulation of Rijtema (1969) is used. Strong precipitation events lead to a stronger rise in soil moisture especially in the upper four layers (0.27 m in total), and to rapid saturation and higher layer and surface runoff. Therefore, the discharge peaks are often overestimated. In contrast, the Campbell (1974) formulation supports a stronger downward water flux leading to lower upper-level runoff; thus the water content of the lower soil layers remains on a higher level and explains the marginal better simulation of the discharge peaks. The deficit of the parameterized lower boundary condition in TERRA-R is also represented in the soil moisture distribution during the simulation. The continuous decrease of the soil moisture in the lower layers using either parameterizations (Fig. 5.4b) leads to their drying out in TERRA-R. This decrease of soil moisture has influence on the generation of base flow.

The vertical soil water movement based on the parameterization of Campbell (1974) improves the simulation of discharge. The model performance is, however, still insufficient. The LHFL is marginally influenced by the formulation of Campbell (1974). In particular, the decrease of discharge and soil moisture during the simulation indicates the need to replace the lower boundary condition. Therefore, in the next step an elimination of the lower boundary parameterization deficit is mandatory. A long-time simulation leading to a significant improved ME is only possible by using a variable ground water table parameterization.

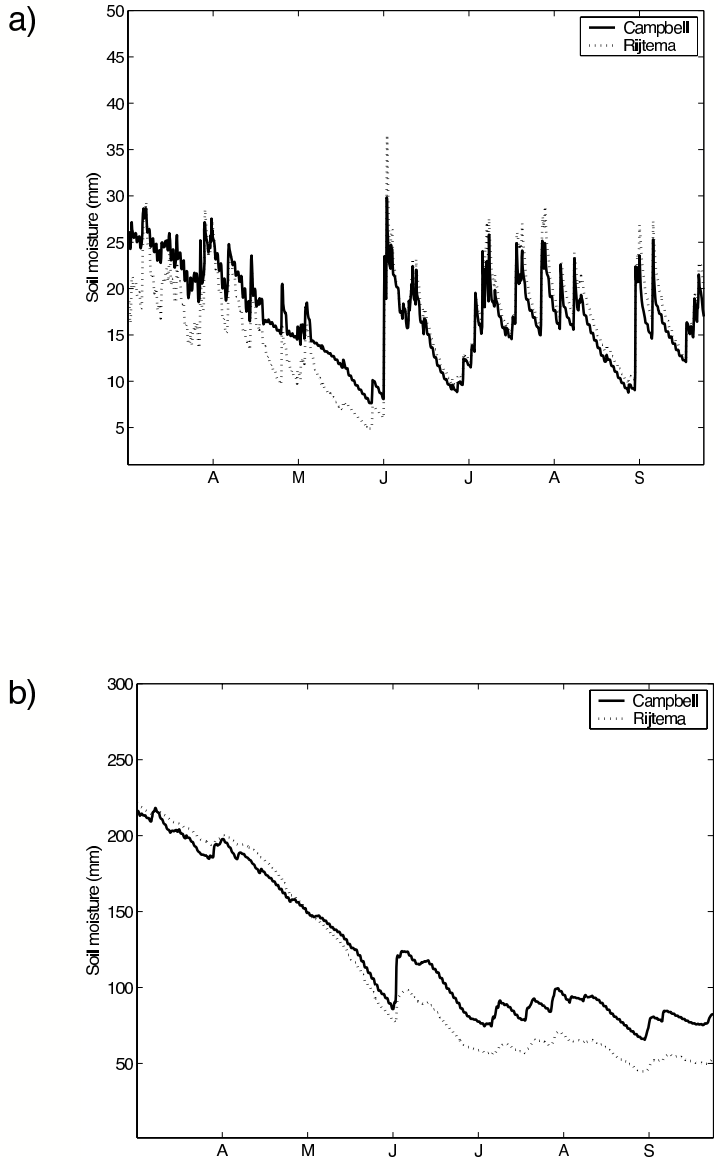

Figure 5.4: **a)** *Total soil moisture content for layer 1 - 4 with an overall thickness of 0.27 m* **b)** *Total soil moisture content for layer 5 - 6 with an overall thickness of 2.16 m*

5.2 Evaluation of SIMTOP

The following Section represents the simulation of discharge with TERRA-R-SIMTOP for the gauging station Menden. The hypothesis is that the SIMTOP approach has the potential to handle the base flow simulation and to remedy the drying out effect during long-time simulations.

The results of the last Section showed an improved simulation of discharge with the vertical soil water movement equations of Campbell (1974). Hence, TERRA-R-SIMTOP uses the formulation of Campbell (1974). First, the comparison with discharge measurements is represented for the summer period 2005. The model run is initialized with saturated soil conditions. In addition, the application of SIMTOP requires the determination of the calibration parameters $R_{sb,max}$ and f (Eq. 3.3.4). The adjustment of both parameters is needed to simulate discharge correctly. Niu et al. (2005) used a wide range of these parameters in order to test the sensitivity of TOPMODEL and SIMTOP in the Community Land Model version 2.0 (CLM 2.0) applied to the Sleepers river catchment located in Vermont, USA. Following the publication of Niu et al. (2005) and sensitivity runs with TERRA-R-SIMTOP for the summer period 2005, the parameters are estimated to $R_{sb,max} = 1.46E-4$ and $f = 2.90$ (Fig. 5.5a, b, green curve).

For an easier comparison both model runs with TERRA-R (Campell (1974) Fig. 5.5a, b, black curve and Rijtema (1969); Fig. 5.5a, b, dashed blue curve) are also shown. Overall, the simulation of discharge with TERRA-R-SIMTOP leads to a significant increase in model efficiency (ME= 0.17) compared with the model performance of TERRA-R (Campell ME= 0.07 and Rijtema ME= -0.61). The main improvement is that the base flow is realistically simulated during the total simulation. Obviously, the SIMTOP parameterization is able to prevent the drying out and therefore to increase the model performance.

Based on the application of TERRA-R-SIMTOP, the first month of the simulation shows an underestimation of the modeled discharge (Fig. 5.5a, green curve). The underestimation is caused by the parameterization of the sub-surface runoff in TERRA-R-SIMTOP. This parameterization leads to a less intensive runoff compared to the sub-surface runoff generated by TERRA-R. Sub-surface runoff in TERRA-R (Eq. 3.2.15) occurs if the total water content of each layer exceeds the field capacity. In contrast, the simplified exponential sub-surface runoff formulation of SIMTOP (Eq. 3.3.4) impeded during saturated soil conditions that the entire water beyond field capacity is directly transferred into sub-surface runoff.

From July to September, the hydrographs are realistically simulated with TERRA-R-SIMTOP during strong precipitation events. Two hydrographs, one be-

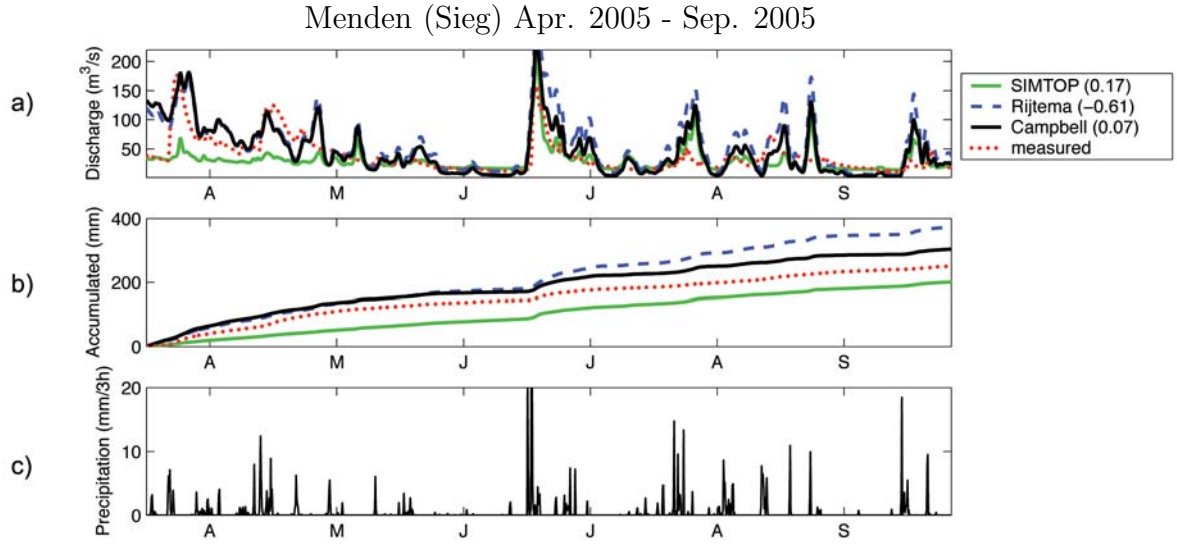

Figure 5.5: *Discharge for gauging station Menden (01.04.05 - 30.09.05) in m^3/s - 3h averages.* **a)** *The solid green curve represents the simulation of discharge with TERRA-R-SIMTOP including the vertical soil water parameterization by Campbell (1974) (calibration parameters $R_{sb,max} = 1.46E-4$, $f = 2.90$), the solid black curve represents the simulation of discharge with TERRA-R including the parameterization by Campbell (1974), the dashed blue curve the simulation of discharge with TERRA-R including the operational vertical soil water parameterization by Rijtema (1969), and the dotted curve represents measured discharge* **b)** *Accumulated discharge - 3h averages converted in mm, the curves are the same according to a),* **c)** *represents the areal precipitation by RADOLAN RW.*

tween end of July and beginning of August and the other at the end of August are overestimated for the version of TERRA-R with an unmodified lower boundary condition. The accumulation of the simulated discharge based on the SIMTOP scheme (Fig. 5.5b, green curve) leads to underestimations, whereas the simulations without SIMTOP result in overestimations. TERRA-R-SIMTOP reproduces discharge which is 50 mm lower than the measured accumulated discharge. The underestimation of the accumulated discharge (Fig. 5.5b) obtained with TERRA-R-SIMTOP is partly caused by the initialization.

The results of the last Section show that modifications of the parameterizations in TERRA-R influence additional variables of the hydrologic cycle. Due to the uniform and realistic simulation of base flow with TERRA-R-SIMTOP it is expected that the latent heat flux (LHFL) is modified compared to model runs without SIMTOP. Therefore, the LHFL is compared with the result of TERRA-R (Fig. 5.6a,b, CTL) which does not consider the variable ground water table parameterization but the vertical soil water formulation based on Campbell (1974). Both simulations are

applied for Menden and Siegburg-Kaldauen during the summer period 2005.

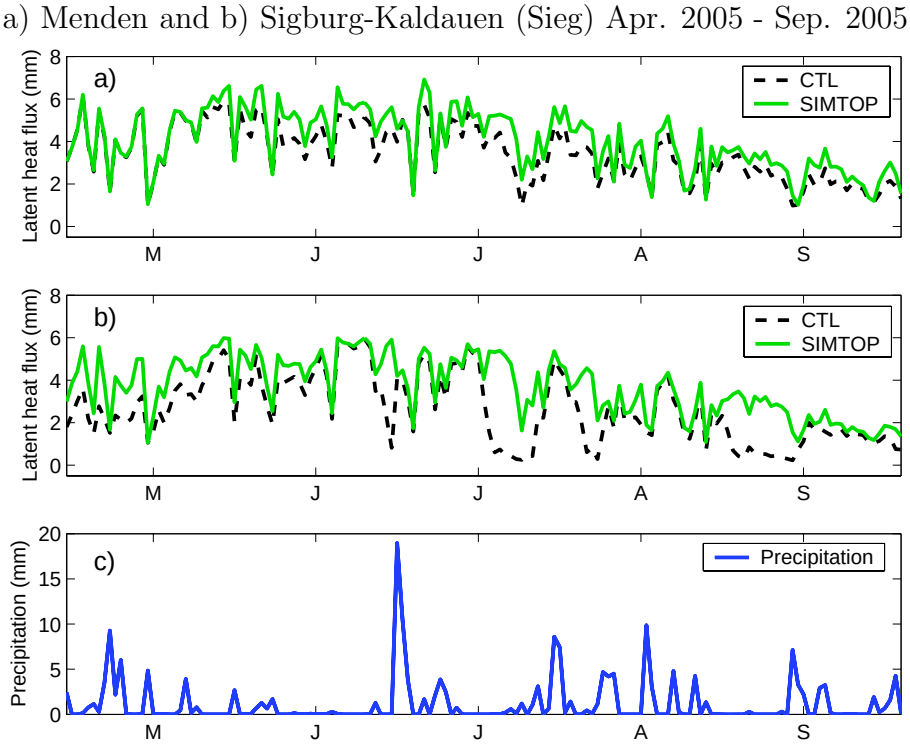

Figure 5.6: *Latent heat flux calculated by TERRA-R-SIMTOP (SIMTOP) and TERRA-R (CTL) with daily averages for the summer period 2005. The solid green curve denotes the calculated latent heat flux with TERRA-R-SIMTOP and the dashed black curve the calculated latent heat flux by TERRA-R as control run (CTL)* **a)** *for gauging station Menden,* **b)** *gauging station Siegburg-Kaldauen and* **c)** *the daily mean areal precipitation by RADOLAN RW*

The differences of the calculated LHFL between TERRA-R and TERRA-R-SIMTOP are larger than in the last Section, where the different evolutions of the LHFL by using the different vertical soil water movement equations were considered. Overall, the LHFL is higher for the simulation with the implemented SIMTOP formulation (Fig. 5.6a,b, SIMTOP). This means that the realistic base flow simulation with SIMTOP leads to a higher soil water content and to a stronger production of LHFL. Both gauging stations indicate also the drying out effects during this time period. In particular, Siegburg-Kaldauen represents a high difference of LHFL between TERRA-R and TERRA-R-SIMTOP. TERRA-R shows a strong decrease of the LHFL (Fig. 5.6b, CTL) whereas the SIMTOP formulation produces a higher LHFL during July and September. The result show the good performance of TERRA-R-SIMTOP for the determination of LHFL due to the realistic evolution

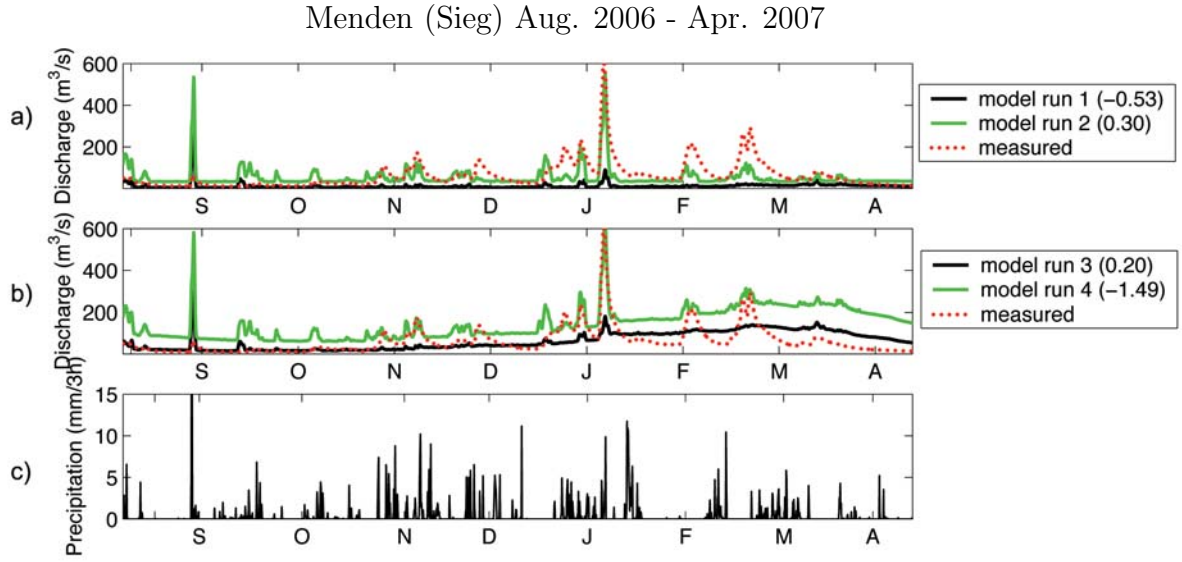

Figure 5.7: *Simulation of discharge (01.08.06 - 30.04.07) for gauging station Menden with TERRA-R-SIMTOP in m^3/s - 3h averages. The model runs are initialized with* **a)** *20% vol. soil moisture and* **b)** *60% vol. soil moisture. The solid black curve represents SIMTOP parameters of $R_{sb,max} = 1.46E-4$, $f = 3.26$, and the operational infiltration rate parameters of I_{K1} and I_{K2} (defined in text). The solid green curve represents SIMTOP parameters of $R_{sb,max} = 4.46E-4$, $f = 2.90$, and modified infiltration rate parameters of I_{K1} and I_{K2} (defined in text); dotted curve represents the measured discharge* **c)** *Areal precipitation by RADOLAN RW.*

of the flux for both gauging stations during the simulation. This means that the implementation of SIMTOP does not lead to a shifting of parameterization deficits e.g. to unrealistic values of the LHFL.

A successful evaluation of SIMTOP requires the test of the calibration parameters $R_{sb,max}$ and f on an additional simulation period. Hence, a model run from August 2006 until April 2007 is executed. A simulation which used the values of $R_{sb,max}$ and f applied during the simulation period 2005 shows an insufficient model efficiency (not shown). Furthermore, additional simulations with different values of $R_{sb,max}$, f, and initial soil water conditions show an overall strong sensitivity of the ground water table parameters. The solid black curve in Figure 5.7a,b represents the evolution of discharge with SIMTOP parameters $R_{sb,max} = 1.46E-4$ and $f = 3.26$. Only the initial soil water conditions are different. The first run is started with 20% vol. soil moisture (Fig. 5.7a, solid black curve) and therefore dry soil conditions whereas the second run is initialized with 60% soil vol. soil moisture (Fig. 5.7b, solid black curve). The latter model run shows the better model performance (ME= 0.20). The simulation of discharge peaks, however, shows poor agreement with

measurements. The first large discharge peak in the simulations can be explained by incorrect precipitation measurements (Fig. 5.7c) because the data set indicates a clear overestimation in the beginning of September. Obviously, a higher initial soil water condition influences the simulation of base flow but has only marginal impact on the simulation of hydrographs. Hence, a sensitivity study was carried out to investigate which additional parameterizations in TERRA-R-SIMTOP influence the simulation of hydrographs.

The analysis shows that a modification of the infiltration rate parameters I_{K1} and I_{K2} from implemented infiltration approach of Holtan (Eq. 3.2.9) indicates variations in the simulation of discharge peaks. The operational parameter of I_{K2} depends on the soil texture and varies between 0.0003 for silty clay, 0.0035 for sand and the uniform parameter I_{K1} is set to 0.0020. This study performed additional simulations for the time period 2006/2007 with changed infiltration rate parameters. During these simulations, I_{K1} is set to 0.0001 and I_{K2} is 80% lower for all soil characteristics. The objective is to reduce the infiltration rate and to obtain an increase of the surface runoff.

The simulation of discharge with changed infiltration rate parameters leads to a better reproduction of discharge peaks (not shown). A simulation with simultaneously modified ground water table parameters ($R_{sb,max} = 4.46E-4$, $f = 2.90$) show the best accordance with discharge measurements. Thus, model run initialized with 20% soil vol. soil moisture (Fig. 5.7a solid green curve) has, in comparison with all tested runs, the best model performance (ME= 0.30). The run describes a realistic simulation of discharge peaks and the best base flow representation during the simulation. Furthermore, the run demonstrates the important influence of the initial soil water conditions additionally to the already selected calibration parameters. A higher contribution of initialized soil water content (Fig. 5.7b, solid green curve) also shows a realistic simulation of discharge peaks but an overestimation of the base flow during the total simulation. The result is an insufficient model efficiency (ME= -1.49).

This Section showed that the implementation of SIMTOP improves clearly the simulation of discharge. In particular, the drying out effects during long-time simulations and drier periods are eliminated. The objective to increase the model efficiency is also achieved. This sensitivity study also shows, however, the combination of different parameterizations with its influencing quantities affect the evolution of discharge peaks and base flow strongly. In addition, the simulation of discharge depends on the soil water initialization. Thus, during time periods (2005; 2006/2007) different model performances and also different evolutions of discharge are shown. The ground water table parameters based on SIMTOP as well as the influencing infiltration rate parameters impact also the model performance. Nevertheless, these results are only based on several single sensitivity runs. Therefore, an extended

sensitivity study based on a statistical analysis is needed, which estimates the most influencing parameters on the simulation of discharge. This study uses a number of runs with different combinations to extract the interactions of the introduced calibration parameters and is described in the following.

5.3 Statistical evaluation of the simulated discharge

The objective of this Section is to analyze the impact of the ground water table parameters, infiltration rate parameters, and the initial soil water conditions on discharge simulations. The last Section showed that it is difficult to estimate a general configuration of these calibration parameters through a simple sensitivity study. Thus, an analysis is needed that evaluates the differences in the LSP response on discharge simulations. This evaluation needs to take into account both the direct and indirect components of the feedback pathways. The direct (or first order) and the indirect (or the interactions) terms often have similar magnitudes but different feedback pathways (Niyogi and Raman 1999). To explicitly resolve these indirect and direct effects, a factorial design experiment is used in this study (Box et al. 1978; Niyogi et al. 2002; Schüttemeyer 2005).

The advantage of a factorial design experiment in comparison to a sensitivity study with a single model run (one-at-time (OAT) method) is that the latter provides only an estimate of the effect of a single variable, while other variables are fixed. The factorial design experiments were also used in earlier land-surface atmosphere studies. Henderson-Sellers (1993) used this technique in conjunction with the BATS scheme. As part of her study, she tested the most important climatological atmospheric forcings, and found that mean monthly temperature and the interaction between mean monthly temperature and total monthly precipitation have a predominant impact on the behavior of BATS. She emphasized that fractional cloudiness and other environmental parameters are also important.

The following Section introduces the theory of the factorial design experiments based on the publications of Henderson-Sellers (1993), Niyogi et al. (2002), and Box et al. (1978). Afterwards, the application and results for simulated discharge in the Sieg river catchment are presented.

5.3.1 Theory of factorial design experiments

In a factorial experiment, all combinations of parameters (factors) for a range of perturbation levels are used to construct the so-called experimental design matrix. Consider the simplest example of two parameters, each to be evaluated at two levels (low [−] and high [+]). As illustrated in Table 5.1, 4 (= 2^2) runs will cover all possibilities for the two parameters A and B. Two of these are the main effects caused by perturbing A or B, the third is the overall average effect, and fourth is the so-called interaction effect between A and B (written as factor $A : B$). If k is the number of parameters and 2 the levels tested in total, 2^k runs must be performed. Different notations are used to describe this experimental design. This study used a plus symbol for a higher value and a minus for a lower.

Table 5.1: *Design matrix for a full factorial, two factor, two-level experiment using minus signs to indicate low levels and plus signs to indicate high levels*

Run	*A*	*B*	*Identification*
1	-	-	*Mean*
2	+	-	*A*
3	-	+	*B*
4	+	+	*A* : *B*

Several algorithms are used to evaluate the factorial design matrix. This study used the Yates algorithm (1970) which is described by Box et al. (1978). If the sign in column j and row i is denoted by S_{ij}, then the effect E_j for the jth parameter (here the first parameter represents the *mean* and other single parameters follow) is given by

$$E_j = \frac{\sum_{i=1}^{R}(S_{ij}V_i)}{P}, \tag{5.3.1}$$

where V_i is the value of the model-simulated outcome (in this study the average discharge; see next Section) derived from the *ith* experimental run, R is the total number of experimental runs undertaken, and P is the number of + signs in the column. The divisor P is used because with the effect of a parameter E_j we describe the change in the response as we move from the - to the + version of the parameter, i.e. from the low to the high level of parameter. For the illustrated two-factor experiment shown in Table 5.1, the parameter $A : B$ represents the interaction effect between A and B. This mode of calculation is easily extendable to much larger matrices and will be used in this study.

For a factorial design study based on the Yates analysis, the data are arranged in the so-called "Yates order": given k factors, the first column consists of $2^{(k-1)}$ minus signs (i.e. the low level of the factor) followed by $2^{(k-1)}$ plus signs (i.e. the high level of the factor). The second column consists of $2^{(k-2)}$ minus signs followed by $2^{(k-2)}$ plus signs and so forth (Box et al. 1978).

Table 5.2 displays the design matrix in Yates order for the analysis in this study. Five variables are varied in TERRA-R-SIMTOP by low and high settings leading to

Table 5.2: *Design matrix for setting the input variable values of the ground water table and infiltration rate parameterization in TERRA-R-SIMTOP. Variables are defined in Table 5.3.*

run	wet	f	$R_{sb,max}$	I_{K1}	I_{K2}
1	-	-	-	-	-
2	-	-	-	-	+
3	-	-	-	+	-
4	-	-	-	+	+
5	-	-	+	-	-
6	-	-	+	-	+
7	-	-	+	+	-
8	-	-	+	+	+
9	-	+	-	-	-
10	-	+	-	-	+
11	-	+	-	+	-
12	-	+	-	+	+
13	-	+	+	-	-
14	-	+	+	-	+
15	-	+	+	+	-
16	-	+	+	+	+
17	+	-	-	-	-
18	+	-	-	-	+
19	+	-	-	+	-
20	+	-	-	+	+
21	+	-	+	-	-
22	+	-	+	-	+
23	+	-	+	+	-
24	+	-	+	+	+
25	+	+	-	-	-
26	+	+	-	-	+
27	+	+	-	+	-
28	+	+	-	+	+
29	+	+	+	-	-
30	+	+	+	-	+
31	+	+	+	+	-
32	+	+	+	+	+

32 different combinations. The following parameters are varied: soil wetness (wet), decay calibration factor of the ground water table parameterization (f), maximum sub-surface runoff calibration parameter of the ground water table parameterization ($R_{sb,max}$; Eq. 3.3.4), maximum infiltration (I_{K1}), and infiltration rate parameter (I_{K2}; Eq. 3.2.9) which depends on the soil texture. The high and low values for the five variables are given in Table 5.3. These values are motivated by the sensitivity

Table 5.3: *Values of input variables used for TERRA-ML simulations for the high (+) and low (-) settings used in the design matrix shown in Table 5.2.*

Variable	High (+)	Low (-)
Wet	1.0	0.2
f	3.56	2.90
$R_{sb,max}$	4.46E-4	0.46E-4
I_{K1}	0.0036	0.0004
I_{K2}	180%	20%

studies in Chapter 5.2. Thus, the lower values of I_{K1} and I_{K2} lead to the best results on the simulation of discharge peaks. In contrast, higher values of both parameters lead to a deterioration. Therefore, this range of parameters is selected for the statistical analysis in order to test the influence of the infiltration rate parameters on the simulation of discharge. The same is considered for the SIMTOP parameters f and $R_{sb,max}$ with the difference that a higher value of $R_{sb,max}$ improves the model performance (Fig. 5.7). In Chapter 5.2, a strong influence of the soil water initialization is demonstrated. Therefore, dry and wet conditions are selected for analyzing the impact of the initialization.

Lenth (1989) presented a method for analyzing the significance of the effects E_j. The following description is based on the notation of Lenth (1989). He denotes the differences between the means at the "high" and the "low" levels as contrasts. Suppose we have j contrasts of interest, let $K_1, K_2, ..., K_j$ denote the true contrast values, and let $E_1, E_2...., E_j$ denote the corresponding estimates. The assumption of Lenth (1989) is that the contrast estimates having the same variance but possibly unequal means.

The essence of the method is to estimate the variance of the contrasts from the smallest (in absolute value) contrast estimates as follows:

$$s_0 = 1.5 \times median\{|E_j|\} \tag{5.3.2}$$

and

$$PSE = 1.5 \times median\{|E_j| : |E_j| < 2.5 s_0\}. \tag{5.3.3}$$

The PSE is 1.5 times the median of all the smaller contrasts, where smaller contrasts are defined as those with absolute values less than 2.5 times 1.5 the median of the absolute value of all contrasts. The PSE is termed the pseudo standard error. Lenth (1989) shows that the PSE is a "fairly good estimate of the variance when the effect are sparse". The effect sparsity means that the number of nonzero or significant effects among the contrasts in a factorial design experiment is expected

to be small. Assuming there are few significant effects E_j, the significant effects show up as outliers. This study uses the method of Lenth (1989) to determine the statistical significance of the effects E_j of the factorial design study.

5.3.2 Results from factorial design

The analysis of the simulated discharge is done for three periods between September 2006 and August 2007. Two periods are characterized by discharge peaks (see Fig. 5.8 A and B) and the third example represents both discharge peaks and drier periods (Fig. 5.8 C). For all three periods, the average discharge of each run is

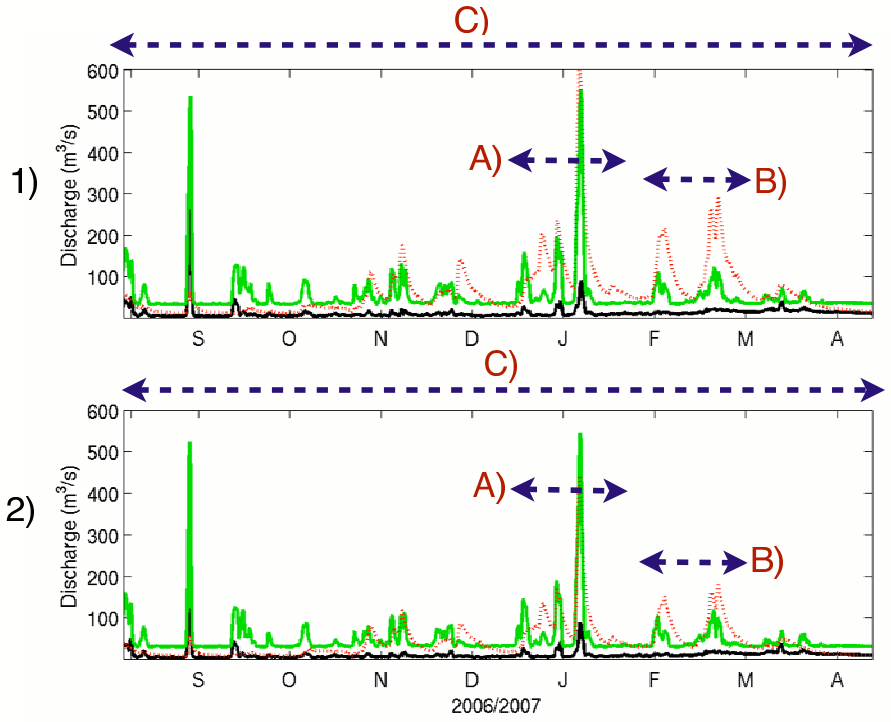

Figure 5.8: *Discharge for gauging stations 1) Menden and 2) Siegburg-Kaldauen (15.08.06 - 30.04.07) in m^3/s - 3h averages. The solid black curve represents SIMTOP parameters $R_{sb,max} = 0.46E-4$ and $f = 3.56$, initial condition 20% vol. soil moisture with a setting of the infiltration rate parameters I_{K1} and I_{K2} to higher values (Tab. 5.3); The solid green curve represents SIMTOP calibration parameters $R_{sb,max} = 4.46E-4$, $f = 2.90$, initial condition 20% vol. soil moisture with changed infiltration rate parameters I_{K1} and I_{K2} to lower values (Tab. 5.3); dotted curve represents measured discharge. A, B and C denote the investigated time periods.*

calculated. With these values the main and interaction effects are calculated (Eq. 5.3.1). All determined effects are normalized by the overall average effect.

The results of the main and interaction effects according to Equation (5.3.1) are shown in a bar plot (Fig. 5.9). Interaction terms are indicated by variables such as $f : R_{sb,max}$, which refers to the interaction between both ground water table parameters. The red line is the significance level (Eq. 5.3.2 - 5.3.3).

a) Results for gauging station Menden

The evaluation indicates a strong influence of the variable ground water table parameterization. Thus, ground water table parameters show a large significance as main effects. The estimated effect of parameter $R_{sb,max}$ has a positive value which means that a higher value of $R_{sb,max}$ leads to a higher discharge in TERRA-R-SIMTOP. This result is also reflected in Figure 5.8: $R_{sb,max} = 0.46E - 4$ (solid black curve) leads to a unrealistic low base flow when compared to the run with $R_{sb,max} = 4.46E{-}4$ (solid green curve). The effect of f is negative during all periods. When setting this parameter to a lower value f shows an opposing behavior. The simulation run in Figure 5.8 (solid green curve) supports this result. Thus, changing f from 3.56 to 2.90 results in higher simulated discharge. The interplay between the ground water table parameters also indicates a significant influence. The interaction combination $f : R_{sb,max}$ indicates a negative performance when setting parameters f and $R_{sb,max}$ from low to high. A reason is the sensitivity of the ground water table parameterization. Hence, the discharge only increases when setting parameter $R_{sb,max}$ to a higher value and f to a lower value.

In Section 5.2 it was concluded that the initialization of soil water (wet) plays an important role for the evolution of discharge. The factorial design experiment shows the same result. The main effect wet has a significant value in all simulated cases. Moreover, the soil wetness is the main effect with the highest positive value. Thus, model runs initialized with a higher amount of soil water lead to a higher generation of discharge. Another significant interaction term is the opposing behavior of soil wetness wet and the ground water table parameter f. An increase of both parameters implies a negative value of the interaction effect $wet : f$. A reason for the negative significant value is the dominance of parameter f of the interaction term $wet : f$. According to Equation (3.3.4), the parameter f describes a decay factor. Setting parameter f to high leads to a stronger damping and to a decrease of discharge. Therefore, parameter f has a stronger influence as the soil water initialization. In contrast, the factorial experiment presents a positive significant value of $wet : R_{sb,max}$ in all examples and indicates that a higher quantity of both parameters increases the simulation of discharge. Overall, the analysis suggests that the effects with the largest values are the soil water initialization wet and the ground water table parameter $R_{sb,max}$. Following, the third largest value is the interaction

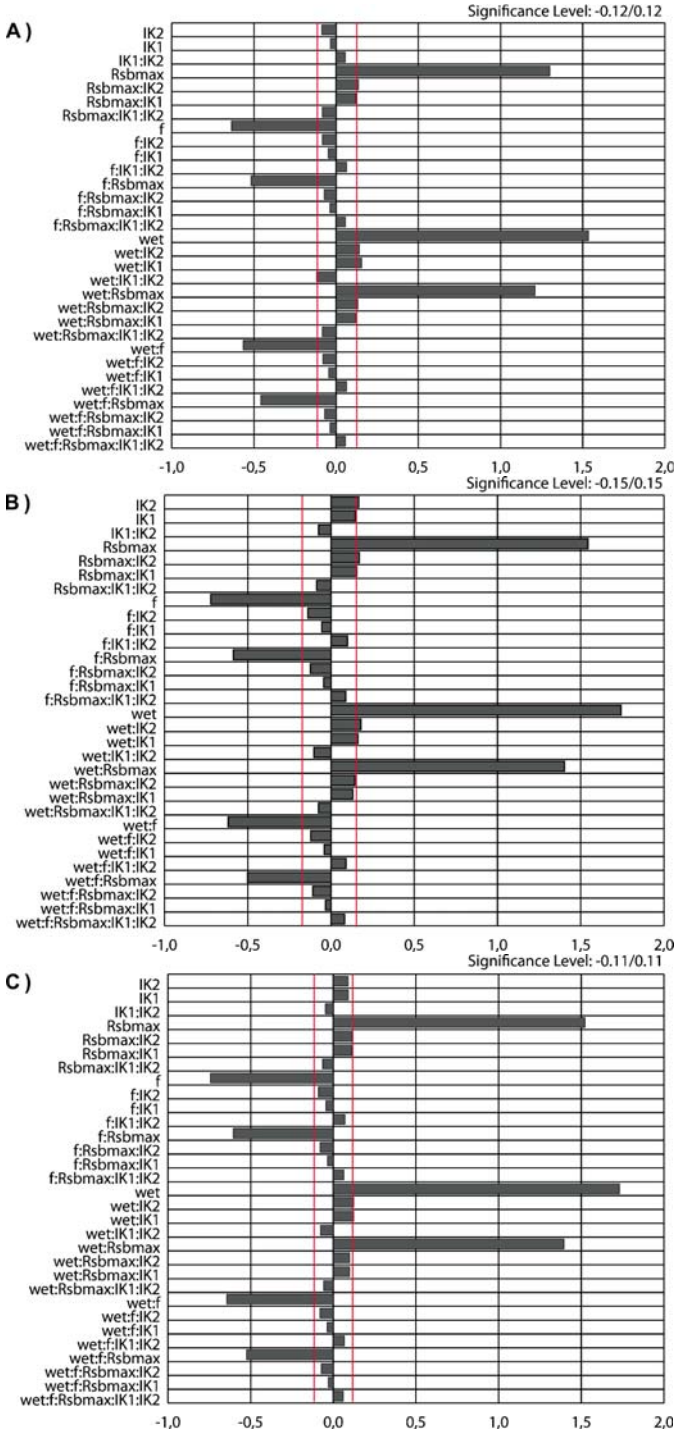

Figure 5.9: *Effects for the simulation of discharge of three different periods according to Figure 5.8 A,B,C. Analysis of the runs which are set from low to high (runs no. 1-32) according to Table 5.2*

between these two parameters $wet : R_{sb,max}$ while the ground water table parameter f is only in the fourth position. Therefore, a simultaneously setting of parameters $R_{sb,max}$ and wet high have a stronger impact as parameter f on the simulation of discharge.

The assumption that the infiltration rate parameterization based on the formulation of Holtan has a significant influence can not be verified. In particular, the first and second periods which are dominated by simulated discharge peaks (Fig. 5.8A,B) only show rarely significant performances of the parameters I_{K1} and I_{K2}. The single simulation runs in the last Section showed nearly realistic simulated hydrographs when setting both parameters to lower values. Hence, it was expected that setting the infiltration rate parameters high would lead to significant negative values and therefore to a decrease of simulated discharge. The interaction effects which contain the infiltration rate parameters also have no or only low significance. This marginal significance is caused by the high influence of the SIMTOP approach as well as the soil wetness. For example, the small significance of the interaction term $wet : I_{K2}$ is caused by the large influence of the initial soil water condition.

To gain deeper insight into the influence of the ground water table parameterization and infiltration rate parameterization on discharge simulation an additional analysis based on the factorial design experiment is performed. The objective is to verify the large impact of the ground water table parameters and the lower influence of the infiltration rate. For this analysis the soil water initialization is not modified. The determination of the effects according to Equation (5.3.1) of a full factorial design requires for the four parameters 16 ($= 2^4$) runs. The estimation of the effects are indicated for a short time period which is dominated by discharge peaks and a long time period (Fig. 5.8 B,C). The first example (Fig. 5.10) shows the effects of the model runs 1-16 and the second example (Fig. 5.11) of the runs 17-32 (Tab. 5.2).

The evaluation of the ground water table parameterization leads to the same results as the already introduced examples. In all examples, significant values of the ground water table parameters are shown. The already obtained results regarding the influence of the infiltration rate parameterization can also be verified during this experimental study. The infiltration rate parameters I_{K1} and I_{K2} have no significant impact.

b) Results for gauging station Siegburg-Kaldauen

The results for the simulation of discharge are comparable to those obtained for Menden concerning the absolute size and the ranking of the effects (Fig. 5.12; Fig. 5.13).

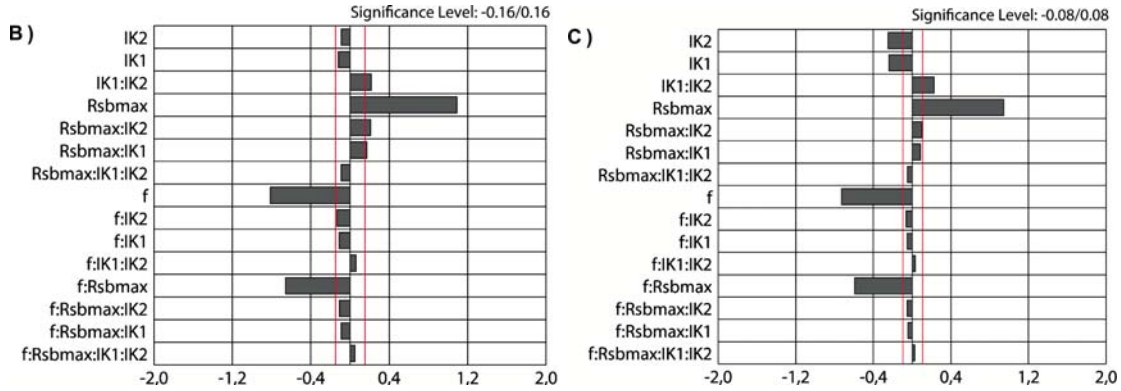

Figure 5.10: *Effects for the simulation of discharge of two different periods according to Figure 5.8 B,C. Analysis of the runs number 1-16 according to Table 5.2.*

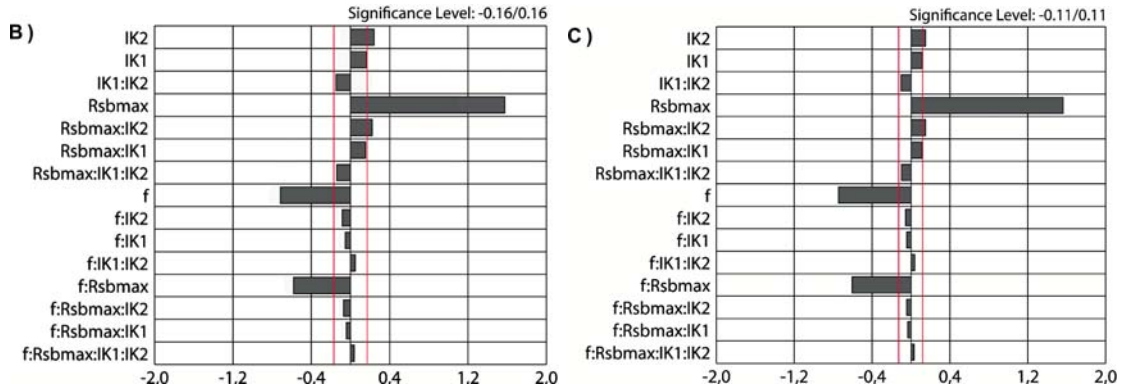

Figure 5.11: *Effects for the simulation of discharge of two different periods according to Figure 5.8 B,C. Analysis of the runs number 17-32 according to Table 5.2.*

The full factorial design experiment evaluating 16 model runs with modified ground water table parameters and infiltration rate parameters ($R_{sb,max}$, f, I_{K1}, I_{K2}) indicates similar significant main and interaction effects compared to gauging station Menden.

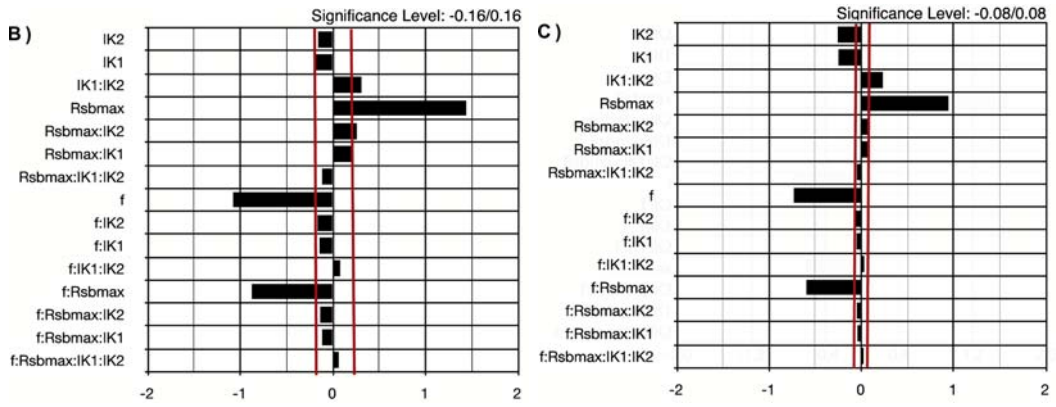

Figure 5.12: *Effects for the simulation of discharge of two different periods according to Figure 5.8 B,C. Analysis of the runs number 1-16 according to Table 5.2.*

The statistical evaluation showed that the initialization of soil water and the ground water table parameters have the largest impact on the simulated discharge. SIMTOP exhibits an important influence on the generated base flow and therefore on the overall simulated discharge. The analyses also indicate the low influence of the infiltration parameterization on discharge simulation.

The best model performance is obtained for runs with a high $R_{sb,max}$ and low f. In addition, the model performance depends strongly on the soil water initialization. The soil wetness is often influenced by the weather situations and the seasons. Due to a higher evaporation, the soil is often drier during the summer months whereas the soil in autumn and winter is often saturated. In August, the optimized discharge simulation is obtained with initial soil water conditions of 20% vol. soil moisture. The ground table parameter should be selected independent from soil water content to $R_{sb,max} = 4.46E-4$ and $f = 2.90$.

Another method to use the optimized soil water initilization is to determine the spin-up timescale of TERRA-R-SIMTOP. The spin-up of a LSP is broadly defined as an adjustment process as the model approaches its equilibrium following initial anomalies in soil moisture content. The spin-up timescale of different LSP schemes was investigated by Yang et al. (1995) during the PILPS (intercomparison of land-surface parameterization schemes) project. They suggest that the most LSP schemes require many years to come to thermal and hydrologic equilibrium with the forcing

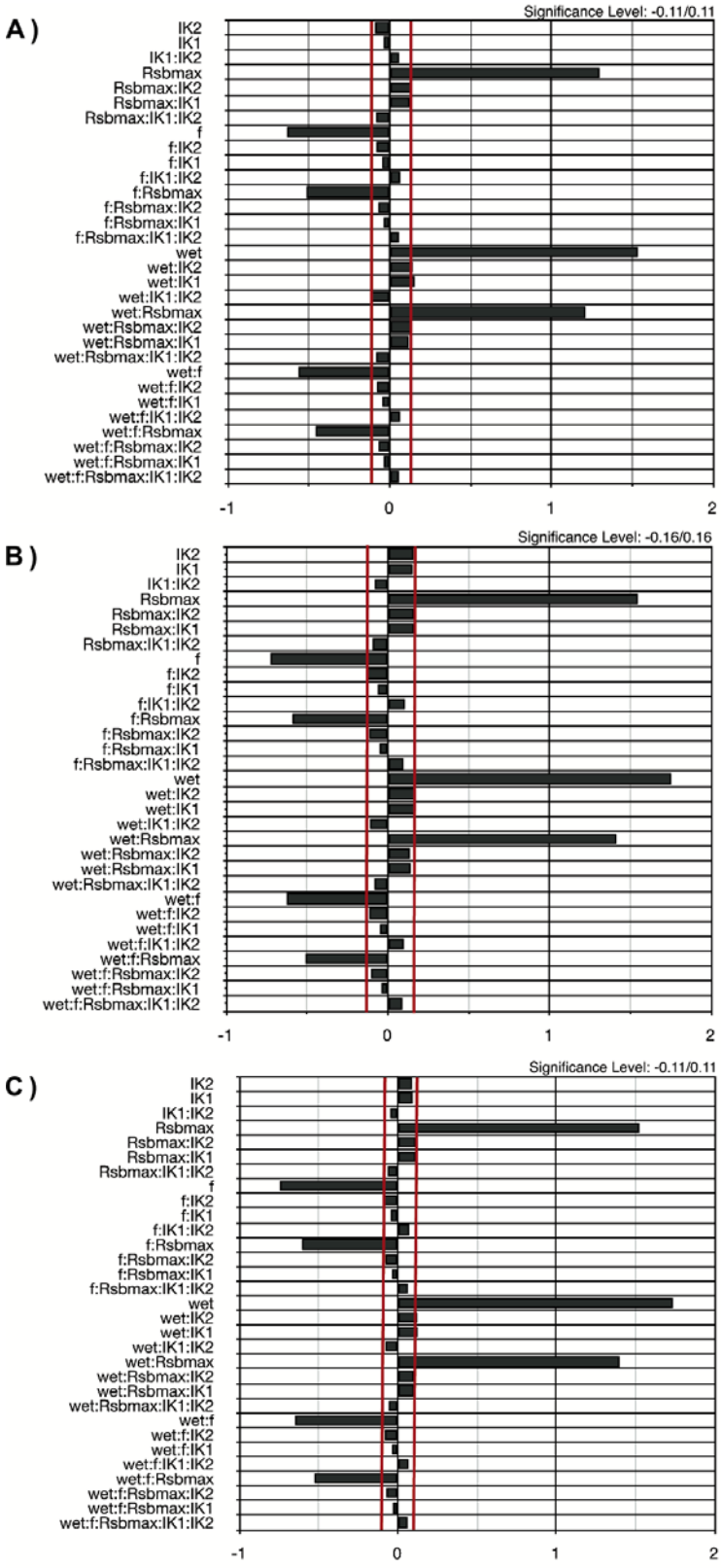

Figure 5.13: *Effects for the simulation of discharge of three different periods according to Figure 5.8 A,B,C. Analysis of the runs of the design matrix which are set from low to high conditions for gauging station Siegburg-Kaldauen (runs no. 1-32) according to Table 5.2.*

meteorology. Therefore, much longer simulation periods are needed to determine the optimized soil water initialization.

Chapter 6

Conclusion and Outlook

The land-surface parameterization TERRA-ML of the operational NWP model system COSMO of DWD has been extended by a river routing scheme (TERRA-R). This study aims at finding the optimized model performance related to the simulation of discharge and studying the influence of different parameterizations on discharge simulation. To this goal, the impact of two formulations of the vertical soil water movement on runoff generation is tested. As a testbed, the uncoupled scheme was implemented for the Sieg catchment and the simulated discharge time series was compared with observations. Based on findings concerning the drying out of the lower soil layers, TERRA-R is extended by an improved parameterization of the ground water table (TERRA-R-SIMTOP). Up to now, the water table is practically kept constant in the operational version of TERRA-ML. Hence, a variable ground water table based on the methodology of Stieglitz et al. (1997) and Niu et al. (2005) as an alternative lower boundary condition was implemented. First results hint at significant improvements in the discharge simulation and also provide the basis for a more detailed model evaluation.

The LSP TERRA-R-SIMTOP also showed uncertainties in the infiltration rate parameterization. A sensitivity study showed small improvements in modelling of hydrographs by changing the infiltration rate parameters. A statistical analysis based on a factorial design experiment quantified the dependence on several parameters for TERRA-R-SIMTOP. The main findings of the factorial design study was a strong sensitivity of the discharge simulation relative to the ground water table parameters. A lower ground water table parameter f and a higher $R_{sb,max}$ lead to an improved model efficiency, which corroborates the results by Niu et al. (2005). The changed infiltration rate parameters showed no significant effect on the simulation of discharge and therefore no improvements for TERRA-R-SIMTOP. In contrast, the initialization of soil water indicates a significant impact for the simulation of

discharge. This means that realistic input information of soil water content is required to yield satisfied discharge simulations. A method is to determine the spin-up timescale of TERRA-R-SIMTOP.

In summary, this study showed that the prediction of discharge with the LSP TERRA-R-SIMTOP of the operational weather forecast model COSMO is possible. The extension with additional parameterizations improved the simulation of discharge with the model system. To achieve a high model performance, the integration of TERRA-R-SIMTOP into a two-way coupled weather forecast system depends on several conditions that are outlined below:

1. Precipitation

The precipitation input represents a major uncertainty for the NWP. This study used a data set which consists of measurements and is available in a high spatial and temporal resolutions (RADOLAN RW). A two-way coupled model system will be forced with precipitation calculated by the COSMO model. This precipitation was already investigated in earlier studies and provide the uncertainties for the future work. Bachner et al. (2008) shows a number of uncertainties for the Climate version of COSMO (CLM). An important result in their study is that the CLM is not able to reproduce the spatial structure of observed precipitation indices within the selected region adequately. Moreover, their study indicates a general low performance in the CLM especially in regions which are dominated by complex terrain. Hence, a higher quality of the simulation of discharge without improvements of the precipitation prediction in NWP models is not feasible.

2. Spatial resolution

TERRA-R and TERRA-R-SIMTOP were applied to the river Sieg catchment with a grid spacing resolution of 1 km x 1 km. Both models had a higher spatial resolution when compared to the resolution of the operational NWP system. In this study, the applied resolution displays more detailed information of vegetation, soil characteristics, and topography. The routing scheme needs as input information the flow direction which is derived from the elevation model. A finer resolution of the elevation model displays the catchment flow properties in more detail and is able to influence the quality of simulated discharge. The parameterization of SIMTOP depends on the calculation of soil moisture by TERRA-ML. A LSP scheme of 1 km x 1 km shows a more detailed soil moisture distribution compared to coarser resolutions (Schmitz 2005) such as the operational COSMO model. Thus, the calculation of the soil moisture distribution by the operational COSMO model could affect the ground water table height of SIMTOP and additionally the quality of base flow. The mosaic approach (Ament and Simmer 2006) can connect the atmosphere and the land-surface by using a finer resolution for the land-surface whereas the atmospheric

resolution is kept as in the operational version.

3. Parameterizations

This study identified model deficiencies, which have not been solved until now. The changed lower boundary condition prevents the drying out of TERRA-R-SIMTOP. Nevertheless the surface runoff component sometimes shows insufficient values during strong precipitation events which are not related to the model input information. The changed infiltration parameterization cannot solve the main deficiencies. Moreover, numerous long time runs are also required for further validation of TERRA-R-SIMTOP in order to quantify the optimized model performance including a new surface runoff parameterization.

4. Prediction technique

A further elimination of uncertainties with TERRA-R-SIMTOP could be achieved by using ensemble-based forecasting methods. For the prediction of discharge various approaches were tested in the past few years. Ensemble based methods use data assimilation approaches which become increasingly popular. State-space filtering methods continuously update the states in the model when new measurements become available. This approach improves model forecast accuracy, and provides a means for explicitly handling the various sources of uncertainty in hydrologic modelling. Most of the techniques based on the ensemble Kalman filter (Evensen 1994) have been shown to have power and flexibility required for data assimilation using conceptual watershed models (Vrugt et al. 2007, 2005, 2006a).

The ensemble-based forecasting methods can lead to a successful validation of TERRA-R-SIMTOP and has also been driven by the project GEWEX/CLIVAR and GLACE (Dirmeyer et al. 2006) introduced in Chapter 1. This project has provided an estimate of the global distribution of land-surface coupling strength during boreal summer based on the results from a dozen weather and climate models. However, there are numerous variations among models, due to sensitivities in the simulation of both the terrestrial and the atmospheric branches of the hydrologic cycle. They found evidences for systematic biases in near-surface temperature and humidity among all models, which may contribute to incorrect surface flux-sensitivities. However, the multi model mean is generally better validated than most or all of the individual models. Hence, an ensemble based forecast system with a multi simulation system could probably help to improve discharge simulations.

Bibliography

Abramopoulos, F., C. Rosenzweig, and B. Choudhury, 1988: Improved ground hydrology calculations for global climate models (GCMs): Soil water movement and evapotranspiration. *J. Climate*, **1**, 921–941.

Ament, F., 2006: *Energy and moisture exchange processes over heterogeneous landsurfaces in a weather prediction model.*. Dissertation, University of Bonn.

Ament, F. and C. Simmer, 2006: Improved representation of land-surface heterogeneity in a non-hydrostatic numerical weather prediction model. *Boundary-Layer Meteorology*, **121 (1)**, 153–174.

Avissar, R., 1992: Conceptual aspects of a statistical-dynamical approach to represent landscape subgrid-scale heterogeneities in atmospheric models. *J. Geophys. Res.*, **97**, 2729–2742.

— 1998: Which type of soil-vegetation-atmosphere transfer scheme is needed for general circulation models: a proposal for a higher order scheme. *J. Hydrol.*, **212-213**, 136–154.

Avissar, R. and R. A. Pielke, 1989: A parameterization of heterogeneous landsurface for atmospheric numerical models and its impact on regional meteorology. *Mon. Wea. Rev.*, **117**, 2113–2136.

Bachner, S., A. Kapala, and C. Simmer, 2008: Evaluation of precipitation characteristics in the CLM and their sensitivity to precipitation. *Meteorol. Z.*, **17**, 407–419.

Baumgartner, A. and H. J. Liebscher, 1990: *Allgemeine Hydrologie Quantitative Hydrologie*. Gebrüder Borntraeger, Bundesanstalt für Gewässerkunde in Koblenz.

Beljaars, A. C. M., P. Viterbo, and M. Miller, 1995: The anomalous rainfall over the united states during july 1993: Sensitivity to land surface parameterization and soil moisture anomalies. *Mon. Wea. Rev.*, **124**, 362–383.

Betts, A., F. Chen, K. Mitchell, and Z. Janjic, 1997: Assessment of the land surface and boundary layer models in two operational versions of the NCEP Eta model using FIFE data. *Mon. Wea. Rev.*, **125**, 2896–2916.

Beven, K. J., 1982: Macropores and water flow in soils. *Water Resour. Res.*, **18**, 1311–1325.

Beven, K. J. and M. J. Kirkby, 1979: A physically based, variable contributing model of basin. *Hydrol. Sc. Bull.*, **24**, 43–69.

Bonan, G. B., 1998: The land surface climatology of the ncar land surface model coupled to the ncar community climate model. *J. Climate*, **11**, 1307–1326.

Box, G., W. Hunter, and J. Hunter, 1978: *Statistics of Experimenters: An Introduction to Design, Data Analysis, and Model Building*. Jon Wiley and Sons, 306 pp.

Box, G. E. P., G. M. Jenkins, and G. C. Reinsel, 1994: *Time series analysis, forcasting and control*, volume 3rd edition. Prentice Hall.

Braun, F. J., 2002: *Mesoskalige Modellierung der Bodenhydrologie*. Dissertation, University of Karlsruhe.

Brooks, R. H. and A. T. Corey, 1964: Hydraulic Properties of Porous Media. *Hydrol. Paper*, **3**.

Busche, H. and B. Diekkrüger, 2005: *Kontinuierliche Modellierung der Bodenerosion im Sieg-Einzugsgebiet. Abschlussbericht der Forschungsstudenten*. GRK 437/3, Meckenheimer Allee 166, D - 53115 Bonn.

Campbell, G. S., 1974: A simple method for determining unsaturated conductivity from moisture retention data. *Soil Science*, **117**, 311–314.

Chen, F., K. Mitchell, and J. Schaake, 1996: Modeling of land surface evaporation by four schemes and comparison with FIFE observations. *J. Climate*, **10**, 1194 – 1215.

Chen, J. and P. Kumar, 2001: Topographic influence on the seasonal and interannual variation of the water and energy balance of basin in North America. *J. Climate*, **14**, 1989 – 2014.

Clapp, R. B. and G. M. Hornberger, 1978: Empirical equations for some soil hydraulic properties. *Water Resour. Res.*, **14 (4)**, 601–604.

Claussen, M., 1999: Area-averaging of surface fluxes in a neutrally stratified, horizontally inhomogeneous atmospheric boundary layer. *Atmos. Environ.*, **24a**, 1349–1360.

Dai, Y. and Q. Zeng, 1997: A land surface model (IAP94) for climate studies, part 1: Formulation and validation in off-line experiments. *Advances in Atmos. Sci.*, **14**, 443–460.

Deardorff, J. W., 1978: Efficient prediction of ground surface temperature and moisture, with inclusion of layer and vegetation. *J. Geophys. Res.*, **83**, 1889–1903.

Dickinson, R. E., A. Henderson-Sellers, and P. J. Kennedy, 1993: *Biosphere-Atmosphere Transfer Scheme (BATS) for the NCAR Community Climate model*. NCAR Technical Note, NCAR/TN-275+STR, 72pp.

Dingman, S. L., 2002: *Physical Hydrology - Second Edition*. Prentice Hall.

Dirmeyer, P. A., A. J. Dolman, and N. Sato, 2008: The global soil wetness project: A pilot project for global land surface modeling and validation. *Bull. Amer. Meteorol. Soc.*, **80**, 851–878.

Dirmeyer, P. A., R. D. Koster, and Z. Guo, 2006: Do global models properly represent the feedback between land and atmosphere. *J. Hydrometeor.*, **7**, 1177–1198.

Doms, G., J. Förstner, E. Heise, H.-J. Herzog, M. Raschendorfer, R. Schrodin, T. Reinhardt, and G. Vogel, 2005: *A description of the Nonhydrostatic Regional Model LM*. Part 2: Physical parameterization, Postfach 100465, 63007 Offenbach, Germany: Deutscher Wetterdienst, Offenbach.

Doms, G. and U. Schättler, 2002: *A description of the Nonhydrostatic Regional Model LM*. Part 1: Dynamics and Numerics, Postfach 100465, 63007 Offenbach, Germany: Deutscher Wetterdienst, Offenbach.

Duband, D., C. Obled, and J. Y. Rodriguez, 1993: Unit hydrograph revisited: an alternate iterative approach to UH and effective precipitation identification. *J. Hydrol.*, **150**, 115 – 149.

Dümenil, L. and E. Todini, 1992: *A rainfall-runoff scheme for use in the Hamburg climate model. – In: J. P. O'Kane (Ed.): Advances in theoretical hydrology, A tribute to James Dooge*. European Geophys. Soc. Series on Hydrological Sciences 1, Elsevier, 129–157.

Eagleson, P. S. and et al., 1991: Opportunities in the hydrologic sciences. *J. Hydrol.*, **150**, 115 – 149.

ECMWF, 2001: *Documentation - Cycle 23r4*. Download version available at http://www.ecmwf.int/research/ifsdocs, Reading UK.

EEA, 2000: *Corine Land Cover (CLC90)*. European Environment Agency a http://dataservice.eea.eu.int/dataservice/, Copenhagen DK.

Ek, M. B. and R. Cuenca, 1994: Variation in soil parameters: Implications for modeling surface fluxes and atmospheric boundary-layer development. *Bound.-Lay. Meteor.*, **70**, 369–383.

Ek, M. B., K. E. Mitchell, Y. Lin, E. Rogers, P. Grunmann, V. Koren, G. Gayno, and J. D. Tarpley, 2003: Implementation of noah land surface model advances in the national centers for environmental prediction operational mesoscale ETA model. *J. Geophys. Res.*, **108(D22)**, doi:10.1029/2002JD003296.

Evensen, G., 1994: Sequential data assimilation with a nonlinear quasi geostrophic model using monte carlo methods to forcast erroro statistics. *J. Gephys. Res.*, **99**, 10143–10162.

Famiglietti, J. S. and E. F. Wood, 1994: Multi-scale modelling of spatially variable water and energy balance processes. *Water Resour. Res.*, **30(11)**, 3061–3078.

Farr, T. G., P. A. Rosen, E. Caro, R. Crippen, R. Duren, S. Hensley, M. Kobrick, M. Paller, E. Rodriguez, L. Roth, D. Seal, S. Shaffer, J. Shimada, J. Umland, M. Werner, M. Oskin, D. Burbank, and D. Alsdorf, 2007: The shuttle radar topography mission. *Rev. Geophys.*, **45**, doi: 10.1029/2005RG000183.

Fread, D. L., 1993: *Flow routing. In: D. R. Maidment - Handbook of Hydrology (eds.)*. McGraw Hill.

Genuchten, M. T. V., 1980: A closed-form equation for predicting the hydraulic conductivity of unsaturated soil. *Soil Sience*, **44**, 892–898.

Graßelt, R., D. Schüttemeyer, K. Warrach-Sagi, F. Ament, and C. Simmer, 2008: Validation of TERRA-ML with discharge measurements. *Meteorol. Z.*, **17 (6)**, 763–773, DOI 10.1127/0941-2948/2008/0334.

Gray, D. M. and T. D. Prowse, 1993: *Snow and Floating Ice. Handbook of Hydrology, Chapter 8, D. R. Maidment Ed.*. McGraw Hill.

Gulden, L. E., E. Rosero, Z.-L. Yang, M. Rodell, C. S. Jackson, G.-J. Niu, P. J.-F. Yeh, and J. Famigliette, 2007: Improving land-surface model hydrology: Is an explicit aquifer model better than a deeper soil profile. *Geophys. Res. L.*, **34(9)**, L09402, doi:10.1029/2007/GL029804.

Hamlet, A. F. and D. Lettenmaier, 1999: Effects of climate change on hydrology and water resources in the columbia river basin. *Am. Water Res. Assoc.*, **35(6)**, 1597–1623.

Henderson-Sellers, A., 1993: A factorial assesment of the sensitivity of the BATS land-surface parameterization schemes. *J. Climate*, **6**, 227–247.

Henderson-Sellers, A., K. McGuffie, and A. J. Pitman, 1996: The project for intercomparison of land-surface parameterization schemes (PILPS): 1992 to 1995. *Climate Dynamics*, **12**, 849–859.

Henderson-Sellers, A., A. J. Pitman, P. K. Love, P. Irannejad, and T. Chen, 1995: The project for intercomparison of land-surface parameterization schemes (PILPS): Phases 2 and 3. *Bull. Amer. Meteor. Soc.*, **76**, 489–503.

Henderson-Sellers, A., Z.-L. Yang, and R. E. Dickinson, 1993: The project for intercomparison of land-surface parameterization schemes. *Bull. Amer. Meteor. Soc.*, **74**, 1335–1349.

Hillel, D., 2004: *Introduction to Environmental Soil Physics*. Academic Press, San Diego.

Hohenegger, C., P. Brockhaus, and C. Schär, 2008a: Towards climate simulations at cloud-resolving scales. *Meteorol. Z.*, **17**, 383–394.

Jacobsen, I. and E. Heise, 1982: A new economic method for the computation of the surface temperature in numericals models. *Contr. Atmos. Phy.*, **55**, 128–141.

Janssen, P. H. M. and P. S. C. Heuberger, 1995: Calibration of process oriented models. *Ecol. Modell.*, **83**, 55–66.

Jarvis, P., 1976: The interpretations of the variations in leafwater potentials and stomatal conductances found in canopies in the field. *Philos. Trans. R. Soc. London*, **Ser. B 273**, 593–610.

Kabat, P., R. W. A. Hutjes, and R. A. Feddes, 1997: The scaling characteristics of soil parameters: From plot scale heterogeneity to subgrid parameterization. *J. Hydrol.*, **190 (3-4)**, 363–396.

Kalnay, E., 2002: *Atmospheric Modeling, Data Assimilation and Predictability*. Cambridge University Press.

Kollet, S. J., I. Cvijanovic, D. Schüttemeyer, R. M. Maxwell, and P. B. A. F. Moene, 2009: The influence of rain sensible heat, subsurface heat convection and the lower temperature boundary condition on the energy balance at the land surface. *Vadose Zone J.*, accepted.

Koren, V., J. Schaake, K. Mitchell, Q. Y. Duan, F. Chen, and J. M. Baker, 1999: A parameterization of snowpack and frozen ground intended for ncep weather and climate models. *J. Geophys. Res.*, **104**, 19569–19585.

Koster, R. D., M. J. Suarez, A. Ducharne, M. Stieglitz, and P. Kumar, 2000: A catchment-based approach to modeling land surface processes in a GCM. Part 1: Model structure. *J. Geophys. Res.*, **105 D**, 24809–24822.

Lenth, R., 1989: Quick and easy analysis of unreplicated fractional factorial. *Technometrics*, **31**, 469–473.

Liang, X., D. P. Lettenmaier, and E. F. Wood, 1996: One-dimensional statistical dynamic representation of subgrid spatial variability of precipitation in the two-layer variable infiltration capacity model. *J. Geophys. Res.*, **101(D16)**, 21403-21422.

Liang, X., D. P. Lettenmaier, E. F. Wood, and S. J. Burges, 1994: A simple hydrologically based model of land surface water and energy fluxes for GSMs. *J. Geophys. Res.*, **99(D7)**, 14415-14428.

Liang, X., D. P. Lettenmaier, E. F. Wood, et al., 1998: The project for intercomparison of land-surface parameterization schemes (PILPS) phase-2c red-arkansas river basin experiment: 2. spatial and temporal analysis of energy fluxes. *J. Global and Planetary Change*, **19**, 137–159.

Lohmann, D., 1996: *Hydrologische Modellierung auf regionaler Skala*. Dissertation University of Hamburg.

Lohmann, D., R. Nolte-Holube, and E. Raschke, 1996: A large-scale horizontal model to be coupled to land surface parameterization schemes. *Tellus*, **48A**, 708–721.

Mahrt, L. and M. Ek, 1984: The influence of atmospheric stability on potential evaporation. *J. Appl. Metorol.*, **23**, 222–234.

Maidment, D. R., 1993: *Precipitation. Handbook of Hydrology, Chapter 1, D. R. Maidment Ed.*. McGraw Hill.

Manabe, S., 1969: Climate and ocean circulation: 1. the atmospheric circulation and the hydrology of the earth's surface. *Mon. Weath. Rev.*, **97**, 739–774.

Mengelkamp, H. T., K. Warrach, and E. Raschke, 1999: SEWAB: A parameterization of the surface energy and water balance for atmospheric and hydrologic models. *Adv. Water Res.*, **23 (2)**, 165–175.

Mesa, O. J. and E. R. Mifflin, 1986: On the relative role of hillslope and network geometry in hydrology response. in: V. k. gupta, i. rodriguez-iturbe and e. f. wood (eds.). *Scale of Problems in Hydrology*, pp. 1–17.

Meyers, T. P. and S. E. Hollinger, 2004: An assessment of storage terms in the surface energy balance of maize and soybean. *Agric. For. Meteor.*, **125**, 105–115.

Ministry of environment, conservation, agriculture and consumer protection NRW, 2004: *Ergebnisbericht Sieg*. Ministry of environment, conservation, agriculture and consumer protection NRW, Schwannstrae 3, 40476 Düsseldorf, www.niederrhein.nrw.de/sieg/index.html.

Mosley, M. and A. I. McKerchar, 1993: *Streamflow. Handbook of Hydrology, Chapter 8, D. R. Maidment Ed.*. McGraw Hill.

Nijssen, B. N., R. Schnur, and D. Lettenmaier, 2001: Global retrospective estimation of soil moisture using the VIC land surface model. *J. Climate*, **14**, 1790–1808.

Niu, G. Y., Y. Z.-L., R. E. Dickinson, and L. E. Gulden, 2005: A simple topmodel-based runoff parameterization (SIMTOP) for use in global climate models. *J. Geophys. Res.*, **110**, D21106, doi:10.1029/2005JD006111.

Niyogi, D. S. and S. Raman, 1999: Uncertainty in the specification of surface characteristics. part 2: Hierarchy of interaction-explicit statistical analysis. *Bound.-Layer Meteor.*, **91**, 341–366.

Niyogi, D. S., X. Yongkang, and S. Raman, 2002: Hydrological land surface response in a tropical regime and a midlatitudinal regime. *Journal of Hydrometeor.*, **3**, 39–56.

Oleson, K. W., G.-Y. Niu, Z.-L. Yang, D. M. Lawrence, P. E. Thornton, P. Lawrence, R. Stockli, R. E. Dickinson, G. Bonan, S. Levis, A. Dai, and T. Qian, 2008: Improvements to the community land model and their impact on the hydrological cycle. *J. Geophys. Res.*, **113**, g01021, doi:10.1029/2007JG000563.

Paulson, C., 1970: The mathematical representation of wind speed and temperature profiles in the unstable atmospheric surface layer. *J. Appl. Meteor.*, **9**, 857–861.

Pielke, R. A., 1984: *Mesoscale meteorological modelling*. Academic Press, Orlando.

Pitman, A., A. Dolman, B. Kuijit, R. Valentini, and D. Baldocchi, 2004: *The Climate near the ground. — In: Kabat, P., M. Claussen, P.A. Dirmeyer, J.H.C. Gashk, L. Bravo de Guenni, M. Meybeck, R.A. Pielke, C.J. Vorosmarty, R.W.A. Hutjes , S. Lutkemaier (Eds.): Vegetation, Water, Humans and the Climate: A new perspective on an interactive system*. Springer Verlag, Heidelberg, 650 pp.

Press, W. H., S. A. Teukolsky, W. T. Vetterling, and B. P. Flannery, 1992: *Numerical Recipes in Fortran*. Cambridge Press.

Program, U. S., 2001: A plan for the new science initiative on the global cycle. *Report from the USGCRP Water Cycle Study Group*, Washington, DC, USA, 118 pp.

Rawls, W. J., L. R. Ahuja, D. L. Brakensiek, and A. Shirmohammadi, 1993: *Infiltration and soil water movement. Handbook of Hydrology, Chapter 5, D. R. Maidment Ed.*. McGraw Hill.

Richards, L. A., 1931: *Capillary conduction of liquids in porous mediums*. Physics 1.

Rijtema, P. E., 1969: *Soil moisture forecasting*. Technical Report Nota 513, Instituut voor Cultuurtechniek en Waterhuishouding, Wageningen.

Rodriguez, J. Y., 1989: *Modelisation pluie-debit par la methode*. These de doctorat, Grenoble, France.

Schär, C., D. Lüthi, U. Beyerle, and E. Heise, 1999: The soil-precipitation feedback: A process study with a regional climate model. *J. Climate*, **12**, 722–741.

Schmitz, R., 2005: *Einfluss der Landoberflaeche auf die Atmosphaere unter besonderer Beruecksichtigung der Bodenfeuchte*. Dissertation, University of Bonn.

Schraff, C. and R. Hess, 2003: *A description of the Nonhydrostatic Regional Model LM. Part 3: Data Assimilation*. www.cosmo-model.org, Deutscher Wetterdienst, Offenbach.

Schrodin, R., 1995: *Dokumentation des EM/DM Systems*. DWD, available at Deutscher Wetterdienst, Postfach 100465, D-63004 Offenbach.

Schrodin, R. and E. Heise, 2001: *The Multi-Layer Version of the DWD Soil Model TERRA-LM*. COSMO Technical Report No. 2, Offenbach.

Schüttemeyer, D., 2005: *The surface energy balance over drying semi-arid terrain in West Africa*. Dissertation, University of Wageningen.

Sellers, P., Y. Mintz, Y. C. Sud, and A. Dalcher, 1986: A simple biosphere model (sib) for use with general circulation models. *J. Atmos. Sci.*, **43**, 505–531.

Seuffert, G., P. Gross, C. Simmer, and E. F. Wood, 2002: The influence of hydrologic modeling on the predicted local weather: Two-way coupling of a mesoscale weather prediction model and a land surface hydrologic model. *J. Hydrometeor.*, **3**, 505–523.

Seuffert, G., H. Wilker, P. Viterbo, J. Mahfouf, M. Drusch, and J.-C. Calvet, 2003: Soil moisture analysis combining screen level parameters and microwave brightness temperatures. *Geophys. Res. Let.*, **30**, 1498, doi:10.1029/2003GL017128.

Shields, F. D. and J. R. Rigby, 2005: River habitat quality from river velocities measured using acoustic doppler currenr profiler. *Environmental Management*, **36 (4)**, DOI 10.1007/s00267-004-0292-6.

Shuttleworth, W. J., 1993: *Evaporation. Handbook of Hydrology, Chapter 4, D. R. Maidment Ed.*. McGraw Hill.

Sivapalan, M., K. Beven, and E. F. Wood, 1987: On hydrologic similarity: 2. A scaled model of storm runoff production. *Water Resour. Res.*, 2266–2278.

Slater, A. G., C. A. Schlosser, C. E. Desborough, A. Pitman, A. Henderson-Sellers, A. Robock, K. Y. Vinnikov, N. Speranskaya, K. Mitchell, A. Boone, H. Braden, F. Chen, P. Cox, P. de Rosnay, R. E. Dickinson, Y.-J. Dai, Q. Duan, J. Entin, P. Etchevers, N. Gedney, Y. Gusev, F. Habbets, J. Kim, V. Koren, E. Kowalczyk, O. Nasonova, J. Noilhan, J. Schaake, A. B. Shmakin, T. Smirnova, D. Verseghy, P. Wetzel, Y. Xue, and Z.-L. Yang, 2001: The representation of snow in land-surface schemes; results from PILPS 2(d). *J. Hydrometeor.*, **2**, 7–25.

Smith, J. A., 1993: *Precipitation. Handbook of Hydrology, Chapter 3, D. R. Maidment Ed.*. McGraw Hill.

Stewart, J. B., 1988: Modelling surface conductance of pine forest. *Agri. For. Meteorol.*, **43**, 19-35.

Stieglitz, M., D. Rind, J. Famigliette, and C. Rosenzweig, 1997: An efficient approach to modeling topographic control of surface hydrology for regional and global climate modeling. *J. Climate*, **10**, 118–137.

Stull, R. B., 1988: *An introduction to boundary layer meteorology*. Kluwer Acad., Norwell, Mass. 666 pp.

Viterbo, P. and C. Beljaars, 1995: An improved land surface parameterization scheme in the ECMWF model and its validation. *J. Climate*, **8**, 2716–2748.

Vrugt, J. A., C. Diks, H. V. Gupta, W. Bouten, and J. M. Verstraten, 2005: Improved treatment of uncertainty in hydrologic modeling: Combining the strengths of global optimization and data assimilation. *Water Resour. Res.*, **41**, doi:10.1029/2004WR003059.

Vrugt, J. A., H. V. Gupta, B. O. Nuallain, and W. Bouten, 2006a: Real-time data assimilation for operation ensemble streamflow forcasting. *J. Hydrometeor.*, **7(3)**, 548 – 565 doi:10.1029/2004WR003059.

Vrugt, J. A. and B. A. Robinson, 2007: Treatment of uncertainty using ensemble methods: Comparison of sequential data assimilation and bayesian model averaging. *Water Resour. Res.*, **43**, doi:10.1029/2005WR004838.

Warrach, K., H. T. Mengelkamp, and E. Raschke, 2001: Treatment of frozen soil and snow cover in the land surface model sewab. *Theoret. Applied Climatol.*, **69**, 23–37.

Warrach, K., M. Stieglitz, H. T. Mengelkamp, and E. Raschke, 2002: Advantages of a topographically controlled runoff simulation in a soil-vegetation atmosphere transfer model. *J. Hydrometeor.*, **3**, 131–147.

Warrach-Sagi, K., V. Wulfmeyer, R. Graßelt, F. Ament, and C. Simmer, 2008: Coupled simulations of the land surface model TERRA-ML with a river routing scheme reveal the impact of the soil parameterization on the water balance. *Meteorol. Z.*, **17 (6)**, 751-762. DOI 10.1127/0941-2948/2008/0343.

Wood, E. F., D. P. Lettenmaier, and V. G. Zartarian, 1992: A land-surface hydrology parameterization with subgrid variability for general circulation models. *Geophys. Res.*, **97**, 2717–2728.

Wulfmeyer, V., A. Behrendt, H.-S. Bauer, C. Kottmeier, U. Corsmeier, A. Blyth, G. Craig, U. Schumann, M. Hagen, S. Crewell, P. D. Girolamo, C. Flamant, M. Miller, A. Montani, S. Mobbs, E. Richard, M. Rotach, M. Arpagaus, H. Russchenberg, P. Schlüssel, M. König, V. Gärtner, R. Steinacker, M. Dorninger, D. D. Turner, T. Weckwerth, A. Hense, and C. Simmer, 2008: The Convective and Orographically-induced Precipitation Study: A Research and Development Project of the World Weather Research Program for improving quantitative precipitation forecasting in low-mountain regions. Doi:10.1175/2008BAMS2367.1.

Yang, Z.-L., R. E. Dickinson, A. Henderson-Sellers, and A. J. Pitman, 1995: Preliminary study of spin-up processes in land surface models with the first stage data of project for intercomparison of land surface parameterization schemes phase 1(a). *J. Geophys. Res.*, **100 (D8)**, 16553–16578.

Yates, F., 1970: *Experimental design - selected papers of Frank Yates*. Griffin, London, ISBN 0852641680.

List of Figures

List of Tables

Danksagung

An dieser Stelle möchte ich mich herzlich bei Prof. Dr. Clemens Simmer für das in mich gesetzte Vertrauen und die Betreuung der Arbeit bedanken. Prof. Dr. Susanne Crewell danke ich für ihre Bereitschaft, die Zweitbegutachtung dieser Dissertation zu übernehemen. Des Weiteren möchte ich mich bei Prof. Dr. Bernd Diekkrüger und Prof. Dr. Armin Skowronek bedanken, die sich bereit erklärt haben im Rahmen der Promotionskommission als Gutachter dieser Arbeit mitzuwirken.

Bedanken möchte ich mich auch bei Prof. Dr. Richard Dikau der als Sprecher des Graduiertenkollegs 437 diese Arbeit mitbetreute sowie bei allen anderen Mitgliedern des Graduiertenkollegs für die fruchtbaren Anregungen und Diskussionen während der Promotionszeit. Der Deutschen Forschungsgemeinschaft DFG danke ich für die Finanzierung dieser Arbeit im Rahmen dieses Graduiertenkollegs 437. Schließlich gilt mein Dank dem Deutschen Wetterdienst für die Zusammenarbeit und Bereitstellung der Daten sowie des Modelles TERRA-ML.

Den Korrektorinnen und Korrektoren dieser Arbeit möchte ich für ihre Geduld und ihren Eifer in dieser Sache danken. Des Weiteren bedanke ich mich bei allen Mitarbeiterinnen und Mitarbeitern des Meteorologischen Institutes für das tolle Arbeitsklima während der gesamten Zeit. Stellvertretend hierfür seien hier insbesondere die derzeitigen und ehemaligen Mitarbeiter des Büro 215 genannt: Marco Milan, Henning Wilker, Daniel Simonis, Ralf Schmitz und Mohammad Reza Marami. Im speziellen danke ich auch Kirsten Warrach-Sagi von der Universität Hohenheim für die vertrauensvolle Zusammenarbeit.

Ganz besonders möchte ich meiner Frau Ute danken die mich durch die gesamte Promotion und das Studium begleitet und tapfer ausgehalten und durch jegliche Art von Problemen geholfen hat und natürlich meiner Tochter Ina die während der Anfertigung dieser Arbeit zur Welt kam und mich zusätzlich motiviert hat diese Dissertation zu schreiben. Darüberhinaus danke ich meiner Familie für die tolle Unterstützung während der gesamten Jahre.